SCAN 2025

20th International Symposium on Scientific Computing, Computer Arithmetic, and Verified Numerical Computations

Universität Oldenburg / Matthias Hornung

Oldenburg, Germany, September 22-26, 2025

Book of Abstracts

Editors:
Ekaterina Auer[1]
Marit Lahme[2]
Andreas Rauh[2]

[1]University of Applied Sciences Wismar,
Department of Electrical Engineering and Computer Science,
Wismar, Germany

[2]Carl von Ossietzky Universität Oldenburg
Department of Computer Science
Distributed Control in Interconnected Systems,
Oldenburg, Germany

Aim of SCAN 2025

The series of International Symposia on Scientific Computing, Computer Arithmetic, and Verified Numerical Computations (SCAN) will be continued with the 20th edition from the 22nd to 26th of September 2025 (Monday to Friday) in Germany.

We are pleased to invite you to the Carl von Ossietzky Universität in the city of Oldenburg, a distinguished location in the German state of Lower Saxony.

SCAN 2025 will be the meeting place for researchers from the fields of reliable computing, software engineering, and uncertainty quantification and those from such wide and varied areas as robotics, control, structural and civil engineering, and signal processing.

Here, long-standing colleagues will be able to meet again in a relaxed though productive setting after a long absence of an in-person SCAN event. The new edition of the conference will continue to further strengthen the exchange of novel scientific ideas and will contain not only classical presentations in a lecture format but also discussion sessions focused on young researchers. In those, PhD students will have the opportunity to present their research activities in more detail and exchange views about them with a broad audience of more experienced scientists or other PhD students.

Conference Venue

Library Auditorium, Uhlhornsweg 49-55, D-26129 Oldenburg:
`https://uol.de/en/campus-map?wo=B`

Seminar Room A01-006, Uhlhornsweg 84, D-26129 Oldenburg:
`https://uol.de/en/campus-map?wo=A01`

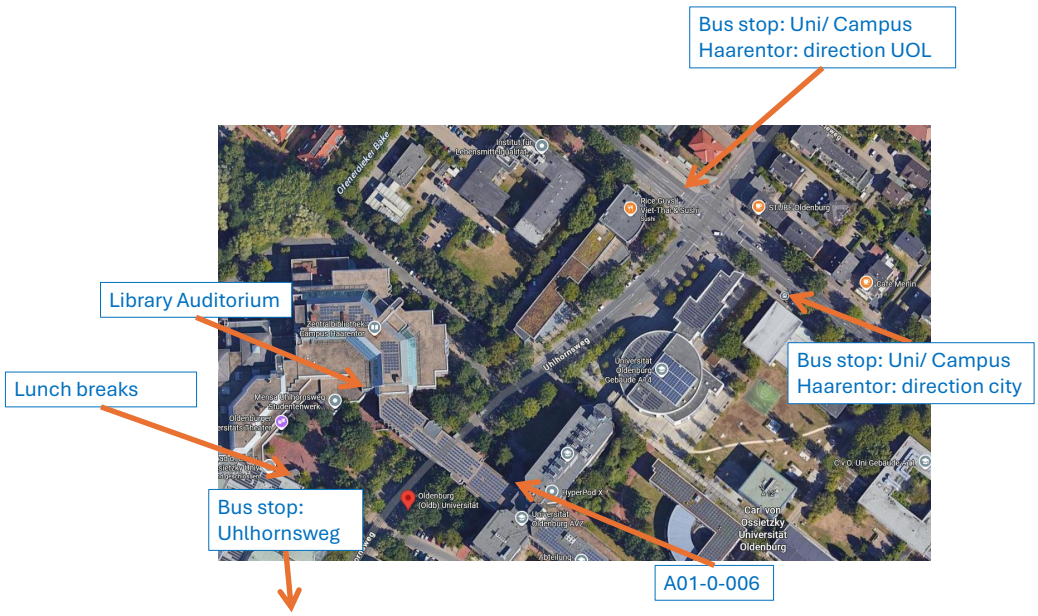


Botanischer Garten (800m)
Exhalle
Alte Maschinenhalle
Pferdemarkt
Landesbibliothek
Neue Donnerschweer Straße
EWE-Arenen Weser-Ems-Hallen
DJH Oldenburg
VHS
Karlstraße
Willy-Brandt-Platz
ZOB
Oldenburg (Oldb) Hbf
Bundesbahnweg
Moslestraße
Horst Janssen-Museum
Stadtmuseum
(Eröffnung 2026)
Oldenburger Computer-Museum e.V.
Bahnhofsgebäude
Bahnhofsviertel
Bahnhofsplatz
Garnisonskirche
Brüderstraße
91er-Straße
Core
Heiligengeisthöfe
Heiligengeiststraße
Peterstraße
Georgstraße
Grüne Straße
Forum St. Peter
Forumskirche St. Peter
Pius-Hospital
Haus für Medienkunst
Theater Laboratorium
Wilhelm 13
Kultur-zentrum PFL
EV-Krhs.
Artothek
Marienstraße
Katharinenstraße
Steinweg
Blumenstraße
Wilhelmstraße
Leo-Trepp-Str.
Kleine Str.
Bahnhofstraße
Osterstraße
Rosenstraße
Werk-schule e.V.
theater hof /19
Kulturetage
Blauschimmel Atelier e.V.
theater wrede+
Klavermannstraße
Güterstraße
Kaiserstraße
Gottorpstraße
Rosenstraße
Ludwig-straße
Bleicherstraße
Schifferstraße
Staustraße
Staulinie
Staugraben
Stau
Lappan
Wallgraben
Heiligengeistwall
Wallstraße
Werkstatt-film e.V.
Sartorius-gang
Elisen-straße
Polizei
Waffenplatz
Herbartgang
Friedenskirche
Friedensplatz
Ofener Straße
Haaren
Julius-Mosen-Platz
Kurwickstraße
Mottenstraße
Lange Straße
Achternstraße
Staupassage
Haus Graf Anton Günther
Thalia Passage
Haarenstraße
Schmale Straße
Schüttingstraße
Herbartstraße
Hausbäke
Theaterwall
Burgstraße
Abraham
Gaststraße
Baumgartenstraße
Nikolaigang
Knick
Bergstraße
Kleine Kirchenstr.
Lambertihof
Degode-haus
Altes Rathaus
Rathaus-markt
Häusing
St. Lamberti-Kirche
Schlosswache
Schlosshöfe
Schloss Landesmuseum Kunst & Kultur
Schlossplatz
Schloßplatz
Schloßwall
Pulverturm
Schlaues Haus
Oldenburgisches Staatstheater
Cäcilienstraße
Cäcilienplatz
Bismarckstraße
Roonstraße
Alter Landtag (150m)
Hindenburgstraße
Lindenallee
Parkstraße
Teichstraße
Holzweg
Dobbenviertel
Moltkestraße
Dobbenstraße
Roggemannstraße
Taubenstraße
Gartenstraße
Schlossgarten
Schlossteich
Elisabeth-Anna-Palais
Tretboot-verleih
Prinzenpalais
Augusteum/ Kunstverein
Paradewall
CADILLAC Zentrum für Jugendkultur
Elisabethstraße
Am Schloßgarten
Herm.-Allmers-Weg
Wilhelm-Wisser-Str.
Fritz-Reuter-Straße
Olantis Huntebad (300m)
Mühlenhunte
Mozart-straße
Schubert-straße
Richard-Wagner-Platz
Händelstraße
Beethovenstraße
Bachstraße
Elisabethstraße
Gerichtsviertel
Koppelstraße
Dammschanze
Damm
Niedersächsisches Landesarchiv
Landesmuseum Natur und Mensch
Gerichtsstraße
Schleusenstraße
Behelfs-brücke
Am Festungsgraben
Dammbleiche
Weidamm
Kanalstraße
Uferstraße
Hunte
Hermannstraße
Ahrensstraße
Am Cäcilien-hof
Blumen-hof
Sterlinger Straße
Gründergasse
Alte Amalienstr.
Friedrichswerk
Mühlgraben
Amalienstraße
Mühlenstraße
Poststraße
Huntestraße
Friederikenstraße
Elimarstraße
Nikolausstraße
Am Wende-hafen
Hafen
Hafenpromenade
Fahrgastschiffanleger (200m)
Ritterstraße
Phillip-Reis-Gang
Taxi
Bus
WC
Pedestrian zone
Parking area
Barrier-free parking space
Barrier-free restroom
Tourist Information
Car park
Barrier-free parking in car park
N

1 **Lappan (city landmark)**
The striking Gothic brick tower was added between 1467 and 1468 and attached ("angelappt") to the Holy Spirit Church which was built in 1394. In 1676 a city fire destroyed the building, but the tower was saved. Its baroque dome was added in 1709. Today it accommodates the Tourist Information Office.

2 **Haus Graf Anton Günther (Count Anton Günther House)**
An original merchant's house with a large fresco (1908) depicting the sovereign Count Anton Günther riding his favourite stallion, Kranich. He was famous for horse breeding (Oldenburg horses).

3 **Degodehaus (Degode House)**
The last remaining typical half-timbered house (1617) from the time before the great city fire. Wilhelm Degode from Jever acquired the house in 1860. Inside there is a painted wooden ceiling from 1645 with an allegorical representation of the continents known of at the time.

4 **Altes Rathaus (Old Town Hall)**
The current city hall is the seat of the Lord Mayor and was built in 1886-1888 on the site of two previous buildings. With its triangular ground plan the neo-Gothic building was intentionally designed to blend into the surrounding public spaces.

5 **St. Lamberti-Kirche (St. Lamberti Church)**
The church was built in around the year 1200 and features a number of architectural contrasts. The neo-Gothic masonry surrounds an impressive interior which was designed in 1791 in a classicist style by Duke Peter Friedrich Ludwig. It was modelled on the Roman Pantheon. The church tower and the four corner towers, which serve as escape routes, were not added until the 19th century.

6 **Schlosswache (Palace Guardhouse)**
The former Palace Guardhouse on the border to the free city was built in 1839 in the classicist style and based on plans drawn up by Heinrich Strack. Until the abdication of the Grand Duke in 1918, the military guard and the pageant of the changing of the guard was a city tradition.

7 **Schloss (Palace)**
The palace is founded on a medieval moated castle which was built around the year 1100 to guard a long-distance trade route. Count Anton Günther had the castle rebuilt from 1607-1615 in the later Renaissance style. Three more extensions were subsequently added, which are visible in the façade. The Landesmuseum Kunst & Kultur (State Museum of Art & Culture) has been housed in the Palace since 1923.

8 **Prinzenpalais (Prince's Palace)**
This classicist building served as a residence, initially for the Russian grandchildren of Duke Peter Friedrich Ludwig, and later for the Oldenburg Grand Duke. Since 2003 it has been part of the State Museum of Art & Culture and houses the Galerie Neue Meister (New Masters Gallery) with paintings and sculptures from the 19th and 20th centuries from the Romantic to the post-war period.

9 **Augusteum (art museum) / Oldenburger Kunstverein (art association)**
Opened in 1867 as the first art museum in the north west (Grand Ducal Painting Gallery). Built in the style of the Florentine Renaissance, it is one of the most beautiful gallery buildings in northern Germany today. As part of the State Museum, it houses the Old Masters Collection with exhibits from the end of the Middle Ages to the dawn of modernity. Founded in 1843, the Oldenburg Art Association is one of the oldest in Germany. It is dedicated to promoting contemporary art and is used as a venue for exhibitions and concerts.

10 **Landesmuseum für Natur und Mensch (State Museum of Man and Nature)**
Founded in 1836 by Grand Duke Paul Friedrich August, it is one of the oldest museums in Germany. It is dedicated to the richness of the landscape of north-western Germany and relates the history of the formation of the moorlands, the Geest (coastal moorlands), the coast and the marshlands and also shows how it has been affected by mankind.

11 **Elisabeth-Anna-Palais (Elisabeth-Anna Palace)**
Hereditary Grand Duke Friedrich August built the palace in 1896 in Dutch brick Renaissance style for his wife Elisabeth Anna of Prussia. After the abdication of the Grand Duke in 1918 it became the property of the state. The Social Court has been housed here since 1954. Exhibitions of artists from the region are regularly held in the foyer.

12 **Schlossgarten (Palace Gardens)**
The park extends over an area of around 16 hectares and was built at the beginning of the 19th century. It was laid out by Duke Peter Friedrich Ludwig in the style of an English landscape garden. The first rhododendrons were planted here in 1828. The Palace Gardens with the ancient trees are a tranquil haven all year round.

13 **Pulverturm (Powder Tower)**
The Powder Tower is the only remaining structure of Oldenburg's city fortifications. It was built in 1529 as a gun turret. In the 18th and 19th centuries it was used to store gunpowder, which is how it was given its name. Since 1996 it has been used as a unique exhibition venue for contemporary art.

14 **Oldenburgisches Staatstheater (Oldenburg State Theatre)**
In 1833 the first wooden theatre was built in Oldenburg. A larger and more imposing new building burned down in 1891. Two years later the theatre was opened in its current impressive form and has a captivating classicist portico. The "Kleines Haus" (Small House) was added as an extension in 1998. The Theatre currently encompasses seven genres.

15 **Peter Friedrich Ludwigs Hospital (Cultural Centre)**
The building was completed in 1841 and originally served as a hospital. It is locally known as the "PFL". It is regarded as the most important example of classicist architecture in Oldenburg. In the spring of 1984, after 143 years the PFL was closed as a hospital. Today it houses the city library and various cultural institutions.

16 **Haus für Medienkunst (House of Media Art)**
The House of Media Art Oldenburg shows and discusses contemporary media art. It presents international, innovative art and invites people to exchange ideas. Dialogue is promoted through changing exhibitions, talks and workshops.

17 **Horst-Janssen-Museum (art museum) and City Museum (under construction)**
The Horst Janssen Museum is dedicated to the visual arts on paper. The permanent exhibition focuses on the life and work of the draughtsman, etcher, woodcutter, poster artist, illustrator, writer and graphic artist Horst Janssen, who grew up in Oldenburg.
The City Museum was built with assets from a foundation set up by the Oldenburg citizen and collector Theodor Francksen. The building is currently under construction (opening 2026).

18 **Oldenburger Computer-Museum e.V. (open Tuesdays from 6 to 9 p.m.)**
The museum contains a display of historical computer systems, focusing on home computers from the 1970s and 80s. Video games, game consoles, arcade machines and pinball machines are also included in the exhibition. The museum is unique in Germany in that the exhibits are still functional and can be used.

19 **Oldenburger Hauptbahnhof (Main Train Station)**
The main train station was inaugurated in 1915 in its present form and architecturally blends into the region with its style of farmhouses of that time. The entire station ensemble with its Art Nouveau structure is protected. The track hall is a unique steel and glass construction and is currently being renovated.

20 **Alter Stadthafen (Old City Port)**
In 1345 Oldenburg was granted city rights and was therefore able to access maritime trade. In the 16th century the city evolved to become a successful maritime shipping port. Today it is one of the most important inland ports in Lower Saxony. The harbour promenade with its restaurants and cafés is a popular destination and meeting place.

Oldenburg-Info im Lappan
Lange Straße 3 | 26122 Oldenburg
www.oldenburg-tourismus.de

Hier dürfen Sie, wenn Sie müssen.

Public toilets
Public toilets are in the city centre are marked with this sign. The public toilets can be used free of charge and are also located in the Oldenburg Tourist Infomation Office in the Lappan.

FSC www.fsc.org RECYCLED Product made from recycled material FSC® C017909

Tourismus & Marketing Oldenburg i.O.

SCAN 2025 – 20th International Symposium on Scientific Computing, Computer Arithmetic, and Verified Numerical Computations

September 22-26, 2025

Carl von Ossietzky Universität Oldenburg

Monday, September 22

CoProD: 17th International Workshop on Constraint Programming and Decision Making – Library Auditorium

8:30-8:35	Opening	
8:35-9:00	Luc Jaulin	Optimal separator for an hyperbola; Application to localization
9:00-9:25	Milan Hladík	Robustness Properties of Absolute Value Linear Programming Problems and Relations to Interval Analysis
9:25:9:50	Ana Tapia-Rosero, Olga Kosheleva, and Vladik Kreinovich	What is the most natural way to propagate subjective interval uncertainty -- and why
9:50-10:15	Niklas Winnewisser, Michael Beer, Olga Kosheleva, and Vladik Kreinovich	How to combine subjective intervals: a natural idea
10:15-10:40	Niklas Winnewisser, Michael Beer, Victor Timchenko, Yuriy Kondratenko, Olga Kosheleva, and Vladik Kreinovich	Why midpoint, why radius (half-width): invariance-based numerical characteristics of an interval and how they are related to color vision and color optical computing
10:40-11:05	Ildar Z. Batyrshin, Luis A. Villa-Vargas, Nailya I. Kubysheva, Olga Kosheleva, Muhammad Ahmad, and Imre J. Rudas	Complex Chemical and Biochemical Reactions: Maybe Fuzzy Techniques Can Help
11:05-11:30	Martine Ceberio, Olga Kosheleva, and Vladik Kreinovich	Why topology helps to detect cyber-intrusions
11:30-11:55	Jean Rendon, Clariandys Rivera, Afshin Gholamy, and Leobardo Valera	Pre-Hashing as a Cryptographic Tool for Securing Entrepreneurial Ideas
11:55-12:20	Andrea Luces, Jean Rendon, Afshin Gholamy, and Leobardo Valera	Predicting Subsurface Soil Parameters Using Surface and Satellite Data with Machine Learning Techniques

Monday, September 22

SCAN 2025: Library Auditorium

14:00-14:30	Opening (Ekaterina Auer, Marit Lahme, Astrid Nieße, Andreas Rauh)	
Moore Prize Lecture (Chair: Vladik Kreinovich)		
14:30-16:00	Tristan Buckmaster, Gonzalo Cao-Labora, Javier Gomez-Serrano	Smooth imploding solutions for 3D compressible fluids
Regular Session: Special Functions (Chair: Luc Jaulin)		
16:30-17:00	Hiroaki Miyauchi, Taisei Asai, Masahide Kashiwagi and Akitoshi Takayasu	Constructing the Bessel function rigorously via the power series arithmetic
17:00-17:30	Lucas Si Larbi, Eric Lucet and Julien Alexandre Dit Sandretto	Interval Uniform, Non-Uniform, Rational, Non-Rational B-spline Curves
PhD Poster Session		

Tuesday, September 23

SCAN 2025: Library Auditorium

Plenary Lecture (Chair: Ekaterina Auer)		
9:00-10:30	Siegfried Rump	Verified error bounds for sparse systems
Regular Session A: Formal Verification (Chair: Takeshi Ogita)		
11:00-11:30	Antoine Besset, Joris Tillet and Julien Alexandre Dit Sandretto	Formal Verification of State and Temporal Properties of Neural Network-Controlled Systems
11:30-12:00	Martin Fränzle, Paul Kröger and Anna Nienaber	Exploiting the Impossible: Towards Resilience of Decision Making Against Misperceptions
12:00-12:30	Ryoki Endo and Xuefeng Liu	Computer-assisted proof of the simplicity of the second Dirichlet eigenvalue for non-equilateral triangles

Tuesday, September 23

SCAN 2025: A01-0-006

Regular Session B: Tools and Implementations (Chair: Simon Rohou)		
11:00-11:30	Ryoga Iwanami	Verry: an open-source package for verified computation written in Python 3
11:30-12:00	Pierre Filiol, Luc Jaulin, Theotime Bollengier and Jean-Christophe LeLann	Hardware accelerated interval arithmetic for mobile robotics using RISC-V ISA extension
12:00-12:30	Jiří Khun and Jan Schmidt	Towards Interval Arithmetic in TensorFlow: A Comparison of Approaches

Wednesday, September 24

SCAN 2025: Library Auditorium

Plenary Lecture (Chair: Nathalie Revol)		
9:00-10:30	Andreas Rauh	Interval and Set-Based Approaches for Control and State Estimation: Their Use for Offline and Online Purposes
Regular Session A: PDEs (Chair: Anna Gierzkiewicz)		
11:00-11:30	Kazuaki Tanaka, Ryoga Iwanami, Kaname Matsue and Hiroyuki Ochiai	Green-Representable Solutions: Reformulating Sub- and Super-solution Theory for Poisson's Equation
11:30-12:00	Taisei Asai, Kazuaki Tanaka, Satoshi Tanaka and Shin'Ichi Oishi	Verified Computation of All Positive Solutions to a Hénon-Type Boundary Value Problem
12:00-12:30	Akitoshi Takayasu and Jean-Philippe Lessard	Semigroup approach for validating solutions to semilinear parabolic PDEs

Wednesday, September 24

SCAN 2025: A01-0-006

Regular Session B: Uncertainty Quantification (Chair: Luc Jaulin)		
11:00-11:30	Olga Kosheleva and Vladik Kreinovich	For statistical analysis of big data, interval uncertainty is needed
11:30-12:00	Jahangir Alam, Ismail Hossain, Tausif Hossain, Md Nuruzzaman Sojib, Olga Kosheleva and Vladik Kreinovich	How to compare situations in which we measure different quantities with different uncertainty
12:00-12:30	Ekaterina Auer and Wolfram Luther	Towards Fair and Explainable Medical Risk Prediction Software via Dempster-Shafer Theory

Department of Computer Science

QR code and link to the detailed conference program

www.uol.de/en/scan2025/program

SCAN 2025 – 20th International Symposium on Scientific Computing, Computer Arithmetic, and Verified Numerical Computations

September 22-26, 2025

Carl von Ossietzky Universität Oldenburg

Thursday, September 25

SCAN 2025: Library Auditorium

Plenary Lecture (Chair: Andreas Rauh)

9:00-10:30	Tino Teige	Bringing Formal Methods from Academia to Real-World Applications in Industry: My Personal Two-Decades-Journey

Regular Session A: Estimation (Chair: Bernd Tibken)

11:00-11:30	Quentin Brateau, Fabrice Le Bars and Luc Jaulin	Separator for the remoteness constraint
11:30-12:00	Damien Esnault, Simon Rohou, Fabrice Le Bars and Luc Jaulin	Computing Interval Detection-Probability Grids via Monte-Carlo method for Underwater Robotics
12:00-12:30	Marit Lahme and Andreas Rauh	Set-Based Identification of Characteristic Curves and Its Challenges for Real-Life Applications

Regular Session A: Linear Systems and Linear Algebra: Library Auditorium (Chair: Siegfried Rump)

14:30-15:00	Haruto Kijima and Takeshi Ogita	Fast Implementation of Interval Matrix Multiplication Using Infimum-Supremum Representation With SIMD Operations
15:00-15:30	Takeshi Terao, Yoshitaka Watanabe and Katsuhisa Ozaki	Verification of Singular Values under Oblique Inner Product Space for Matrices
15:30-16:00	Katsuhisa Ozaki and Toru Koizumi	Tight Enclosure of Matrix Multiplication using Fused Multiply-Add

Regular Session A: Neural Networks: Library Auditorium (Chair: Vladik Kreinovich)

16:30-17:00	Attila Szász and Balázs Bánhelyi	Parameter Robustness of Neural Networks
17:00-17:30	Tibor Csendes	Interval Based Verification of Adversarial Example Free Zones for Neural Networks

Thursday, September 25

SCAN 2025: A01-0-006

Regular Session B: Uncertainty Quantification (Chair: Tibor Csendes)

11:00-11:30	Olga Kosheleva and Vladik Kreinovich	Inconsistencies in Fuzzy Estimations: Kaucher Arithmetic Naturally Appears
11:30-12:00	Miroslav Svitek, Olga Kosheleva and Vladik Kreinovich	Shapley Value Under Interval Uncertainty Revisited: Why Seemingly Natural Axiomatic Approach Is Not Fully Adequate
12:00-12:30	Luc Jaulin	A new wrapper for a reliable resolution of underdetermined nonlinear equations

Regular Session B: Optimization (Chair: Julien Alexandre Dit Sandretto)

14:30-15:00	Milan Hladík	Linear Programming Problems with Absolute Values and Interval Uncertainty
15:00-15:30	Cyril Kotecký and Milan Hladík	Complementary stability in quadratic interval programming
15:30-16:00	Christophe Jermann, Nathalie Revol and Christine Solnon	B&P algorithms for continuous constraint problems: a survey of branching strategies

Regular Session B: Dynamic Systems (Chair: Simon Rohou)

16:30-17:00	Ramiz Dilji, Bernd Tibken, Robert Dehnert, Youping Fan, Regina Deisling and Laura Ackerschott	Estimation of the Domain of Attraction for Nonlinear Systems using the Bihari Inequality
17:00-17:30	Andreas Rauh and Marit Lahme	Observer-Based Approaches for a Verified Simulation and Pseudo State Estimation of Fractional Dynamic Systems

Friday, September 26

SCAN 2025: Library Auditorium

Plenary Lecture (Chair: Andreas Rauh)

9:00-10:30	Christoph Matheja	Automated Verification of Discrete Probabilistic Programs

Regular Session A: Dynamic Systems (Chair: Robert Dehnert)

11:00-11:30	Robert Szczelina, Anna Gierzkiewicz and Jakub Kural	Investigating chaos in Delay Differential Equations with rigorous numerical methods
11:30-12:00	Jakub Kural, Anna Gierzkiewicz and Robert Szczelina	Computer assisted proof of existence of periodic solutions to ENSO delay differential equation model
12:00-12:30	Théo Le Terrier, Marie Babel and Vincent Drevelle	Ultra-wideband Based Smart Wheelchair Pose Estimation using Interval Analysis

Regular Session A: Dynamic Systems (Chair: Marit Lahme)

14:00-14:30	Andreas Rauh and Friederike Bruns	Set-Based Contracts for Systematic Controller Tuning in Interconnected Dynamic Systems
14:30-15:00	Anna Gierzkiewicz, Maciej Capinski and Pau Martin	Oscillating orbits in the Sitnikov model: equal masses case
15:00-15:30	Mohamed Fnadi and Régis Lherbier	Interval Particle Filter for LiDAR-Based Object Tracking
16:00	**Closing of SCAN 2025**	

Friday, September 26

SCAN 2025: A01-0-006

Regular Session B: Optimization (Chair: Ekaterina Auer)

11:00-11:30	Mihály Gencsi and Boglárka G.-Tóth	Improvements of the Geometrical Test in Interval Branch and Bound methods
11:30-12:00	Verlein Radwan, Simon Rohou and Gilles Trombettoni	Exhaustive Interval-based 2-D Shape Registration Under Similarity Transformation
12:00-12:30	Maël Godard, Luc Jaulin and Damien Massé	Adaptative parallelepipedic approximation of the image of a set by a nonlinear function

Regular Session B: Optimization (Chair: Nathalie Revol)

14:00-14:30	Yuki Uchino, Katsuhisa Ozaki and Toshiyuki Imamura	High-Performance Emulation of Matrix Multiplication using INT8 Matrix Engines and its Error Analysis
14:30-15:00	Lorenz Gillner and Ekaterina Auer	Efficient Acceleration Strategies for Interval Branch-and-Bound Type Methods
15:00-15:30	Diego Romano, Ekaterina Auer, Francesco Gregoretti and Lorenz Gillner	GPU-Accelerated Algorithmic Differentiation For Reliable Computing: Comparing Different Architectures

Department of Computer Science

QR code and link to the detailed conference program

www.uol.de/en/scan2025/program

Contents

Author-Sorted List of Contributions

Monday, September 22, 2025

Library Auditorium

8:30–12:20	**CoProD:** 17th International Workshop on Constraint Programming and Decision Making
12:30–14:00	Lunch Break – Food truck
14:00–14:30	Opening
14:30–16:00	**Moore Prize Lecture** Tristan Buckmaster, Gonzalo Cao-Labora, Javier Gomez-Serrano: *Smooth imploding solutions for 3D compressible fluids*
16:00–16:30	Coffee Break
16:30–17:00	**Regular Session: Special Functions**
16:30–17:00	Hiroaki Miyauchi, Taisei Asai, Masahide Kashiwagi: and Akitoshi Takayasu: *Constructing the Bessel function rigorously via the power series arithmetic*
17:00–17:30	Lucas Si Larbi, Eric Lucet and Julien Alexandre Dit Sandretto: *Interval Uniform, Non-Uniform, Rational, Non-Rational B-spline Curves*
17:30–18:30	**PhD Poster Session**

All posters presented in this PhD session are included subsequently together with the associated abstract.

Constructing the Bessel function rigorously via the power series arithmetic

Hiroaki Miyauchi[1], Taisei Asai[2], Masahide Kashiwagi[2], Akitoshi Takayasu[3]

[1] Graduate School of Science and Technology, University of Tsukuba
s2530138@u.tsukuba.ac.jp
[2] Faculty of Science and Engineering, Waseda University
captino@fuji.waseda.jp
kashi@waseda.jp
[3] Institute of Systems and Information Engineering, University of Tsukuba
takitoshi@risk.tsukuba.ac.jp

Keywords: Power series arithmetic, Bessel function, Interval arithmetic

Introduction

This study introduces a verified numerics framework for integrals involving the Bessel function that arise in the analysis of nonlinear elliptic boundary value problems. Existing quadrature schemes rarely control rounding and truncation errors rigorously, and the accuracy of their results cannot be guaranteed. In particular, to the best of our knowledge no existing approach encloses in interval form integrals of the type

$$\int_0^1 \prod_{i=1}^{p+1} J_{n_i}(\nu_{n_i,m_i} r) r dr, \quad n_i = 0, 1, 2, \ldots, \quad m_i = 1, 2, 3, \ldots,$$

where $J_n(x)$ is the n-th order Bessel function of the first kind and $\nu_{n,m}$ denotes the m-th positive root of $J_n(x)$. This integral corresponds to the Galerkin projection in semilinear elliptic equations (1) shown at the end of this abstract.

There exist methods for rigorously computing the Bessel function, for example, within the Arb library [1]. This is a C library for rigorous real and complex arithmetic with arbitrary precision based on ball arithmetic that implements algorithms for computing $J_n(x)$ and $Y_n(x)$ (the n-th order Bessel function of the second kind) in the real and complex domains. However, Arb lacks built-in tools for verifying quadratures of the Bessel function. This makes it difficult to account for truncation errors in such quadratures directly.

With the background mentioned above, we have developed a method that performs verified numerics for integrals involving the Bessel function, enclosing the integral values directly and rigorously in interval form.

In this talk, providing the Bessel function using the power series arithmetic in the kv library [2], a collection of C++ libraries for verified numerical computations, we can obtain rigorous enclosures of the Bessel function via interval arithmetic. We apply the Schlömilch's diffrential recurrence formula [3] to construct the power series expansion of $J_n(x)$. All coefficients of the power series up to degree n are rigorously included in the interval coefficients. The remainder term is also rigorously included

in the coefficient of the highest degree. This yields a verified power series representation of $J_n(x)$. Additionally, the verified power series representation provides interval inclusion of the values of integrals such as

$$\int_0^1 J_0(\nu_{0,1}r)rdr, \quad \int_0^1 J_0(\nu_{0,1}r)^3rdr.$$

Selected results in practice

Furthermore, using the power series expression, the verified quadrature of the Bessel function is rigorously included as follows:

$$\begin{aligned}
\int_0^1 J_0(\nu_{0,1}r)rdr &\in \left[0.2158774035098^{4231}_{3808}\right] \\
\int_0^1 J_0(\nu_{0,1}r)^3rdr &\in \left[0.09746130106859^{7087}_{4366}\right] \\
\int_0^1 J_1(\nu_{0,1}r)J_1(\nu_{0,2}r)rdr &\in \left[-2.35055030994e^{-15}, 2.39776731456e^{-15}\right] \\
\int_0^1 J_0(\nu_{0,1}r)J_1(\nu_{1,1}r)J_2(\nu_{2,1}r)rdr &\in \left[0.036053739292^{458323}_{183674}\right] \\
\int_0^1 J_8(\nu_{8,1}r)J_9(\nu_{9,1}r)J_{10}(\nu_{10,1}r)rdr &\in \left[0.00464011953^{73457745}_{52999569}\right],
\end{aligned}$$

where the interval $[0, 1]$ is partitioned into sixteen sub-intervals and the Bessel function is expanded by the power series up to the degree 20.

For applications of the provided method, we aim to consider verified numerics for solutions to semilinear elliptic equations on the unit disk.

$$\begin{cases} -\Delta u = f(u) & \text{in } \Omega \\ u = 0 & \text{on } \partial\Omega, \end{cases} \tag{1}$$

where $\Omega = \{(r, \theta) \mid 0 \le r \le 1, 0 \le \theta \le 2\pi\} \in \mathbb{R}^2$, $f(u)$ is a polynomial of order p.

Since the Bessel function is the eigenfunction of the Laplacian on the unit disk, we can expect a highly accurate approximation of the boundary value problems. To this end, the methods for integrals introduced in this abstract are essential. This prospective application to the problem in (1) serves as the primary motivation for this study.

References

[1] Johansson, F: Arb kibrary (2013). https://arblib.org/index.html

[2] Kashiwagi, M.: kv library (2016). http://verifiedby.me/kv/index-e.html

[3] Watson, G.N: A Treatise on The Theory of Bessel Functions, Cambridge (1966).

Constructing the Bessel function rigorously via the power series arithmetic

Hiroaki Miyauchi[1] Taisei Asai[2] Masahide Kashiwagi[2] Akitoshi Takayasu[3]

[1] Graduate School of Science and Technology, University of Tsukuba [2] Faculty of Science and Engineering, Waseda University [3] Institute of Systems and Information Engineering, University of Tsukuba

1. Background

Verified numerical computation of solutions to nonlinear boundary value problems is a fundamental challenge in scientific computing. On the unit disk, Fourier-Bessel expansions naturally appear, which require the evaluation of multiple integrals of Bessel functions: to ensure reliable error bounds. The Fourier-Bessel expansion leads to the

$$\int_0^1 \left(\prod_{i=1}^{p+1} J_{n_i}(\nu_{n_i,m_i} r)\right) r\,dr, \quad u_i = 0, 1, 2, \ldots, \quad m_i = 1, 2, \ldots,$$

where $J_n(x)$ is the Bessel function of the first kind and $\nu_{n,m}$ denotes the m-th positive root of J_n. Existing quadrature schemes rarely provide rigorous control of rounding and truncation errors, so the reliability of such integrals cannot be guaranteed. This motivates us to develop a verified numerics framework based on *Power Series Arithmetic* (PSA).

2. Objective

The goal of this study is to establish a verified numerics framework for integrals involving Bessel functions that naturally arise in Fourier-Bessel expansions of nonlinear elliptic boundary value problems. Specifically, we construct rigorous power series representations of $J_n(x)$ using Type-II Power Series Arithmetic (PSA) in the kv library. This approach encloses all coefficients and remainder terms in interval form, enabling verified evaluation of Bessel integrals such as

$$\int_0^1 J_0(\nu_{0,1} r)\, r\,dr, \quad \int_0^1 J_1(\nu_{0,1} r)^3\, r\,dr,$$

which cannot be rigorously handled by conventional quadrature methods. The verified quadrature developed here is designed as a foundation for reliable Galerkin projections and residuals bounds in semilinear elliptic PDEs on the unit disk.

3. Methods (Type-II PSA for $J_n(x)$)

Type-II Power Series Arithmetic (PSA).
We are using Type-II PSA for verified computations. On a fixed domain $[t_1, t_2]$, truncated power series are stored with interval coefficients. Terms up to degree n are kept explicitly, and all higher-order contributions are absorbed in to the top coefficient, enduring rigorous error control.

Construction of Bessel functions.
Schlömilch's differential recurrence provides a basis for recursive differentiation:

$$J_n'(x) = \tfrac{1}{2}\big(J_{n-1}(x) - J_{n+1}(x)\big).$$

More generally, higher derivatives satisfy

$$J_n^{(k)}(x) = \frac{1}{2^k}\sum_{r=0}^{k}(-1)^r \binom{k}{r} J_{n-k+2r}(x).$$

Using these formulas, we construct verified Taylor expansions of $J_n(x)$, enclosing all coefficients and the remainder in interval form. This yields a power series representation that is both rigorous and directly usable in computations.

Verified quadrature.
To evaluate integrals of Bessel functions required in Galerkin projections, we proceed as follows:

- "The interval $[0, 1]$ is subdivided into smaller subintervals, so that polynomial approximations remain accurate."
- "On each subinterval, $J_n(x)$ is expanded by Type-II PSA up to degree n, and the product of series is computed with interval coefficients."
- "Term-by-term integration is carried out analytically, which provides an interval polynomial $y(t)$. evaluating $y(\Delta)$ yields an enclosure of the integral over that subinterval."
- "The contributions of all subintervals are summed, resulting in a global enclosure of the target integral."

4-1. Results: Verified Maclaurin expansions of $J_0(x)$

As a demonstration, we present a verified Maclaurin expansions of $J_0(x)$ on the interval $[0, 1]$ using Type-II PSA with degree 4.

$$\begin{aligned} J_0(x) \in\ & [0.999999, 1.00001] + [-8.9 \times 10^{-16},\ 8.9 \times 10^{-16}]\, x \\ & + [-0.250001, -0.249999]\, x^2 + [-1.7 \times 10^{-16},\ 1.7 \times 10^{-16}]\, x^3 \\ & + [0.005291, 0.020030]\, x^4 \end{aligned}$$

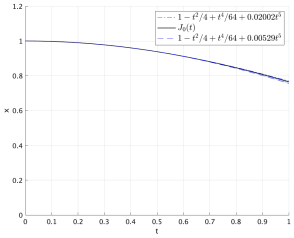

$J_0(x)$: **Overall comparison**

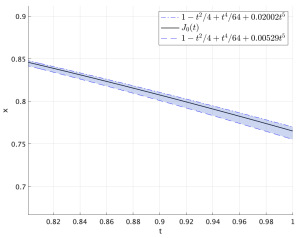

$J_0(x)$: **Focused view**

4-2. Results: Verified integrals

The following examples show verified enclosures of Bessel integrals, which play a central role in Galerkin projections for semilinear elliptic PDEs. In these computations, the interval $[0, 1]$ is partitioned into sixteen sub-intervals, and the Bessel functions are expanded by power series up to degree 20.

$$\int_0^1 J_0(\nu_{0,1} r)\, r\,dr \in \left[0.2158774035098^{4231}_{3808}\right]$$

$$\int_0^1 J_0(\nu_{0,1} r)^3\, r\,dr \in \left[0.0974613010685^{7087}_{4366}\right]$$

$$\int_0^1 J_1(\nu_{0,1} r) J_1(\nu_{0,2} r)\, r\,dr \in \left[-2.35055030994 \times 10^{-15},\ 2.39776731456 \times 10^{-15}\right]$$

$$\int_0^1 J_0(\nu_{0,1} r) J_1(\nu_{1,1} r) J_2(\nu_{2,1} r)\, r\,dr \in \left[0.0360537392^{458323}_{183674}\right]$$

$$\int_0^1 J_8(\nu_{8,1} r) J_9(\nu_{9,1} r) J_{10}(\nu_{10,1} r)\, r\,dr \in \left[0.00464011953^{73457745}_{52999569}\right]$$

5. Discussion & Conclusion

Our study demonstrates that Type-II PSA provides a rigorous way to represent Bessel functions and to evaluate their integrals with guaranteed error bounds. By enclosing both coefficients and remainder terms in interval form, we obtained verified power series expansions and quadrature results that are not achievable by conventional methods. These verified integrals form the essential components of Galerkin projections for semilinear elliptic PDEs on the unit disk.

$$\begin{cases} -\Delta u = f(u) & \text{in } \Omega \\ u = 0 & \text{on } \partial\Omega, \end{cases} \tag{1}$$

$\Omega = \{(r, \theta) \mid 0 \le r \le 1, 0 \le \theta \le 2\pi\} \in \mathbb{R}^2$, $f(u)$ is a polynomial of order p. While the proposed Type-II PSA framework ensures rigorous enclosures, its computational cost increases rapidly with higher series degrees and finer partitions. This indicates that PSA alone is not sufficient for practical large-scale computations. A promising direction is to design hybrid methods that use PSA where it is most effective and rely on asymptotic expansions or optimized recurrence relations in other regions, thereby achieving both rigor and efficiency.

6. Outlook

Building on this framework, we plan to:

- "Integrate verified quadrature into full residual-norm estimation for elliptic PDEs (1)."
- "Develop hybrid algorithms that use PSA near the origin and asymptotic expansions for large arguments."
- "Extend the method to more general oscillatory integrals and higher-dimensional spectral problems."

These advances aim to establish a practical and scalable tool for verified numerical analysis of nonlinear elliptic PDEs, contributing to reliable scientific computing in broader contexts.

References

Johansson, F. *Arb library* `https://arblib.org/`
Kashiwagi, M. *kv library* `http://verifiedby.me/kv/index-e.html`
Watson, G. N. *A Treatise on the Theory of Bessel Functions*, Cambridge, 1966

Interval Uniform, Non-Uniform, Rational, Non-Rational B-spline Curves

Lucas Si Larbi[1,2], Eric Lucet[1] and Julien Alexandre dit Sandretto[2]

[1] Université Paris Saclay, CEA, List, F-91120 Palaiseau, France
{lucas.silarbi,eric.lucet}@cea.fr
[2] ENSTA Paris, Institut Polytechnique de Paris, F-91120 Palaiseau, France
julien.alexandre-dit-sandretto@ensta-paris.fr

Keywords: Interval Methods , B-spline curves

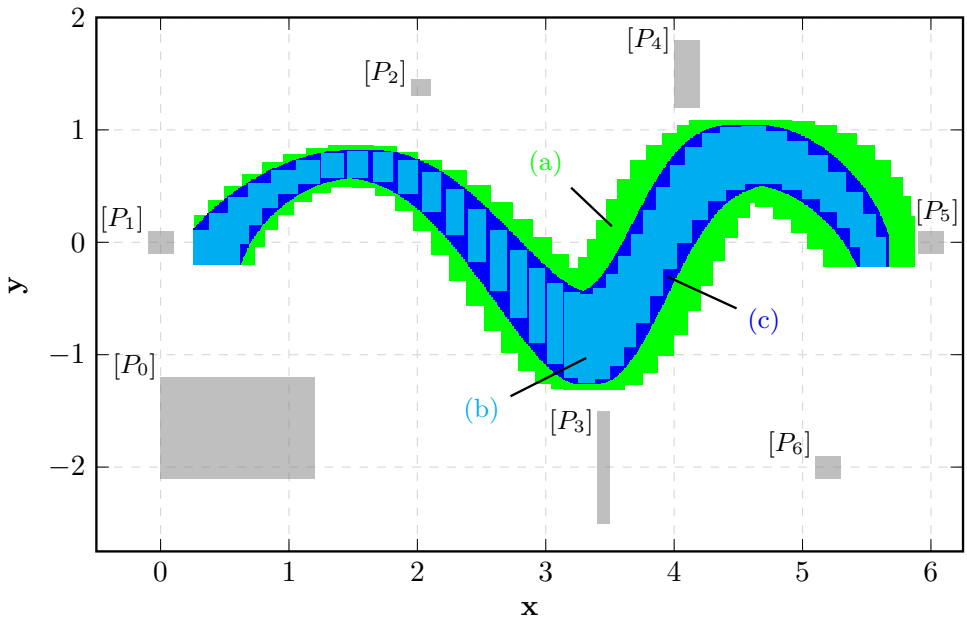

Figure 1: (a) Exactly evaluated Interval U-NR-BS. (b) Pseudo-Interval U-NR-BS built from the successive midpoints of parameter discretized intervals of (a). (c) Interval U-NR-BS with a finner parameter discretization than (a). These three curves are made from the same control boxes $[P_i]$.

Uniform or Non-Uniform, Rational or Non-Rational B-Spline curves (U-NU-R-NR-BS) are widely used in computer aided design, computer graphics, and robotics [3, 6]. These polynomial curves have powerful properties and, using the deBoor-Cox recurrence formula [1, 2], they are simple to compute. U-NU-R-NR-BS are parameterized and defined by a finite number of control points. A natural way to bound these curves is to consider both the parameter and control points as intervals. However, as they are constructed from a sum of polynomial basis functions, and, as the pessimism of the natural interval evaluation is cumulative, the resulting bounds are often worthless. It is therefore necessary to bound basis functions with other approaches. In general, to reduce the pessimism, the centered form, the Taylor form or the affine arithmetic are used [5]. For the same reason, the modal arithmetic was

used to evaluate interval Bézier curves in [4]. Another elegant way to avoid interval dependencies is to discretize the parameter of basis functions [7, 8, 9]. These last are therefore exactly evaluated. The discretized basis obtained generates non-continuous U-NU-R-NR-BS. This pseudo-interval approach is only suitable for applications that do not require interval guarantees, see Figure 1.

We propose: (i) a comprehensive analysis of interval extensions of U-NU-R-NR-BS; (ii) operators on interval U-NU-R-NR-BS such as $\cap$, $\cup$; (iii) operators between interval U-NU-R-NR-BS and real numbers or matrices; (iv) discussion about the wrapping effect.

Acknowledgement

Contributions from CEA List were carried out in the scope of REFLEX project, as part of the MOBILEX Challenge. This project received funding from the French Defense Innovation Agency (AID) and the French National Research Agency (ANR) and, in partnership with the French National Center for Space Studies (CNES) and the French Agency for Transport Innovation (AIT).

References

[1] M. G. COX, The numerical evaluation of b-splines. *IMA Journal of Applied Mathematics*, 10(2):134–149, 1972. DOI: 10.1093/imamat/10.2.134.

[2] C. De Boor, *On calculating with B-splines.* Jour. Approx. Theory, Vol. 6, pp. 50-62, 1972.

[3] D. González *et al.*, "A review of motion planning techniques for automated vehicles," *IEEE Transactions on Intelligent Transportation Systems* DOI: 10.1109/TITS.2015.2498841.

[4] N. T. Hayes. Introduction to Modal Intervals, *prepared for the IEEE 1788 Working Group.*

[5] L. Jaulin *et al.*, *Applied Interval Analysis with Examples in Parameter and State Estimation, Robust Control and Robotics.* 2001. DOI: 10.1007/978-1-4471-0249-6.

[6] L. Piegl and W. Tiller, *The NURBS Book.* Monographs in Visual Communication. Springer Berlin Heidelberg, 1996. DOI: 10.1007/978-3-642-59223-2.

[7] T. W. Sederberg and R. T. Farouki Approximation by interval Bezier curves, *IEEE Computer Graphics and Applications.* DOI: 10.1109/38.156018.

[8] G. Shen and N. M. Patrikalakis, Numerical and geometric properties of interval b-splines. *International Journal of Shape Modeling.* DOI: 10.1142/S0218654398000040.

[9] L. Si Larbi, E. Lucet and J. A. D. Sandretto, Optimal Path Planner over Receding Horizon using Interval Analysis, *Summer Workshop on Interval Methods, 2024.*

Interval Uniform, Non-Uniform, Rational, Non-Rational B-spline Curves

Lucas SI LARBI[1,2], Eric LUCET[1] and Julien ALEXANDRE DIT SANDRETTO[2]

SCAN2025

Objective: Use B-spline curves as a support solution of an Interval branch and Bound (IB&B)

B-spline u, Pi

Made from:
- A discretized parameter u.
- Some control points Pi.

General B-spline properties:
- Local modification.
- Definition of the entire curve only with several control points.
- Setting of the degree of the curve.
- Basis:

$$N_{i,0}(u) = \begin{cases} 1 & if \quad u_i \le u \le u_{i+1} \\ 0 & otherwise \end{cases}$$

$$N_{i,p}(u) = \frac{u - u_i}{u_{i+p} - u_i} N_{i,p-1}(u) + \frac{u_{i+p+1} - u}{u_{i+p+1} - u_{i+1}} N_{i+1,p-1}(u)$$

Drawbacks:
- Not compatible with an IB&B.
- Not continuous.

Non-uniform | Uniform

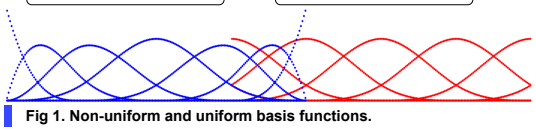

Fig 1. Non-uniform and uniform basis functions.

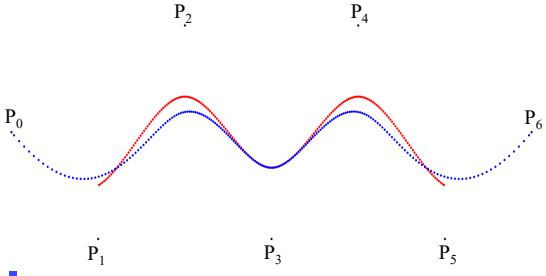

Fig 2. Uniform (open) and non-uniform (semi-open, clamped) B-splines.

Non-Rational | Rational

$$C(u) = \sum_{i=0}^{n} N_{i,p}(u) P_i \qquad C(u) = \frac{\sum_{i=0}^{n} \omega_i N_{i,p}(u) P_i}{\sum_{i=0}^{n} \omega_i N_{i,p}(u)}$$

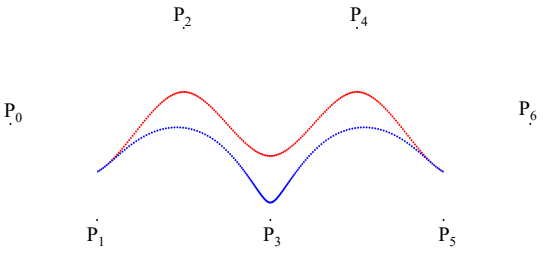

Fig 3. Uniform non-rational and rational B-splines. The rational equation allows us to increase the weight ω_i of certain control points. In this figure, the weight ω_3 of the control point P_3 was increased.

Pseudo-Interval B-spline u, [Pi]

Made from:
- A discretized parameter u.
- Some control boxes [Pi].

Advantages:
- Properties of B-splines remain valid.
- Compatible with an IB&B.
- Avoid the dependency problem because the only redundant variable is u, which is not an interval. The basis therefore remains the same as for B-spline curves.
- **Drawback:** Not continuous.

Non-uniform | Uniform

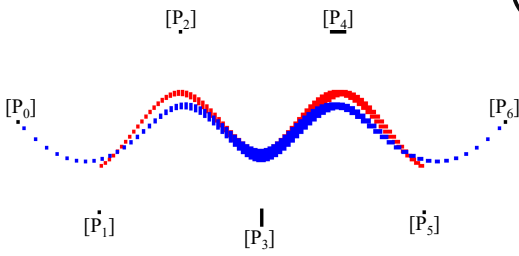

Fig 4. Uniform and non-uniform pseudo-interval B-splines. Curve boxes diameters are directly linked to control boxes diameters. It is therefore possible to optimize the curve by using an IB&B.

Non-Rational | Rational

$$[C](u) = \sum_{i=0}^{n} N_{i,p}(u)[P_i] \qquad [C](u) = \frac{\sum_{i=0}^{n} \omega_i N_{i,p}(u)[P_i]}{\sum_{i=0}^{n} \omega_i N_{i,p}(u)}$$

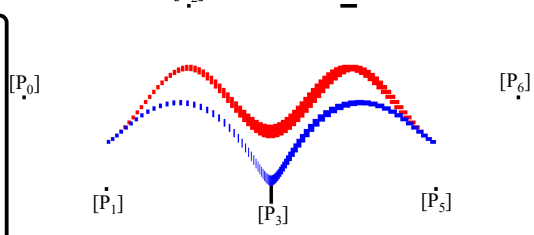

Fig 5. Uniform non-rational and rational pseudo-interval B-splines.

Interval B-spline [u], [Pi]

Made from:
- A bisected interval parameter [u].
- Some control boxes [Pi].

Advantages:
- Properties of B-splines remain valid.
- Compatible with an IB&B.
- Continuous and guaranteed.

Drawback:
- Basis functions are more difficult to compute.
- The wrapping effect depend on the control boxes positions.

Basis forms:

With: $N = [N_{i,p}]$; $mu = mid([u])$; $dN = \frac{d[N_{i,p}]}{d}$

- Centered:

$$N([u]) \subset N(mu) + dN([u])([u] - mu)$$

- Taylor 1:

$$N([u]) \subset N(mu) + dN(mu)([u] - mu) + d^2N([u])(\frac{([u] - mu)^2}{2}$$

Perspectives:
- Reduce the wrapping effect.
- Unlink the wrapping effect and the position of control boxes.
- Replace control boxes by control zonotopes.

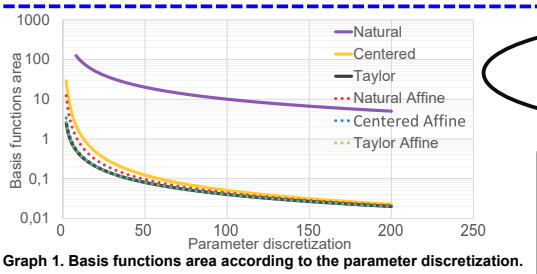

Graph 1. Basis functions area according to the parameter discretization.

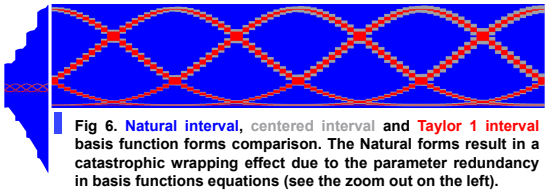

Fig 6. Natural interval, centered interval and Taylor 1 interval basis function forms comparison. The Natural forms result in a catastrophic wrapping effect due to the parameter redundancy in basis functions equations (see the zoom out on the left).

Non-uniform | Uniform

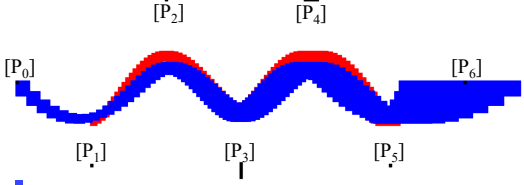

Fig 7. Uniform and non-uniform interval B-splines with basis functions evaluated by using the Taylor 1 interval affine form.

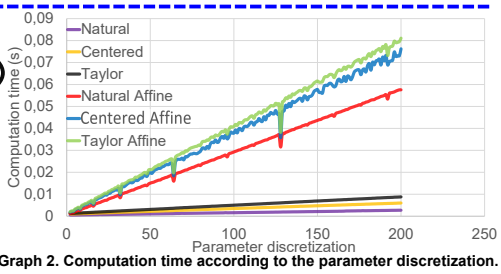

Graph 2. Computation time according to the parameter discretization.

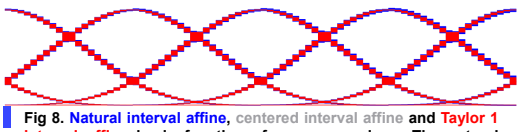

Fig 8. Natural interval affine, centered interval affine and Taylor 1 interval affine basis functions forms comparison. The natural interval affine form is better than the interval centered form.

Non-Rational | Rational

$$[C]([u]) = \sum_{i=0}^{n} [N_{i,p}]([u])[P_i] \qquad [C]([u]) = \frac{\sum_{i=0}^{n} \omega_i [N_{i,p}]([u])[P_i]}{\sum_{i=0}^{n} \omega_i [N_{i,p}]([u])}$$

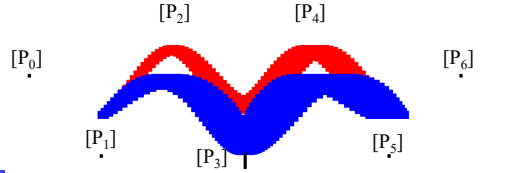

Fig 9. Uniform non-rational and rational interval B-splines with basis functions evaluated by using the Taylor 1 interval affine form.

L. Si Larbi, E. Lucet, J. A. D. Sandretto, Optimal local path Planner over Receding Horizon using Open Interval B-spline, Acta Cybernetica, 2025 (in proceeding).
L. Si Larbi, E. Lucet, J. A. D. Sandretto, Interval Uniform, Non-Uniform, Rational, Non-Rational B-spline Curves, SCAN2025.
G. Shen, N. M. Patrikalakis, Numerical and geometric properties of interval B-splines. International Journal of Shape Modeling, 1998.
L. Piegl, W. Tiller, The NURBS Book. Monographs in Visual Communication. Springer Berlin Heidelberg, 1996.

1 Université Paris-Saclay, CEA, LIST, DIASI/SRI/LCSR, Palaiseau, France
2 U2IS, ENSTA Paris, Institut Polytechnique de Paris, Palaiseau, France

Tuesday, September 23, 2025

Library Auditorium

9:00–10:30	**Plenary Lecture** Siegfried Rump: *Verified error bounds for sparse systems*
10:30–11:00	Coffee Break
11:00–12:30	**Regular Session A: Formal Verification**
11:00–11:30	Antoine Besset, Joris Tillet and Julien Alexandre Dit Sandretto: *Formal Verification of State and Temporal Properties of Neural Network-Controlled Systems*
11:30–12:00	Martin Fränzle, Paul Kröger and Anna Nienaber: *Exploiting the Impossible: Towards Resilience of Decision Making Against Misperceptions*
12:00–12:30	Ryoki Endo and Xuefeng Liu: *Computer-assisted proof of the simplicity of the second Dirichlet eigenvalue for non-equilateral triangles*
12:30–14:00	Lunch Break – Food truck
14:00–17:00	**Social Program – Guided Lab Tour at the ForWind Institute**

Verified Error Bounds for Sparse Systems

Siegfried M. Rump

Institute for Reliable Computing
Hamburg University of Technology
D-21073 Hamburg, Germany

Faculty of Science and Engineering
Waseda University
169–8555 Tokyo, Japan
rump@tuhh.de

The solution of sparse systems is ubiquitous in numerical computations. Despite several efforts, there were no satisfactory method for computing verified bounds for the solution and it was mentioned as "Grand Challenge".

In this talk we present two algorithms to compute entrywise error bounds for the solution of general real or complex sparse systems with condition number up to the limit 10^{16}. Our algorithms split into three subalgorithms for symmetric positive definite, symmetric indefinite and general input matrix A. A key point is a factorization of A into $L_1 L_2$ such that L_1 and L_2 have identical sets of singular values with the smallest one close to $\sigma_{\min}(A)^{1/2}$. A mathematically correct lower bound on $\sigma_{\min}(L_1) = \sigma_{\min}(L_2)$ is then computed using $L_1^T L_1$. Based on that a second method exploring the inertia of a symmetric/Hermitian matrix is presented. It is often slower but more stable, i.e., it may produce verified inclusions where the first method fails.

We show how to compute inclusions with almost maximal accuracy for all entries, i.e., all bounds differ by few bits. That is based on a fast method to compute accurate approximations and bounds for extremely ill-conditioned dot products with a very efficient Matlab implementation.

Both approaches are used to compute verified error bounds for the solution of least squares problems and for underdetermined linear systems. Inclusions of the solution of general real or complex systems of nonlinear equations with sparse Jacobi matrix are computed by transforming the problem into a linear system with point matrix and interval right hand side.

All algorithms are implemented in pure Matlab/Octave and included in Version 14 of INTLAB, the Matlab/Octave toolbox for verified computations.

Formal Verification of State and Temporal Properties of Neural Network-Controlled Systems

Antoine Besset[1], Joris Tillet[1] and Julien Alexandre dit Sandretto[1]

[1] ENSTA Paris, Institut Polytechnique
U2IS
Palaiseau, France
{antoine.besset,joris.tillet,alexandre}@ensta.fr

Keywords: Signal Temporal Logic, Verification of Neural Network, Interval Methods, Cyber-Physical Systems

Ensuring the safety of Neural Network Controlled Systems (NNCS) remains a major challenge due to the opaque nature of neural networks, especially when temporal properties are involved. This paper presents an interval analysis-based framework for verifying both state and temporal properties of NNCS using Signal Temporal Logic (STL) specifications [1, 2, 3, 4]. We introduce an STL monitoring algorithm based on interval analysis, featuring adaptive time sampling and formal guarantees of satisfaction over continuous domains. The STL formalism allows a rich temporal property specification while our approach is broadly applicable to neural networks when activation functions can be expressed as Ordinary or Differential Algebraic Equations (ODEs/DAEs). Reachability analysis, following the differential approach of [5], employs an ODE solver with affine arithmetic to ensure tight enclosures and dependency tracking. We demonstrate the effectiveness of the method on two case studies, involving both NNCS and systems with temporal constraints.

To express temporal properties, we adopt a temporal logic formalism known as Signal Temporal Logic (STL) [1, 2]. It has been applied in the domains of robotics and control. STL formulas allow the expression of various temporal properties using explicit time bounds, combining logical connectives with bounded Until temporal operators ($U_{[a,b]}$) [1]. The syntax of STL is defined recursively as follows:

$$\phi := \mu \mid T \mid \neg\phi \mid \phi_1 \vee \phi_2 \mid \phi_1 \, U_{[a,b]} \, \phi_2. \tag{1}$$

We extend the verification of predicate (μ) with an inclusion predicate ($\mathcal{X}^\mu$) to verify properties on reachable tubes $y(t, [y_0]) \subseteq ([\tilde{y}], t)$, $\forall t \in [t_0, T]$, [3, 4]. A reachable set at t is $[\tilde{y}](t)$.

$$([\tilde{y}], t) \vDash \mu_i := \begin{cases} 1, & \text{if } [\tilde{y}](t) \subset \mathcal{X}^\mu, \\ 0, & \text{if } [\tilde{y}](t) \cap \mathcal{X}^\mu = \emptyset, \\ [0,1], & \text{otherwise.} \end{cases} \tag{2}$$

To evaluate satisfaction, we extend the STL syntax with the Boolean Interval Arithmetic [6, 7], enabling sound reasoning under uncertainty.

To conduct reachability analysis of an NNCS, one effective approach is to exploit the differential properties of its activation functions [5]. For instance, in the case of the sigmoid activation function $\sigma(x)$, it can be represented in the form of an ordinary differential equation (ODE) as follows:

$$\frac{d\sigma}{dx}(x) = \sigma(x)(1 - \sigma(x)). \tag{3}$$

This formulation enables the use of ODE solvers within an affine arithmetic framework to compute guaranteed enclosures of the solutions while preserving the dependencies between individual neurons in the network. Supporting a broad spectrum of neural network architectures and expressive temporal logic specifications, the framework enables formal verification of practical NNCS scenarios. Comparative analysis with a Monte Carlo-based method highlights its precision and formal soundness.

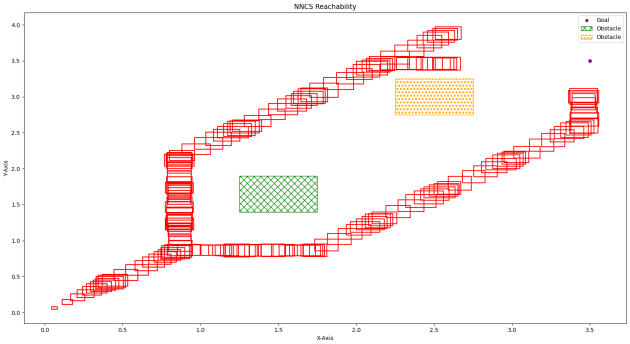

Figure 1: The 20-second simulation illustrates branching in the neural network output, with reachable tubes depicted in red. The axes indicate the position of the NN-controlled robot in meters. Branching arises from uncertainty in output classification. Left deviations around obstacles result in longer trajectories to the goal.

Acknowledgement

The authors acknowledge support from the French Interdisciplinary Center for Defense and Security (CIEDS) with the STARTS project.

References

[1] O. Maler and D. Nickovic, "Monitoring temporal properties of continuous signals," in *Formal Techniques, Modelling and Analysis of Timed and Fault-Tolerant Systems*, ser. Lecture Notes in Computer Science, vol. 3253. Springer, 2004, pp. 152–166.

[2] E. Bartocci, J. Deshmukh, A. Donzé, G. Fainekos, O. Maler, D. Ničković, and S. Sankaranarayanan, "Specification-based monitoring of cyber-physical systems: A survey on theory, tools and applications," *Lecture Notes in Computer Science*, vol. 10457, pp. 135–175, 2018.

[3] F. Lercher and M. Althoff, "Using four-valued signal temporal logic for incremental verification of hybrid systems," in *Proc. of Computer Aided Verification (CAV)*, vol. 14683. Springer Nature Switzerland, 2024, pp. 259–281.

[4] J. Tillet, A. Besset, and J. Alexandre dit Sandretto, "Guaranteed satisfaction of a signal temporal logic formula on tubes," *Acta Cybernetica*, 2025, accepted.

[5] R. Ivanov, J. Weimer, R. Alur, G. J. Pappas, and I. Lee, "Verisig: Verifying safety properties of hybrid systems with neural network controllers," 2018.

[6] J. Alexandre dit Sandretto and A. Chapoutot, "Logical differential constraints based on interval boolean tests," in *Fuzzy Techniques: Theory and Applications*. Springer International Publishing, 2019, vol. 1000, pp. 788–792.

[7] L. Jaulin, M. Kieffer, O. Didrit, and E. Walter, "Applied interval analysis," in *Applied Interval Analysis*, L. Jaulin, M. Kieffer, O. Didrit, and E. Walter, Eds. Springer, 2001, pp. 11–43.

Formal Verification of State and Temporal Properties of Neural Network-Controlled Systems

Antoine Besset, Joris Tillet, and Julien Alexandre dit Sandretto

Projet STARTS
Sécurité et Probabilité de Succès
(SafeTy And pRobAbiliTy Success)
starts.ensta-paris.fr

Summary : Ensuring the safety of Neural Network Controlled Systems (NNCS) remains a major challenge due to the opacity of neural networks, especially when temporal properties are involved. By combining **interval analysis** with **reachability techniques**, we ensure compliance with **spatial and temporal specifications** formally expressed using **Signal Temporal Logic (STL)**. The proposed framework provides a rigorous method for guaranteeing the correctness of uncertain dynamical systems controlled by a neural network.

Cyber-physical systems

Consider a continuous dynamical system modeled by the following differential equation:

$$\dot{y}(t) = f(y(t), w(t)), \quad y(t) \in \mathbb{R}^n, \ w(t) \in \mathcal{W}, \tag{1}$$

where $y(t)$ is the state of the system, $w(t)$ is a bounded external input, and $\mathcal{W} \subseteq \mathbb{R}^p$ is a compact set. For any initial state $y_0 \in \mathbb{R}^n$ and any measurable input $w : \mathbb{R}^+ \to \mathcal{W}$, the system admits a unique trajectory denoted by $\xi(\cdot, y_0, w)$.
In the presence of **bounded uncertainty**, the objective is to determine **the set of possible trajectories** over the interval $[t_0, T]$. The set of reachable states at time $t \in \mathbb{R}^+$ from an initial set $\mathcal{Y}_0 \subseteq \mathbb{R}^n$ is defined as:

$$\text{Reach}_t(\mathcal{Y}_0, \mathcal{W}) = \{\xi(t, y_0, w) \mid y_0 \in \mathcal{Y}_0, \ w(s) \in \mathcal{W}, \ \forall s \in [0, t]\}. \tag{2}$$

A **continuous-time representation** on $[t_j, t_{j+1}]$, $\bigcup_{j=0}^{N-1}[t_j, t_{j+1}] = [t_0, T]$, called a ***tube*** and denoted $[\tilde{y}](t)$ for $t \in [t_0, T]$, is essential for preserving the set of all possible system behaviors [6]. This *tube* enables the analysis of the satisfaction of a temporal logic formula.

Combining STL and reachability analysis

To formally analyze the system behavior, we use *interval analysis* [5] and introduce a **set - valued extension of predicates**:

$$([\tilde{y}], t) \vDash \mu_i := \begin{cases} 1, & \text{if } [\tilde{y}](t) \subset \mathcal{X}^{\mu}, \\ 0, & \text{if } [\tilde{y}](t) \cap \mathcal{X}^{\mu} = \emptyset, \\ [0, 1], & \text{otherwise.} \end{cases} \tag{3}$$

Propagation in temporal logic is handled using **Boolean intervals** [2, 7], e.g [3].:
$0 \wedge [0, 1] = 0, \quad 0 \vee [0, 1] = [0, 1], \quad 1 \wedge [0, 1] = [0, 1], \quad 1 \vee [0, 1] = 1.$

Signal temporal logic

We use the formalism of **Signal Temporal Logic (STL)** [4]:

$$\varphi := \top \mid \mu \mid \neg\varphi \mid \varphi_1 \wedge \varphi_2 \mid \varphi_1 \, \mathbf{U}_{[t_1,t_2]} \varphi_2$$

where the temporal operator **U** (*Until*) specifies that a property must hold until another becomes true within a given time interval. The operator **F** (*Finally*) expresses that a goal must be reached within a time window, while **G** (*Globally*) states that a property must hold throughout a time interval.

Example: an automaton executing a periodic task.

$$\varphi = \mathbf{G}_{[0,5]}(v \Rightarrow \mathbf{F}_{[3.5,4.5]} w) \ \wedge \ \mathbf{G}_{[0,8]}(\neg p) \ \wedge \ \mathbf{F}_{[8,9]} q$$

- $\mathbf{G}_{[0,5]}(v \Rightarrow \mathbf{F}_{[3.5,4.5]} w)$: Always on $[0, 5]$s, if v is reached then w must follow within 3.5–4.5s.
- $\mathbf{G}_{[0,8]}(\neg p)$: The obstacle p must never be encountered during the first 8s.
- $\mathbf{F}_{[8,9]} q$: The stand-by zone q must be reached between 8s and 9s.

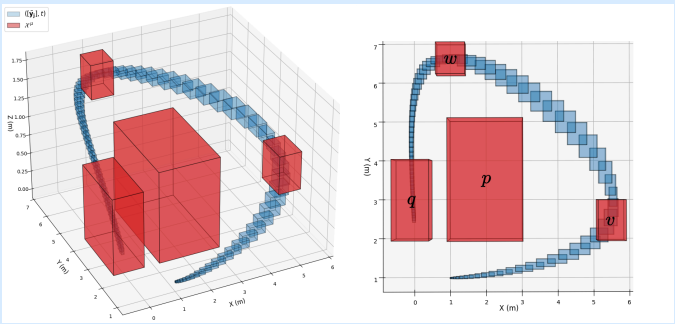

Tube $([\tilde{y}], t)$ *in blue and zones* $(\mathcal{X}^{\mu})$ *in red.*

Application : A robot controlled by a neural network

A robot is controlled by a **neural network**, whose internal behavior is **difficult to interpret**. The presented methods provide **formal guarantees** that it **reaches its goal**, avoids obstacles, and does so within a **given time bound**, even in the presence of uncertainties [1]. The system employs a neural network to choose, from a set of motion primitives, the action that drives it toward the goal while avoiding obstacles. An example of specification could be:

$$\varphi = \neg C \, \mathbf{U}_{[t_1,t_2]} \, T.$$

This means that no collision ($\neg C$) must occur until the target (T) is reached, within the given time horizon $[t_1, t_2]$.

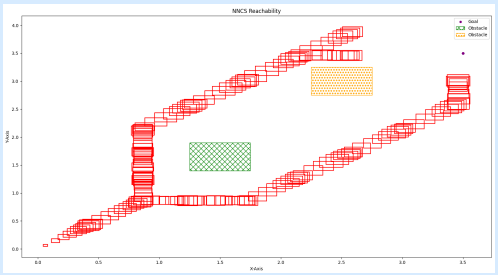

The reachable tube by the robot is shown in red, obstacles are in green and yellow, the target point is in purple.

Set propagation in neural network

To conduct reachability analysis of NNCS, activation functions such as the sigmoid can be expressed as ODEs, e.g.

$$\frac{d\sigma}{dx}(x) = \sigma(x)(1 - \sigma(x)).$$

This allows ODE solvers to be combined with **affine arithmetic**, where uncertain quantities are represented as

$$x = x_0 + x_1\varepsilon_1 + \cdots + x_n\varepsilon_n, \quad \varepsilon_i \in [-1, 1].$$

Using shared noise symbols preserves dependencies between neurons, enabling **accurate error tracking** and avoiding the overestimation of interval arithmetic.

References

[1] Antoine Besset, Julien Alexandre dit Sandretto, and Joris Tillet. Real-time guaranteed monitoring for a drone using interval analysis and signal temporal logic. In *Proceedings of the 2025 IEEE/RSJ IROS*, Hangzhou, China, 2025. IEEE.
[2] Antoine Besset, Joris Tillet, and Julien Alexandre dit Sandretto. Uncertainty removal in verification of nonlinear systems against signal temporal logic via incremental reachability analysis. In *Proceedings of the 64th IEEE CDC*. IEEE, 2025.
[3] Luc Jaulin, Michel Kieffer, Olivier Didrit, and Eric Walter. Applied interval analysis. In Luc Jaulin, Michel Kieffer, Olivier Didrit, and Eric Walter, editors, *Applied Interval Analysis*, pages 11–43. Springer, 2001.
[4] Oded Maler and Dejan Nickovic. Monitoring temporal properties of continuous signals. In *Formal Techniques, Modelling and Analysis of Timed and Fault-Tolerant Systems*, volume 3253, pages 152–166. Springer, 2004.
[5] Ramon E. Moore. *Interval Analysis*. Series in Automatic Computation. Prentice Hall, 1966.
[6] Julien Alexandre Dit Sandretto and Alexandre Chapoutot. Validated explicit and implicit runge-kutta methods. *Reliable Computing*, 22, 2016. Special issue devoted to material presented at SWIM 2015.
[7] Joris Tillet, Antoine Besset, and Julien Alexandre Dit Sandretto. Guaranteed satisfaction of a signal temporal logic formula on tubes. *Acta Cybernetica*, 2025. Accepted, to appear.

U2IS, ENSTA – Institut Polytechnique de Paris, 828 boulevard des Maréchaux, 91120 Palaiseau, France

Exploiting the Impossible: Towards Resilience of Decision Making Against Misperceptions

Martin Fränzle, Paul Kröger, and Anna Nienaber

Carl von Ossietzky Universität Oldenburg
Foundations and Applications of Systems of Cyber-Physical Systems
D-26111 Oldenburg, Germany
{martin.fraenzle,paul.kroeger,anna.nienaber}@uni-oldenburg.de

Keywords: Highly automated vehicles, learning-enabled cyber-physical systems, perception chain, decision making, robustification, symbolic-numeric computation

Introduction

One of the key challenges for safety-critical cyber-physical systems (CPSes) such as (highly) autonomous vehicles is decision making under the inevitable presence of uncertainties in environmental perception. Wrong control decisions within such systems may incur a substantial risk to life, health, or property. Achieving high confidence for guard conditions enabling safety-critical actions is thus crucial, even if they rely on uncertain percepts. However, the safety targets for, e.g., safety-critical manoeuvres of vehicles are typically orders of magnitude higher than, e.g., the statistical figures for the reliability of at least current learning-enabled object classification algorithms.

The perception and decision chain consequently needs to incorporate mechanisms for substantially improving the confidence in critical guard conditions, i.e., to reduce the risk of erroneously performing an unsafe manoeuvre to a frequency considerably below the risk of individual misperceptions, e.g., misclassifications. These mechanisms should, however, not impede performance, i.e., they should retain liveness of the system in that they reduce the rate of erroneously admitting a safety-critical action drastically, yet do not significantly reduce the overall likelihood of permitting the respective action.

We present a symbolic-numeric method that systematically rewrites critical guard conditions s.t. the resulting conditions are more resilient against misperceptions than the original conditions in that they are compatible with a given safety target, e.g. a societally accepted upper bound of the risk of erratically activating a safety-critical manoeuvre due to a false positive in a guard evaluation, while liveness in terms of the true positive rate of guard evaluation simultaneously is maximised.

Approach

Figure 1 illustrates a traffic situation in which the blue ego car (no. 1) shall overtake the orange car (no. 2) iff, first, the orange car is detected as an obstacle and, second, an overtaking manoeuvre is safe, i.e., iff there is no oncoming traffic (such

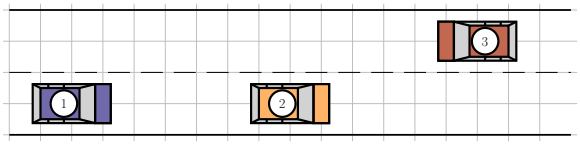

Figure 1: A traffic situation.

as the red car no. 3) with which car 1 could collide. In this –for the sake of conciseness over-simplified– example, the physical environment is partitioned into grid elements and the overtaking manoeuvre could be guarded by a complex Boolean condition describing conditions on the occupancy of the grid elements, which in turn is evaluated separately by a suitable but inherently uncertain object detection and classification algorithm, usually of machine-learning type.

Such safe-guarding conditions are prone to induce unnecessary risk by demanding potentially unsafe overtaking manoeuvres as soon as a single grid element is (mis-) perceived.

Incorporating environmental invariants can alleviate the problems described above: A car can usually neither occupy a single grid element only nor be distributed over non-adjacent grid elements. Our method exploits (formalisations of) such invariants. Given an invariant, we systematically rewrite a given guard by treating percepts not satisfying the invariant as don't cares and generally remapping percepts s.t. the robustness of the guard condition against misperceptions increases. Robustness increases in that the rate of erratically evaluating the guard to be satisfied, i.e., its false-positive rate, is reduced to below a pre-defined threshold, while the true positive rate gets maximised in order to guarantee performance.

We implemented and evaluated our approach by an algorithm that is based on reduced ordered binary decision diagrams (RoBDD) and akin to RoBDD don't care optimisation. The algorithm is symbolic-numeric in that it attaches probabilities to the elements of an RoBDD and adjusts those numerically during the RoBDD operations underlying its don't care optimisation.

Acknowledgement

This work was partially supported by the German Research Foundation (DFG) as part of PreCePT (FR 2715/6-1).

References

[1] M. Fränzle and A. Hein. Safer Than Perception: Increasing Resilience of Automated Vehicles Against Misperception. *Bridging the Gap Between AI and Reality* (AISoLA 2023), LNCS 14129, 415–433, 2024.

[2] Anna Nienaber. Increasing Resilience of Automated Vehicles Against Misperception. Bachelor's thesis, Carl von Ossietzky Universität Oldenburg, 2025. Unpublished.

Computer-assisted proof of the simplicity of the second Dirichlet eigenvalue for non-equilateral triangles

Ryoki Endo[1], Xuefeng Liu[2]

[1] Graduate School of Science and Technology, Niigata University
8050 Ikarashi 2-no-cho, Nishi-ku, Niigata City, Niigata 950-2181, Japan
endo@m.sc.niigata-u.ac.jp
[2] Department of Information and Sciences, Tokyo Woman's Christian University
2-6-1 Zempukuji, Suginami-ku, Tokyo 167-8585, Japan
xfliu@cis.twcu.ac.jp

Keywords: Simplicity of eigenvalues, Dirichlet eigenvalue, Verified computation, Computer-assisted proof

The rich relationship between Laplacian eigenvalues and shapes gave birth to the field of spectral geometry, which continues to attract researchers from various disciplines. In this talk, we provide a computer-assisted proof for a conjecture about Dirichlet eigenvalues posed by R. Laugesen and B. Siudeja in Henrot's book "Shape Optimization and Spectral Theory" [1]:

Conjecture 1 (Conjecture 6.47 of [1])**.** *The second Dirichlet eigenvalue is simple on every non-equilateral triangle.*

The proof of this conjecture is given by two parts.

In Part 1, we provided a partial result confirming the conjecture for the case of nearly degenerate triangles [2]:

Theorem 1. *The second Dirichlet eigenvalue is simple for every non-equilateral triangle with its minimum normalized height* [1] *less than or equal to* $\tan(\pi/60)/2$.

To achieve this, we derived explicit estimates for the k-th Dirichlet eigenvalues on the collapsing triangle:

For $s \in (-1, 1)$ and $t > 0$, let $T(s, t)$ be the triangular domain with vertices $(-1, 0), (1, 0)$ and (s, t); see Figure 1.

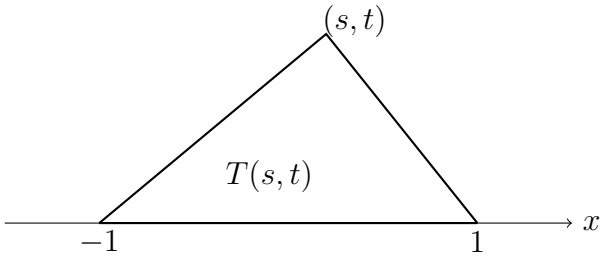

Figure 1: Shape of triangle $T(s, t)$

[1]The minimum normalized height of a triangle is the height measured relative to its longest side, with the triangle scaled such that the longest side has unit length.

Letting $t_0 = \tan(\pi/60)/2$,

$$\frac{\bar{\mu}_k(s)}{1 + t_0^{\frac{2}{3}}/(3\pi^2)\bar{\mu}_k(s)} \leq t^{\frac{4}{3}} \left(\lambda_k(s,t) - \frac{\pi^2}{t^2} \right) \leq \hat{\mu}_k^{t_0}(s) \quad (\forall t \in (0, t_0], \quad k = 1, 2, \cdots), \quad (1)$$

where $\hat{\mu}_k^{t_0}(s)$ is the k-th eigenvalue of a Schrödinger operator over a bounded interval, and $\bar{\mu}_k(s)$ is the k-th eigenvalue a Schrödinger operator on $\mathbb{R}$. It is worth pointing out that the values or bounds of the involved eigenvalues are all computable by utilizing the recently developed methods for rigorous eigenvalue estimation [4].

The estimation for eigenvalues in (1) allows us to separate $\lambda_2(s,t)$ and $\lambda_3(s,t)$ for $t \in (0, t_0]$, confirming the simplicity of the second eigenvalue for nearly degenerate triangles.

Part 2 completes the proof by covering the case of non-degenerate triangles [3]:

Theorem 2. *The second Dirichlet eigenvalue is simple for every non-equilateral triangle with its minimum normalized height greater than or equal to* $\tan(\pi/60)/2$.

The methodology developed for this part provides a new way to stably compute eigenfunctions for clustered eigenvalues [5].

Acknowledgement

Both authors are supported by Japan Society for the Promotion of Science. The first author is supported by JSPS KAKENHI Grant Number JP24KJ1170. The last author is supported by JSPS KAKENHI Grant Numbers JP22H00512, JP24K00538, JP21H00998 and JPJSBP120237407.

References

[1] Henrot, A. Shape optimization and spectral theory. De Gruyter Open Poland (2017).

[2] Endo, R., Liu, X. The second Dirichlet eigenvalue is simple on every non-equilateral triangle Part I: Nearly degenerate triangles. Journal of Differential Equations 447, 113629 (2025).

[3] Endo, R., Liu, X. The Second Dirichlet Eigenvalue is Simple on Every Non-equilateral Triangle, Part II: Nearly Equilateral Triangle. arXiv:2305.14063 (2024).

[4] Liu, X. Guaranteed Computational Methods for Self-Adjoint Differential Eigenvalue Problems. Springer Nature (2024).

[5] Endo, R., Liu, X. Stable computation of Laplacian eigenfunctions corresponding to clustered eigenvalues. arXiv:2506.07340 (2025).

Tuesday, September 23, 2025

A01-0-006

11:00–12:30	**Regular Session B: Tools and Implementations**
11:00–11:30	Ryoga Iwanami: *Verry: an open-source package for verified computation written in Python 3*
11:30–12:00	Pierre Filiol, Luc Jaulin, Theotime Bollengier and Jean-Christophe Le Lann: *Hardware accelerated interval arithmetic for mobile robotics using RISC-V ISA extension*
12:00–12:30	Jiří Khun and Jan Schmidt: *Towards Interval Arithmetic in TensorFlow: A Comparison of Approaches*

Verry: an open-source package for verified computation written in Python 3

Ryoga Iwanami

Waseda University
Graduate School of Fundamental Science and Engineearing
3-4-1 Okubo, Shinjuku-ku, Tokyo, 169-8555, Japan
iwanami.ryoga@akane.waseda.jp

Keywords: delay differential equation, ordinary differential equation, Python

In this talk, we present an overview of *Verry* [1], a verified computation library written in Python 3. Verry aims to provide a comprehensive implementation of various rigorous numerical algorithms for ODEs (e.g., [2], [3], [5], and [6]) and DDEs. We have released solvers based on [2] and [3] at this time.

Since they solve the same problem, these algorithms have many common parts. We removed duplicate code by separating the algorithms into several routines. This separation also enables us to combine each routine depending on the problem.

Here is an overview of the separation. Assume that a symbol put brackets around, like $[x]$, always denotes an interval. Consider the initial value problem

$$\begin{cases} \mathrm{d}y/\mathrm{d}t = f(t,y) & \text{if } t \in (t_0, t_{\mathrm{bound}}), \\ y \in [y_0] & \text{if } t = t_0, \end{cases}$$

where $[y_0] \subseteq \mathbb{R}^N$ is a non-empty bounded interval, and $f(t,y)$ is a smooth function. A number of rigorous numerical algorithms for ODEs calculate the enclosure of the solution $y = \Phi(t, t_0, y_0)$ by the following iteration:

0. Initialize $k = 0$.
1. Set a coarse enclosure $[p_k^{\mathrm{c}}(h)]$ and verify that $\Phi(t_k + h, t_k, y_k) \in [p_k^{\mathrm{c}}(h)]$ holds for all $h \in [0, t_{k+1} - t_k]$ and $y_k \in [y_k]$, where t_{k+1} is predefined or adaptively determined. Then refine $[p_k^{\mathrm{c}}(h)]$ into the tight enclosure $[p_k(h)]$.
2. Calcurate $[y_{k+1}]$ such that $\Phi(t_{k+1}, t_0, y_0) \in [y_{k+1}]$ holds for all $y_0 \in [y_0]$.
3. Increment k; then go to step 1 unless t_k has reached t_{bound}.

Note that one may obtain $[y_{k+1}]$ by evaluating an expression $[p_k(t_{k+1} - t_k)]$ directly; however, due to the *wrapping effect* [4], it induces an explosion of $\mathrm{diam}[y_k]$.

We implemented separately steps 1 and 2 as abstract classes and showed the conditions that these subclasses must satisfy to cooperate with ODE solvers. For example, step 2 is implemented as an abstract class `Tracker`. The requirements that any `x` being an instance of `Tracker` must satisfy are as follows:

1. `x` corresponds to some pair (c, S), where $S \subseteq \mathbb{R}^N$ is star-shaped at c.

2. `x.sample()` returns c, and `x.hull()` returns an interval vector containing S.

3. Given $[A] \subseteq \mathbb{R}^{N\times N}$ and $[b] \subseteq \mathbb{R}^N$, `x.update(A, b)` updates (c, S) to (c', S') such that $A(y-c)+b \in S'$ holds for all $y \in S$, $A \in [A]$, and $b \in [b]$. Note that $F(S) \subseteq S'$ holds if $F \in C^1(\bar{S}, \mathbb{R}^N)$, $F(c) \in [b]$, and $\{DF(y) \mid y \in S\} \subseteq [A]$.

These properties enable `Tracker` to track the trajectory of a given discrete dynamical system $y_{n+1} = F_n(y_n)$ $(n = 0, 1, 2, \dots)$. Hence, we can compute step 2 by applying `Tracker` to the system $y_{n+1} = \Phi(t_{n+1}, t_n, y_n)$.

Verry can also solve boundary value problems via the shooting method, and delay differential equations via the method of steps. We will show some numerical experiments.

References

[1] R. Iwanami, *Verry*, https://python-verry.github.io/verry (13 June 2025).

[2] M. Kashiwagi, *Power series arithmetic and its application to numerical validation*, in Proceedings of the 1995 Symposium on Nonlinear Theory and its Applications, Las Vegas, NV, 1995, pp. 251–254.

[3] R. J. Lohner, *Enclosing the Solutions of Ordinary Initial and Boundary Value Problem*, in Computerarithmetic, E. Kaucher, U. Kulisch, and Ch. Ullrich, eds., B. G. Teubner, Stuttgart, 1987, pp. 225–286.

[4] R. J. Lohner, *On the ubiquity of the wrapping effect in the computation of error bounds*, in Perspectives on Enclosure Methods, U. W. Kulisch, R. J. Lohner, and A. Facius, eds., Springer-Verlag, Vienna, 2001, pp. 201–206.

[5] N. S. Nedialkov and K. R. Jackson, *An Interval Hermite–Obreschkoff Method for Computing Rigorous Bounds on the Solution of an Initial Value Problem for an Ordinary Differential Equation*, in Developments in Reliable Computing, T. Csendes, ed., Springer-Verlag, Dordrecht, 1999, pp. 289–310.

[6] M. Neher, K. R. Jackson, and N. S. Nedialkov, *On Taylor Model Based Integration of ODEs*, SIAM J. Numer. Anal., 45 (2007), pp. 236–262, doi:10.1137/050638448.

Hardware accelerated interval arithmetic for mobile robotics using RISC-V ISA extension

Pierre Filiol[1], Théotime Bollengier[1],
Luc Jaulin[1] and Jean-Christophe Le Lann[1]

[1] Labsticc, Ensta
29238 Brest Cedex 3 - France
{pierre.filiol, theotime.bollengier, luc.jaulin, lelannje}@ensta.fr

Keywords: Interval Arithmetics, RISC-V, Hardware Acceleration, Robotics

Introduction

A lot of recurring tasks encountered in robotics such as localization or robust control involve solving a set of equations and inequalities or find the optimal solution to a particular cost function. Interval analysis [1, 2] is an efficient numerical method to compute a guaranteed approximation of the solution set for such problems even in nonlinear cases (which is the norm in real-world applications). More precisely, elementary interval contractors can be used in combination with algorithms such as HC4-revise [4] to build more complex contractors and compute an inner and outer approximation of a solution set $\mathbb{S}$ for a particular constraint satisfaction problem.

The robotics community traditionally relies on a set of software libraries which implement the IEEE-1788 standard to various extents and provide the most-commonly used interval operators and contractors. The latter are then used as building blocks for more complex and specific problems. This paper advocates in favor of a novel approach which tackles interval arithmetic and contractor algebra directly at hardware level. The advantages of this strategy have been detailed in [5] and notably include the ability to implement efficient primitives where the trade-off between speed and precision can be adjusted to satisfy the need of embedded robotics without sacrificing the guarantees offered by interval analysis. The proposed acceleration is implemented as a RISC-V custom ISA extension called *xinterval* which provides hardware instructions for recurring elementary contractors and expose them in C language.

General Approach

In [3], we designed a RISC-V custom extension called *xinterval* which adds native support for IEEE-1788 interval arithmetic. The new hardware instructions correspond to the most commonly-used interval arithmetic operators and transcendental functions which can then be used to build portable elementary interval contractors. The integration in the RISC-V architecture is achieved by using the double precision floating-points registers to fit the interval model depicted in Figure 1. The implementation has been performed in VHDL and partially relies on the FloPoCo library for IEEE-754 algorithms.

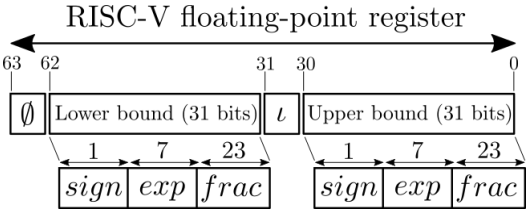

Figure 1: Interval representation in xinterval

In [6] we presented an iterative process to validate the *xinterval* architecture and measure the performance obtained on a FPGA device. This allows us to execute high-level robotics applications such as localization algorithms and compute fine-grained runtime metrics.

In the proposed paper, we compare the performances obtained on two textbook robotics localization algorithms (navigation in a field of landmarks and simple SLAM) for a traditional non-accelerated and a *xinterval*-based implementation. Our first results indicate speedup ranging from 3 to 10 depending of the complexity of the considered contractors.

Conclusion

This work proves the viability of interval arithmetic in hardware by providing a custom RISC-V extension prototype and a validation platform to execute standard robotic localization algorithms. The upcoming works involve refinement of our interval primitives to increase the potential speedups.

References

[1] R. E. Moore. *Interval Analysis. Printice-Hall, 1966.*

[2] R. Guyonneau, S. Lagrange, L. Hardouin and P. Lucidarme, Guaranteed Interval Analysis Localization for Mobile Robots. *Advanced Robotics*, 28(16), pp. 1067-–1077, 2014.

[3] P. Filiol. Efficient Hardware Primitives for Interval Contractors in Robotics and Integration to a Custom RISC-V ISA Extension. 23rd IEEE International NEWCAS Conference, June 22-25th, Paris, 2025.

[4] F. Benhamou, F. Goualard, L. Granvilliers, and J.F. Puget, Revising hull and box consistency. In Proceedings of the International Confer- ence on Logic Programming, pages 230–244, Las Cruces, NM, 1999. DOI: 10.7551/mitpress/4304.003.0024.

[5] P. Filiol, T. Bollengier, L. Jaulin and J.-C. Le Lann, "RISC-V Based Hardware Acceleration of Interval Contractor Primitives in the Context of Mobile Robotics", Acta Cybernetica, 26(4), pp. 889-912, 2024.

[6] P. Filiol, T. Bollengier, L. Jaulin and J.-C. Le Lann, "An Iterative Design and Validation Methodology for RISC-V Custom Extension", publication pending.

Towards Interval Arithmetic in TensorFlow: A Comparison of Approaches

Jiří Khun, Jan Schmidt

Department of Digital Design
Faculty of Information Technology
Czech Technical University in Prague
Thákurova 9, 160 00 Praha, Czech Republic
{jiri.khun|jan.schmidt}@fit.cvut.cz

Keywords: Interval arithmetic, constraint satisfaction problems, TensorFlow, IBEX, IEEE-1788, StableHLO, XLA, expression trees, parallelization, acceleration

Introduction

Interval arithmetic [4] is essential in many scientific and engineering fields, but its adoption is often hindered by computational complexity. Specialized software tools are commonly used to address this challenge.

Modern frameworks for deep learning offer efficient graph execution and support for multiple hardware backends. This raises the question of whether such infrastructure can also accelerate other classes of numerical computations, such as interval arithmetic, without developing specialized tools.

We would like to demonstrate that, with targeted modifications, the widely used deep learning framework TensorFlow [1] can serve as a fast and reliable platform for interval computations.

Our approach leverages TensorFlow's powerful infrastructure that can provide parallelization, optimization, and hardware acceleration. The work lays the foundation for further developments, including the application of TensorFlow to solving interval constraint satisfaction problems (CSPs) [2], which is one of our intended targets.

Background

A variety of frameworks enable reliable interval arithmetic (e.g., INTLAB, MPFI, C-XSC, IntervalArithmetic.jl), while advanced solvers such as IBEX [5] and CODAC offer comprehensive support for interval CSPs, contractor programming, and are widely used in engineering and validated numerics.

TensorFlow supports execution on CPUs, GPUs, and TPUs via device-specific kernels, the full graph-level optimization is achieved through the XLA compiler [6]. XLA fuses operations, applies advanced optimizations. The adoption of StableHLO, a hardware-independent IR, enables standardized model export and greater interoperability with compilers such as XLA and IREE, enhancing portability in machine learning workflows.

This raises the important question whether applications in other domains (such as CSP) require specialized implementations for each backend, or if a generic, IR-based approach can deliver sufficient efficiency across diverse hardware platforms.

Main results

We implemented and benchmarked three approaches for interval arithmetic in TensorFlow: (i) a native functional variant using tensor operations, (ii) an object-oriented approach (with ExtensionType), and (iii) custom C++ kernels via TensorFlow's plugin interface. All implementations leverage TensorFlow's graph execution for optimized performance, with all experiments performed on CPU.

Benchmarking on large expression trees demonstrated that the native approach, thanks to the XLA optimizer, consistently yields the fastest execution times, especially as the number of operations increases. The custom kernel approach is also efficient, benefiting from direct C++ execution, while the object-oriented variant incurs significant overhead from object construction and method dispatch.

For large expression graphs (tested up to 50,000 operations), the native TensorFlow implementation consistently achieved the fastest execution among the evaluated variants while maintaining IEEE-1788 [3] compliance. When compared to IBEX, a state-of-the-art interval solver, TensorFlow's graph-based execution outperforms the traditional "eager" evaluation in IBEX by two to three orders of magnitude for large graphs, and approaches the efficiency of IBEX's highly optimized compiled ("lazy") mode. These results demonstrate that modern machine learning frameworks can deliver scalable and competitive performance for interval arithmetic, provided they leverage graph compilation and optimization.

These results confirm that efficient, scalable interval computations can be achieved in TensorFlow with minimal modifications by leveraging graph compilation and optimization. This suggests that a generic IR-based approach can deliver sufficient performance without backend-specific implementations, opening new possibilities for advanced numerical methods in machine learning and scientific computing workflows.

References

[1] M. Abadi et al. TensorFlow: Large-Scale Machine Learning on Heterogeneous Distributed Systems. arXiv:1603.04467, 2015. `https://arxiv.org/abs/1603.04467`.

[2] F. Benhamou, W. J. Older, and A. Vellino. Constraint Logic Programming on Boolean, Integer and Real Intervals. *Journal of Symbolic Computation*, 1994.

[3] IEEE Standards Association. IEEE Standard for Interval Arithmetic. *IEEE Std 1788-2015*, 2015. `https://doi.org/10.1109/IEEESTD.2015.7140721`.

[4] R. E. Moore. On computing the range of a rational function of n variables over a bounded region. *Computing*, 16:1–15, 1976.

[5] J. Ninin and G. Chabert. Global Optimization Based on Contractor Programming: An Overview of the IBEX Library. In *MACIS 2015, LNCS 9582*, Springer, 2016. `https://doi.org/10.1007/978-3-319-32859-1_47`.

[6] TensorFlow Team. XLA Overview. `https://www.tensorflow.org/xla`, Accessed: 2024-06-02.

Towards Interval Arithmetic in TensorFlow: A Comparison of Approaches

Jiří Khun Jan Schmidt

Department of Digital Design
Faculty of Information Technology
Czech Technical University in Prague
Czech Republic

DEPARTMENT OF DIGITAL DESIGN

FACULTY OF INFORMATION TECHNOLOGY CTU IN PRAGUE

Motivation / Introduction

Interval arithmetic [4] is a key tool for handling uncertainty and ensuring reliable results in optimization, control, and validated numerics. Despite its importance, practical adoption is often hindered by **high computational cost** and the lack of efficient, parallel or hardware-accelerated implementations.

Existing frameworks (INTLAB, MPFI, C-XSC, IntervalArithmetic.jl) and solvers (IBEX [5], CODAC) offer solid functionality, but are mostly CPU-bound and would require dedicated GPU/TPU backends for scalable performance.

Meanwhile, modern ML frameworks like TensorFlow [1] provide **graph execution**, advanced compiler optimizations (XLA [6], IREE), and automatic acceleration on CPUs, GPUs, and TPUs. These capabilities can be leveraged to evaluate expression trees in interval arithmetic, which is a key step towards building efficient interval CSP solvers [2].

Question: Can TensorFlow, a mainstream ML framework, become an efficient platform for interval computations?

Our goal: Demonstrate scalable, efficient interval arithmetic in TensorFlow, with compatibility to IEEE-1788 [3], laying the foundation for future interval CSP solvers.

Approach

We explored three possible implementations of interval arithmetic in TensorFlow, all executed in **graph mode** with compiler optimizations (XLA/IREE):

- **Native (functional):** direct composition of interval operations from basic tensor ops; benefits most from XLA/IREE graph fusion, which also enables efficient outward rounding (IEEE-1788) with minimal performance overhead.
- **Composite (object-oriented):** based on `tf.experimental.ExtensionType`; simple API, but high Python overhead.
- **Custom kernels (C++ ops):** implemented via TensorFlow plugin API; efficient runtime, but higher development cost, compiled side-by-side with standard TF operations.

All implementations rely on **graph execution**, enabling optimization, parallelism, and hardware acceleration (CPU, GPU, TPU).

Results

We benchmarked expression trees up to 50,000 operations (CPU run, Intel Core i7-12700H, 64GB RAM).

TF variants: Native is consistently fastest (thanks to XLA fusion). Custom kernels are close in performance, but require more development effort. Composite suffers from Python overhead and does not scale as well.

Expression tree evaluation – TF variants

Operations	TF native	TF composite	TF custom
10	85.2 (2.0)	191.6 (8.8)	79.9 (4.4)
100	88.5 (5.3)	198.8 (10.9)	78.5 (3.8)
1000	86.1 (5.6)	226.4 (8.9)	84.4 (5.1)
5000	90.1 (5.1)	441.7 (36.9)	98.5 (5.1)
10000	91.1 (4.9)	955.9 (6.0)	114.3 (21.9)
25000	85.0 (2.3)	1094.2 (17.4)	96.9 (10.4)
50000	94.0 (3.6)	728.9 (34.7)	96.4 (2.0)

Mean execution times (μs) and standard deviations.

Performance remains stable even for large expression trees (50k ops), demonstrating scalability of the TensorFlow-based approaches.

Results (cont.)

The plot shows the increasing Python overhead for the composite type, while native stays flat and custom remains close.

Expression tree evaluation – TF variants

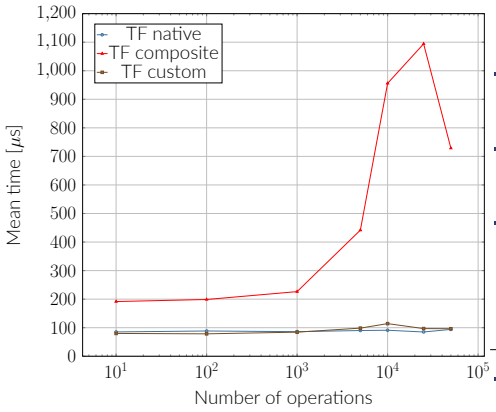

TF vs IBEX: We compared TF native against IBEX in eager and lazy modes to evaluate competitiveness with an established interval solver. IBEX in eager mode is among the fastest eager interval arithmetic frameworks, while IBEX in lazy (graph) mode is widely regarded as the state-of-the-art solver in terms of performance.

Expression tree evaluation – TF vs. IBEX

Operations	TF native	IBEX eager	IBEX lazy
10	85.2 (2.0)	15.1 (1.7)	4.1 (0.2)
100	88.5 (5.3)	112.6 (3.6)	3.9 (0.2)
1000	86.1 (5.6)	1113.9 (15.7)	4.5 (0.0)
5000	90.1 (5.1)	5533.8 (46.9)	5.1 (0.2)
10000	91.1 (4.9)	13033.6 (375.8)	4.8 (0.1)
25000	85.0 (2.3)	33789.4 (1939.1)	4.9 (0.7)
50000	94.0 (3.6)	74208.8 (893.7)	4.3 (0.1)

Mean execution times (μs) and standard deviations for TF native, IBEX eager, and IBEX lazy.

The plot shows IBEX eager slowing linearly with the number of operations, contrasted with the near-constant performance of TF native and IBEX lazy.

Expression tree evaluation – TF vs. IBEX

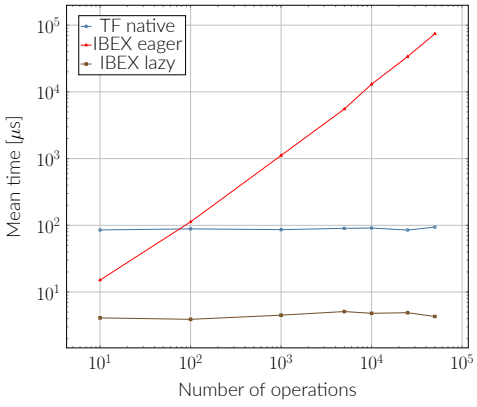

TF native outperforms IBEX eager by 2–3 orders of magnitude, and approaches IBEX lazy performance for large graphs, showing similar scalability without slowdown on larger instances. This demonstrates that ML frameworks can rival even the most efficient traditional solvers.

Key Insights / Discussion

- **Graph execution matters:** TF graph mode with XLA/IREE gives 2–3 orders of magnitude speedup over eager-style execution.
- **Native wins:** Functional TF native is fastest (despite the overhead of outward rounding); custom C++ ops are competitive, while composite suffers from Python overhead.
- **Scalability:** TF native scales comparably to IBEX lazy, remaining efficient even for large expression trees (50k+ ops).
- **Portability:** ML frameworks provide parallelism and CPU/GPU/TPU backends, unlike most traditional interval solvers.
- **Future integration:** StableHLO IR + XLA/IREE suggests portable pipelines for interval arithmetic solving and other use-cases (e.g., CSP).

Future Directions

- Extend from interval arithmetic to **interval CSP solving** (consistency, branching, backtracking).
- Integrate **automatic differentiation** for constraint propagation (potentially leveraging TensorFlow's built-in autodiff).
- Exploit **GPU/TPU acceleration** and distributed execution for larger problems.
- Build on **StableHLO IR** for portable pipelines across frameworks.
- Apply to domains such as **control, optimization, and formal verification**.

Conclusions

- TensorFlow graph execution enables efficient, IEEE-1788 compliant interval arithmetic.
- Native implementation is fastest; custom kernels are competitive; composite design suffers from Python overhead.
- TF native outperforms IBEX eager (the fastest among eager frameworks) by 2–3 orders of magnitude and scales comparably to IBEX lazy, the state-of-the-art graph-based approach.
- ML frameworks can provide a scalable foundation for interval arithmetic and validated numerics.

This opens a path to parallel, portable, high-performance interval computation and possibly interval CSP solvers on ML infrastructures.

References

[1] M. Abadi et al. *TensorFlow: Large-Scale Machine Learning on Heterogeneous Distributed Systems*. arXiv:1603.04467, 2015.

[2] F. Benhamou, W. J. Older, A. Vellino. Constraint Logic Programming on Boolean, Integer and Real Intervals. *J. Symb. Comput.*, 1994.

[3] IEEE Standards Association. *IEEE Standard for Interval Arithmetic*. IEEE Std 1788-2015, 2015.

[4] R. E. Moore. On computing the range of a rational function of n variables over a bounded region. *Computing*, 16:1–15, 1976.

[5] J. Ninin, G. Chabert. Global Optimization Based on Contractor Programming: An Overview of the IBEX Library. In *MACIS 2015*, LNCS 9582, Springer, 2016.

[6] TensorFlow Team. *XLA Overview*. `https://www.tensorflow.org/xla`, accessed 2024-06-02.

ORCID: 0000-0002-0524-1503

SCAN 2025, Oldenburg, Germany

jiri.khun@fit.cvut.cz

Wednesday, September 24, 2025

Library Auditorium

9:00–10:30	**Plenary Lecture** Andreas Rauh: *Interval and Set-Based Approaches for Control and State Estimation: Their Use for Offline and Online Purposes*
10:30–11:00	Coffee Break
11:00–12:30	**Regular Session A: PDEs**
11:00–11:30	Kazuaki Tanaka, Ryoga Iwanami, Kaname Matsue and Hiroyuki Ochiai: *Green-Representable Solutions: Reformulating Sub- and Super-solution Theory for Poisson's Equation*
11:30–12:00	Taisei Asai, Kazuaki Tanaka, Satoshi Tanaka and Shin'Ichi Oishi: *Verified Computation of All Positive Solutions to a Hénon-Type Boundary Value Problem*
12:00–12:30	Akitoshi Takayasu and Jean-Philippe Lessard: *Semigroup approach for validating solutions to semilinear parabolic PDEs*
12:30–14:00	Lunch Break – Food truck
14:00–21:30	**Social Program – Trip to Bad Zwischenahn and Dinner**

Interval and Set-Based Approaches for Control and State Estimation: Their Use for Offline and Online Purposes

Andreas Rauh

Carl von Ossietzky Universität Oldenburg
Distributed Control in Interconnected Systems
D-26111 Oldenburg, Germany
andreas.rauh@uni-oldenburg.de

Keywords: Interval methods, Set-based state estimation, Robust control, Optimization under uncertainty, Neural networks, Fuel cells

Introduction

Control and state estimation procedures need to be robust against imprecisely known parameters, uncertainty in initial conditions, and external disturbances. Interval methods and other set-based techniques form the basis for the implementation of powerful approaches that can be used to identify parameters of dynamic system models in the presence of the aforementioned uncertainties. Moreover, they are applicable to a verified feasibility and stability analysis of controllers and state estimators [1,3,7].

In addition to offline approaches for analysis, interval and set-based methods have also been developed in recent years which are allow to solve the associated design tasks and to implement reliable techniques that are applicable online. The latter approaches include online parameter adaptation techniques for nonlinear variable-structure controllers, interval observers, and fault diagnosis techniques [3,4,5,7]. In this talk, an overview of the methodological background will be presented, together with a review of practical applications for which interval and set-valued approaches have been employed successfully.

Modeling, Parameter Identification, and Verified State Estimation

Although, for example, many dynamic system models in (control) engineering, especially in the frame of thermo-fluidic applications, are described after a first-principle modeling by state equations that have certain monotonicity properties, other applications in the domain of mechanics as well as for electro-chemical energy storage may require specific changes of coordinates to obtain these properties. In the domains of parameter identification as well as state and disturbance estimation, the most important monotonicity property that allows for a simplification of the aforementioned tasks is the cooperativity of the state equations. As far as the application domains mentioned above are concerned, these properties originate from the conservation of mass or energy [4].

In such cases, a decoupling of lower and upper bounding systems — that enclose all possible state trajectories — can be obtained. This property does not only

allow for the simplification of the task of parameter identification but also for the implementation of real-time capable state estimation procedures.

For systems with periodically recurring trajectories (and also disturbance profiles), recent investigations have shown that the corresponding procedures can also be extended to a learning-type technique. This technique especially allows for enhancing the bounds of estimated state trajectories in each successive execution of the same task and exploits a formulation that uses the iteration counter as a second independent dimension in addition to time [2].

Verified Control Implementation and Robust Model-Predictive Control

On the basis of the set-based state estimates described in the previous section, real-time capable robust control implementations can be derived that prevent the violation of state constraints with certainty. Moreover, it is possible to implement robust predictive control laws in a similar manner. For the case of a nonlinear state feedback, interval extensions of sliding mode and backstepping control approaches have been published which allow for a guaranteed stabilization of the system dynamics and for a guaranteed prevention of overshooting certain thresholds for the state variables under constraints on the inputs and their respective variation rates. A practical application of this technique is the temperature control of a solid oxide fuel cell stack [3,7].

For the second class of controllers, a novel combination of set-based and neural network modeling was recently developed and integrated into a sensitivity-based predictive control scheme that maximizes the degree of fuel utilization of a fuel cell. The approach can be implemented for time-varying desired electric power profiles so that operating points stay within the region of Ohmic polarization, which is crucial for preventing accelerated aging of the fuel cell stack [5].

Combination of Set-Based and Stochastic Uncertainty Representations

In the final part of this talk, a combination of stochastic and set-based (in this case, ellipsoidal) uncertainty representations will be considered. This approach allows, on the one hand, for a rigorous quantification of predefined confidence levels in stochastic state estimation procedures. On the other hand, it allows for handling nonlinearities in such a way that the previously mentioned tolerance bounds are definitely not determined in an overly optimistic manner [6].

References

[1] E. Auer, L. Senkel, S. Kiel and A Rauh, Control-Oriented Models for SO Fuel Cells from the Angle of V&V: Analysis, Simplification Possibilities, Performance, *Algorithms*, 10, 140, 2017.

[2] T. Chevet, A. Rauh, T.N. Dinh, J. Marzat, T. Raïssi, Robust Interval Observer for Systems Described by the Fornasini-Marchesini Second Model, *IEEE Control Systems Letters*, 6, 1940–1945, 2021.

[3] N. Cont, W. Frenkel, J. Kersten, A. Rauh and H. Aschemann, Interval-Based Modeling of High-Temperature Fuel Cells for a Real-Time Control Implementation Under State Constraints, *IFAC-PapersOnLine*, 53, 12542–12547, 2020.

[4] S. Ifqir, A. Rauh, J. Kersten, D. Ichalal, N. Ait-Oufroukh and S. Mammar. *Interval Observer-Based Controller Design for Systems with State Constraints: Application to Solid Oxide Fuel Cells Stacks*, Proceedings of the Intl. Conf. on Methods and Models in Automation and Robotics, MMAR 2019, Miedzyzdroje, Poland.

[5] A. Rauh and E. Auer, *Comparison of Stochastic and Interval-Based Modeling Approaches for the Online Optimization of the Fuel Efficiency of SOFC Systems*, Proceedings of the 9th Intl. Conf. on Systems and Control (ICSC), 2021, Caen, France.

[6] A. Rauh, T. Chevet, T.N. Dinh, J. Marzat, T. Raïssi, *Robust Iterative Learning Observers Based on a Combination of Stochastic Estimation Schemes and Ellipsoidal Calculus*, Proceedings of the 25th Intl. Conf. on Information Fusion (FUSION), 2022, Linköping, Sweden.

[7] A. Rauh, L. Senkel and H. Aschemann, Interval-Based Sliding Mode Control Design for Solid Oxide Fuel Cells With State and Actuator Constraints, *IEEE Transactions on Industrial Electronics*, 62(8), 5208–5217, 2015.

Green-Representable Solutions: Reformulating Sub- and Super-solution Theory for Poisson's Equation

Kazuaki Tanaka[1], Ryoga Iwanami[1], Kaname Matsue[2] and Hiroyuki Ochiai[2]

[1] Waseda University, Tokyo, Japan
tanaka@ims.sci.waseda.ac.jp, iwanami.ryoga@akane.waseda.jp
[2] Kyushu University, Fukuoka, Japan
{kmatsue, ochiai}@imi.kyushu-u.ac.jp

Keywords: Poisson's equation, Green's function, Fundamental solution, Sub- and Super-solutions, Solution enclosure, Corner singularities

Introduction

We consider the weak solution $u \in H_0^1(\Omega)$ of the following boundary value problem

$$\begin{cases} -\Delta u = f & \text{in } \Omega, \\ u = 0 & \text{on } \partial\Omega, \end{cases} \tag{1}$$

where $\Omega \subset \mathbb{R}^N$ $(N > 1)$ is a bounded polytopic domain, and f is a given function that satisfies $f \in L^1(\Omega)$ for $N = 1$ and $f \in L^p(\Omega)$ for some $p > N/2$ when $N \geq 2$. The motivation of this research is to find upper and lower solutions that enclose the exact solution of this problem. However, with traditional definitions of upper and lower solutions, smoothness of functions is implicitly required, which made it impossible to represent upper and lower solutions using piecewise linear functions. To overcome this challenge, it is necessary to relax the conditions that upper and lower solutions must satisfy.

Green-Representable Solutions

We introduce a new framework based on fundamental solutions. For an evaluation point $s_{\mathrm{int}} \in \Omega$, we construct test functions of the form

$$\phi_{s_{\mathrm{int}}}(x) := a_{\mathrm{int}}\Gamma(s_{\mathrm{int}}, x) + H_{s_{\mathrm{int}}}(x), \tag{2}$$

where Γ is the fundamental solution satisfying $-\Delta\Gamma(s, x) = \delta(x - s)$, with explicit forms depending on dimension. a_{int} is a non-zero coefficient, and $H_{s_{\mathrm{int}}}$ is harmonic in some domain containing $\overline{\Omega}$.

Definition 1 (Local Green-representability)**.** *A solution $u \in H_0^1(\Omega)$ of the problem* (1) *is said to be Green-representable with respect to $\phi_{s_{\mathrm{int}}}$ (or simply $\phi_{s_{\mathrm{int}}}$-Green-representable for short) if, for a fixed s_{int}, there exists a test function $\phi_{s_{\mathrm{int}}}$ of the form above such that*

$$a_{\mathrm{int}}u(s_{\mathrm{int}}) = \langle f, \phi_{s_{\mathrm{int}}} \rangle + \int_{\partial\Omega} \frac{\partial u}{\partial n}\phi_{s_{\mathrm{int}}} d\gamma. \tag{3}$$

Definition 2 (Global Green-representability)**.** *A solution u of the problem* (1) *is said to be Green-representable with respect to mapping $\Phi : s_{\text{int}} \mapsto \phi_{s_{\text{int}}}$ (or simply Φ-Green-representable for short) if u possesses the regularity $u \in H_0^1(\Omega) \cap W^{1,q}(\Omega)$ for some $q > N$, and there exists a mapping Φ that assigns to each point $s_{\text{int}} \in \Omega$ a test function $\phi_{s_{\text{int}}}$ such that u is $\phi_{s_{\text{int}}}$-Green-representable.*

The following is our main theorem and its corollary for two-dimensional polygonal domains.

Theorem 1 (Main Theorem)**.** *Let $\Omega \subset \mathbb{R}^N$ ($N > 1$) be a bounded N-dimensional polytopic domain and let $f \in L^p(\Omega)$ with $p > N/2$. Then, a solution $u \in H_0^1(\Omega)$ of the problem* (1) *is locally Green-representable with respect to any fixed evaluation point in Ω.*

Corollary 1. *Let $\Omega \subset \mathbb{R}^2$ be a bounded polygonal domain (possibly non-convex) and let $f \in L^p(\Omega)$ with $p > 1$. Then a solution $u \in H_0^1(\Omega)$ of the problem* (1) *is globally Green-representable with respect to any mapping Φ constructed using fundamental solutions.*

Generalized Sub- and Super-Solutions

Building on this representability, we define generalized sub- and super-solutions:

Definition 3 (Green-representable super-solution)**.** *A function $\overline{u} \in W^{1,q}(\Omega)$ ($q > N$) is a Green-representable super-solution if there exists a nonnegative constant c and a mapping $\Phi : s_{\text{int}} \mapsto \phi_{s_{\text{int}}}$ such that*

$$\langle \nabla \overline{u}, \nabla \phi_{s_{\text{int}}} \rangle \geq \langle f, \phi_{s_{\text{int}}} \rangle + c \int_{\partial\Omega} \frac{\partial \phi_{s_{\text{int}}}}{\partial n} d\gamma \tag{4}$$

and

$$\overline{u} - c \geq 0 \quad \text{on } \partial\Omega. \tag{5}$$

A corresponding definition applies to sub-solutions by reversing the inequalities. This generalization allows piecewise linear functions to serve as sub- and super-solutions—a capability not available in the classical framework.

Theorem 2 (Comparison)**.** *Let u be a Green-representable solution with respect to mapping Φ, and assume that for all s_{int}, we have $\frac{\partial \phi_{s_{\text{int}}}}{\partial n} \leq 0$ on $\partial\Omega$. Let $\overline{u}$ and $\underline{u}$ be a Green-representable sub-solution and super-solution, respectively, with respect to the same mapping Φ. Then,*

$$\underline{u} - \gamma_{s_{\text{int}}} \leq u \leq \overline{u} + \gamma_{s_{\text{int}}} \quad \text{in } \Omega, \tag{6}$$

where $\gamma_{s_{\text{int}}} := \frac{1}{a_{\text{int}}} \int_{\partial\Omega} \frac{\partial u}{\partial n} \phi_{s_{\text{int}}} d\gamma$.

In the talk, we will present numerical examples in one and two dimensions. In particular, for two-dimensional cases, we demonstrate pointwise evaluations in non-convex domains where the solution lacks sufficient regularity.

Verified Computation of All Positive Solutions to a Hénon-Type Boundary Value Problem

Taisei Asai[1], Kazuaki Tanaka[2], Satoshi Tanaka[3] and Shin'ichi Oishi[4]

[1] Faculty of Science and Engineering, Waseda University
3-4-1 Okubo, Shinjuku, Tokyo 169-8555, Japan
captino@fuji.waseda.jp
[2] Global Center for Science and Engineering, Waseda University
3-4-1 Okubo, Shinjuku, Tokyo 169-8555, Japan
tanaka@ims.sci.waseda.ac.jp
[3] Mathematical Institute, Tohoku University
Aoba 6-3, Aramaki, Aoba-ku, Sendai 980-8578, Japan
satoshi.tanaka.d4@tohoku.ac.jp
[4] Faculty of Science and Engineering, Waseda University
3-4-1 Okubo, Shinjuku, Tokyo 169-8555, Japan
oishi@waseda.jp

Keywords: Verified numerical computation, All-solution search, Bifurcation analysis, Hénon-type equation

We consider the Hénon-type equation, which is a two-point boundary value problem:

$$\begin{cases} -u'' = (|x|^l + \lambda)u^p, \quad x \in (-1,1), \\ u(-1) = u(1) = 0, \end{cases} \tag{1}$$

where the parameters l and λ satisfy $l \geq 0$ and $\lambda \geq 0$, and the exponent p satisfies $p > 1$. In this context, an "even solution" refers to a function u that is both a solution of (1) and an even function, satisfying $u(-x) = u(x)$ for all $x \in (-1,1)$.

The case $\lambda = 0$ corresponds to the one-dimensional Hénon equation $-u'' = |x|^l u^p$, and problem (1) was introduced in [1] as part of a study on the symmetry of its solutions. In recent years, the Hénon-type equation has attracted attention due to the possibility of possessing more multiple solutions than the original Hénon equation, and the bifurcation structure of such solutions has been the subject of active research.

According to the study [2], for fixed $p > 1$, the uniqueness of positive even solutions holds on most of the first quadrant $(l, \lambda) \subset \mathbb{R}^2$, and only a very narrow region remains as a candidate for the existence of multiple positive even solutions. However, while sufficient conditions for multiple solutions have been studied, the overall bifurcation structure—including the precise branching points—has not been fully understood.

In this study, we rigorously determined the number of positive solutions of (1), including both even and non-even ones. The all-solution search is a method for rigorously identifying all solutions of a differential equation within a given parameter range. However, a fundamental difficulty in implementing this method arises from the fact that the set of parameters used to determine solutions (e.g., initial values) is non-compact. For example, to find all solutions of problem (1), one would, in principle,

need to explore the infinite range $-\infty < u'(-1) < \infty$, which is computationally infeasible.

To overcome this difficulty, we first established a priori estimates of the solutions. Proposition 1 gives an upper bound on the maximum value $\|u\|_\infty$ of any positive solution, while Propositions 2 and 3 provide explicit upper and lower bounds on the initial condition $u'(-1)$, thereby reducing the search domain to a compact set.

Based on these theoretical results, we constructed the initial value domain depending on the type of solution. For even solutions, we fixed $u'(0) = 0$ and varied $u(0)$ within the bound given by Proposition 1. For general positive solutions (including non-even ones), we fixed $u(-1) = 0$ and varied $u'(-1)$ within the bounds specified in Propositions 2 and 3. Here again, the upper bound from Proposition 1 plays a key role in computation: if the value of the function exceeds this bound during the numerical process, the trajectory can immediately be ruled out as a solution to (1), saving unnecessary computations.

Using these settings, we carried out an efficient and exhaustive numerical search with the kv library [3].

Here, $\mathrm{B}(x, y) := \int_0^1 t^{x-1}(1-t)^{y-1}dt$ denotes the beta function.

Proposition 1. *Let u be a positive solution of (1) with $l \geq 0$, $\lambda \geq 0$, and $p > 1$. Then*

$$\|u\|_\infty \leq 2\left(\mathrm{B}(l+1, p+2) + \frac{\lambda}{p+2}\right)^{-\frac{1}{p-1}}.$$

Proposition 2. *Let u be a positive solution of (1) with $l \geq 0$, $\lambda \geq 0$, and $p > 1$. Then*

$$u'(-1) \geq \frac{1}{2}\left(B(l+1, 2) + \frac{\lambda}{2}\right)^{-\frac{1}{p-1}} = \frac{1}{2}\left(\frac{1}{(l+1)(l+2)} + \frac{\lambda}{2}\right)^{-\frac{1}{p-1}}.$$

Proposition 3. *Let u be a positive solution of (1) with $l \geq 0$, $\lambda \geq 0$, and $p > 1$. Then*

$$u'(-1) \leq \sqrt{\frac{2(1+\lambda)}{p+1}} \cdot 2^{\frac{p+1}{2}} \left(\mathrm{B}(l+1, p+2) + \frac{\lambda}{p+2}\right)^{-\frac{p+1}{2(p-1)}}.$$

Acknowledgement

This work was supported by JSPS KAKENHI Grant Numbers JP23K19016, JP25K17304.

References

[1] S. Tanaka: Morse index and symmetry–breaking for positive solutions of one–dimensional Hénon type equations, *Journal of Differential Equations*, 255:7 (2013), 1709–1733.

[2] N. Shioji, S. Tanaka, K. Watanabe: Multiple existence of positive even solutions for a two point boundary value problem on some very narrow possible parameter set, *Journal of Mathematical Analysis and Applications*, 513:1 (2022), 126182.

[3] M. Kashiwagi: kv library, (2025). `http://verifiedby.me/kv/`

Semigroup approach for validating solutions to semilinear parabolic PDEs

Akitoshi Takayasu[1] and Jean-Philippe Lessard[2]

[1] University of Tsukuba
Institute of Systems and Information Engineering
1-1-1 Tennodai, Tsukuba, Ibaraki 305-8573, Japan
takitoshi@risk.tsukuba.ac.jp

[2] McGill University
Department of Mathematics and Statistics
805 Sherbrooke West, Montreal, QC, H3A 0B9, Canada
jp.lessard@mcgill.ca

Keywords: Semilinear parabolic PDEs, Initial value problems, Spectral methods, Semigroup theory, Computer-assisted proofs

Introduction and contributions

Recent advances in computer-assisted proofs for dynamical systems have been driven primarily by progress in the study of the global dynamics of infinite-dimensional problems, such as the rigorous construction of invariant objects, forward integration of time-dependent partial differential equations (PDEs), and the validation of connections between equilibria. In particular, solving the initial value problem (IVP) for PDEs has emerged as a central topic in this field. Over the past decades, several standard methodologies for rigorously integrating IVPs have been established, including the *fully spectral approach* [1], the *autonomous semigroup approach* [2], and the *non-autonomous semigroup approach* [3].

In this talk, we present our recent advances in the non-autonomous semigroup approach for semilinear parabolic PDEs, focusing on the validation of long-time existence of solutions and their asymptotic behavior. More precisely, we consider a class of IVP of the general form

$$\begin{cases} u_t = (\lambda_0 + \lambda_1\Delta + \lambda_2\Delta^2)u + \Delta^p N(u), & t > 0, \quad x \in \Omega, \\ u(0,x) = u_0(x), & x \in \Omega, \end{cases}$$

where $p \in \{0,1\}$, N is a polynomial satisfying both $N(0) = 0$ and its Fréchet derivative $DN(0) = 0$, $u_0(x)$ is a given initial data. The parameters λ_0, λ_1, λ_2 are chosen so that the PDE is parabolic. The assumption of the PDE being semilinear implies that the degree p of the Laplacian in front of the nonlinear term N is less than the one of the differential linear operator $\lambda_0 + \lambda_1\Delta + \lambda_2\Delta^2$. This form of PDEs covers wide variety of PDEs, such as the nonlinear heat, the Swift–Hohenberg, Cahn–Hilliard, Ohta–Kawasaki, phase-field-crystal (PFC), and Navier–Stokes, etc.

Our approach reformulates the IVP as a zero-finding problem in a Banach space of time-dependent Fourier coefficients. A Newton-like operator is explicitly constructed

using the linearized *evolution operator* derived from semigroup theory. The inverse of the Fréchet derivative is realized by the variation-of-constants formula, for which we develop rigorous numerical bounds using a decomposition into finite and infinite Fourier modes. A key feature of our approach is the explicit control of the evolution operator, which allows us to validate contraction properties of the Newton-like operator and thus prove the existence and local uniqueness of solutions in a neighborhood of numerical approximations.

Furthermore, we extend this approach to a multi-step framework, enabling rigorous forward integration over long time intervals. In other words, this development relates to the challenge of efficiently controlling the *wrapping effect* in infinite-dimensional problems, which is an essential problem in the field of interval analysis. By using the semigroup property, we rigorously control the evolution operator over multiple time intervals and thereby validate the contraction property of the Newton-like operator over long time. This leads to more efficient rigorous integration of IVPs. In the talk, we demonstrate the effectiveness of this improved approach using the Swift–Hohenberg equation and the Ohta–Kawasaki equation, the latter of which includes derivatives in the nonlinear term.

Finally, we discuss the parallelizability of the method, which makes it computationally efficient for high-dimensional systems. The non-autonomous semigroup-based rigorous integrator thus provides a unified and feasible framework for studying long-time dynamics of evolutionary PDEs through validated numerics.

Acknowledgement

AT is partially supported by the Top Runners in Strategy of Transborder Advanced Researches (TRiSTAR) program conducted as the Strategic Professional Development Program for Young Researchers by the MEXT and JSPS KAKENHI Grant Numbers 25K00922, 24K00538, and 22K03411.

References

[1] M. Cadiot, J.-P. Lessard. Recent advances about the rigorous integration of parabolic PDEs via fully spectral Fourier-Chebyshev expansions. arXiv:2502.20644 [math.AP], 2025.

[2] J. B. van den Berg, M. Breden, R. Sheombarsing. Validated integration of semilinear parabolic PDEs. *Numerische Mathematik*, 156:1219–1287, 2024.

[3] G. W. Duchesne, J.-P. Lessard, A. Takayasu. A Rigorous Integrator and Global Existence for Higher-Dimensional Semilinear Parabolic PDEs via Semigroup Theory. *Journal of Scientific Computing*, 102:62, 2025.

Wednesday, September 24, 2025

A01-0-006

11:00–12:30	**Regular Session B: Uncertainty Quantification**
11:00–11:30	Olga Kosheleva and Vladik Kreinovich: *For statistical analysis of big data, interval uncertainty is needed*
11:30–12:00	Jahangir Alam, Ismail Hossain, Tausif Hossain, Md Nuruzzaman Sojib, Olga Kosheleva and Vladik Kreinovich: *How to compare situations in which we measure different quantities with different uncertainty*
12:00–12:30	Ekaterina Auer and Wolfram Luther: *Towards Fair and Explainable Medical Risk Prediction Software via Dempster-Shafer Theory*

For statistical analysis of big data, interval uncertainty is needed

Olga Kosheleva[1] and Vladik Kreinovich[2]

[1]Department of Teacher Education, University of Texas at El Paso
El Paso, TX 79968, USA, olgak@utep.edu
[2]Department of Computer Science, University of Texas at El Paso
El Paso, TX 79968, USA, vladik@utep.edu

Keywords: Statistical analysis, Big Data, Macronumerosity, Interval Uncertainty

Formulation of the problem

A usual statistical approach to processing data $x_1, \ldots, x_n$ is to come up with a model – e.g., based on the training part of the data – and then test whether this model adequately describes the remaining testing part of the data.

For example, if it turns out that the observations are consistent with a normal distribution with mean m and standard deviation σ, then we can use the chi-square criterion and check whether we have

$$\chi^2_{n,1-\alpha} \le \sum_{i=1}^{n} \frac{(x_i - m)^2}{\sigma^2} \le \chi^2_{n,\alpha}$$

for appropriate values $\chi^2_{n,1-\alpha}$ and $\chi^2_{n,\alpha}$.

These tests are designed in such a way that:

- when the actual distributions is the assumed one, this test returns "true" with frequency close to 1, while
- when the actual distribution is different from the assumed one, for sufficiently large n – above a certain threshold n_0 – the corresponding test fails with frequency close to 1.

This traditional statistical approach has worked successfully for more than a century. However, with the emergence of big data, when we have millions and even billions of data points, this traditional statistical approach often fails. The reason for this failure is clear (see, e.g., [1, 2]): in most applications areas – e.g., in econometrics – all statistical models are approximate. When n was reasonably small, much smaller than the threshold value n_0, the tests still worked. However, big data often means $n > n_0$, so the tests fail. As a result, either we cannot find a model that fits the training data, or, if such a model is found, we cannot show that it fits the testing data. This phenomenon is known as *macronumerosity*.

This is well-known problem in many application areas – e.g., in modeling climate change.

Intervals form a natural solution

That the model is approximate means that there are some close values $\widetilde{x}_i \approx x_i$ that fit this model. A typical statistical idea would be to find the distribution for the approximation error $\Delta x_i \stackrel{\text{def}}{=} \widetilde{x}_i - x_i$, but in this case, we would still assume some exact distribution for x_i, so this brings us back to the same problem.

From the interval viewpoint, a natural solution out of this seemingly vicious circle is not to assume any specific distribution for Δx_i, but instead to use interval uncertainty, i.e., to assume that all the values Δx_i are within an interval $[-\Delta, \Delta]$. In this case, for each model and each corresponding test $C(x_1, \ldots, x_n) \le C_0$ that is not satisfied for the actual data, we can describe the degree to which data fits the model by the smallest Δ for which some Δ-close values $\widetilde{x}_i$ satisfy the test. Usually, the values Δx_i are small, so we can ignore terms quadratic in Δx_i; in this linear approximation, we have:

$$\Delta = \frac{|f(x_1, \ldots, x_n) - C|}{\sum\limits_{i=1}^{n} |C_{,i}|},$$

where $C_{,i}$ are partial derivatives of C with respect to x_i.

Then, e.g., between two models with the same number of parameters, we can select the model with the smallest Δ.

References

[1] A. Nichols and M. E. Schaffer, "Practical steps to improve specification testing", In: N. N. Thach, D. T. Ha, N. D. Trung, and V. Kreinovich (eds.), *Prediction and Causality in Econometrics and Related Topics*, Springer, Cham, Switzerland, 2022, pp. 75–88.

[2] M. E. Schaffer, "Null hypothesis misspecification testing revisited: how (not) to test orthogonality conditions", In: V. Kreinovich, W. Yamaka, and S. Leurcharusmee (eds.), *Data Science for Econometrics and Related Topics*, Springer, Cham, Switzerland, to appear.

How to compare situations in which we measure different quantities with different uncertainty

Jahangir Alam[1], Ismail Hossain[1],
Tausif Hossain[1], Md Nuruzzaman Sojib[1],
Olga Kosheleva[2], and Vladik Kreinovich[1]

[1]Department of Computer Science
University of Texas at El Paso, El Paso, TX 79968, USA
malam10@miners.utep.edu, ihossain@miners.utep.edu,
mhossain15@miners.utep.edu, msojib@miners.utep.edu,
vladik@utep.edu
[2] Department of Teacher Education, University of Texas at El Paso
El Paso, TX 79968, USA, olgak@utep.edu

Keywords: Measurements, Interval uncertainty, Mission to the unknown

Formulation of the problem

In many practical situations, we need to design a device for measuring several quantities – e.g., a device to send on a space mission. Often, this is largely a mission to the unknown – we do not know a priori which measurements will be more important.

In the ideal world, we should measure each of the quantities of interest with maximum accuracy. However, in practice, there are limits on the size and weight of the device, so our options are limited. Under such restrictions, we may have different possible sets of accuracies $a = (a_1, \ldots, a_n)$ for measuring the desired n quantities.

Which options should we select?

Let us formulate this problem in precise terms

To select the best option, we need to describe the relation "better of or the same quality" – which we will denote by $a \succeq b$. This relation should be reflexive ($a \succeq a$) and transitive (if $a \succeq b$ and $b \succeq c$, then $a \succeq c$). Of course, if all measurement are more accurate, i.e., if $a_i \le b_i$ for all i, then we should have $a \succeq b$ – and if also $a_i < b_i$ for some i, we should have $b \not\succeq a$.

Since we do not know which quantity is more important, the relation should not change if we swap some quantities. In precise terms, for each permutation π, if $a \succeq b$, then we should have $\pi(a) \succeq \pi(b)$. Finally, the selection should not depend on what measuring unit we use for each quantity: e.g., for measuring length, we can use meters or centimeters. If we switch to a unit which is λ_i times smaller, all numerical values are multiplied by λ_i. Thus, for each tuple $\lambda = (\lambda_1, \ldots, \lambda_n)$, if $(a_1, \ldots, a_n) \succeq (b_1, \ldots, b_n)$, then we should have $(\lambda_1 \cdot a_1, \ldots, \lambda_n \cdot a_n) \succeq (\lambda_1 \cdot b_1, \ldots, \lambda_n \cdot b_n)$. This is known as *scale-invariance.*

Our result: formulation

It turns out that for permutation-invariant and scale-invariant relations, $a \succeq b$ is equivalent to $a_1 \cdot \ldots \cdot a_n \le b_1 \cdot \ldots \cdot b_n$.

Our result: meaning

This result has the following natural interpretation. If we start with some area of values of size $X = X_1 \times \ldots \times X_n$, then we have X_1/a_1 possible different measured values of x_1, etc., with the total of $N = (X_1/a_1) \cdot \ldots \cdot (X_n/a_n)$ combinations. Here, $N = X/(a_1 \cdot \ldots \cdot a_n)$. So, the smaller the product of a_i's, the more alternatives we get and thus, the more information we gain about the studied object.

Proof

For $n = 2$, for all a_1 and a_2, due to permutation-invariance, we have $(\sqrt{a_1}, \sqrt{a_2}) \sim (\sqrt{a_2}, \sqrt{a_1})$, where $a \sim b$ means $a \succeq b$ and $b \succeq a$. For $\lambda_1 = \sqrt{a_1}$ and $\lambda_2 = \sqrt{a_2}$, scale-invariance implies that $(a_1, a_2) \sim (\sqrt{a_1 \cdot a_2}, \sqrt{a_1 \cdot a_2})$. So, by transitivity, if the two options have the same product $a_1 \cdot a_2$, they are equivalent.

For $n > 2$, we can similarly prove that if we replace two values a_i and a_{i+1} with another two values with the same product, the options remain equivalent. Thus, if we start with any option $a = (a_1, \ldots, a_n)$ with $s \stackrel{\text{def}}{=} \sqrt[n]{a_1 \cdot \ldots \cdot a_n}$, then we first replace a_1 and a_2 with s and $(a_1 \cdot s_2)/s$. Then, for each k, once we have an equivalent option $(s, \ldots, s, a'_{k+1}, a'_{k+2}, \ldots, a'_n)$, we replace a'_{k+1} and a'_{k+2} with s and $(a'_{k+1} \cdot a'_{k+2})/s$, etc. At the end, we will be able to conclude that the original option a is equivalent to $(s, \ldots, s)$. For such options, the smaller s, the better – and if s is smaller, then s^n is also smaller.

Thus, the relative quality of different options is indeed determined by the product s^n of their accuracies: the smaller this product, the better.

Towards Fair and Explainable Medical Risk Prediction Software via Dempster-Shafer Theory

Ekaterina Auer[1] and Wolfram Luther[2]

[1] University of Applied Sciences Wismar,
Department of Electrical Engineering and Computer Science,
D-23966 Wismar, Germany
ekaterina.auer@hs-wismar.de
[2] University of Duisburg-Essen
Computer Science/AI
D-47057 Duisburg, Germany
wolfram.luther@uni-due.de

Keywords: Algorithmic Fairness, Explainability, Dempster-Shafer Theory, Interval Methods

Fairness in software is a dynamic, interdisciplinary field that is evolving rapidly and has significant implications across many areas of modern life. It plays a critical role in such varied domains as law (e.g., for assessing the risk of criminal re-offense), finance (e.g., for evaluating creditworthiness), engineering (e.g., for autonomous vehicle decision-making), medicine (e.g., predicting cancer risk), and even social media (e.g., mitigating filter bubbles). Numerous definitions of this so-called *algorithmic fairness* exist, and some of them are inherently contradictory, for example, when ethical norms or standards of social responsibility come into conflict [3]. In contexts involving non-polar predictions, that is, predictions where the goals of (groups of) individuals and decision-makers are aligned, fairness can often be understood as the absence of bias, the presence of which is easier to assess. This perspective is especially relevant in medical applications.

Even in non-polar predictions, conflicting interpretations of fairness may arise, for example, from considering the group versus individual perspective. Resolving these conflicts requires a meta-level analysis that takes into account the broader social and algorithmic context, prevailing notions of justice, and the utilities of both decision-makers and decision recipients. In this contribution, we propose a meta-fairness metric designed to aid in selecting or combining fairness definitions in a principled and explainable manner. To support this, we advocate for the use of the Dempster-Shafer theory (DST) [5] as a foundation for handling uncertainty and integrating diverse fairness viewpoints.

We illustrate meta-fairness using the problem of classifying individuals at potential risk of hereditary breast cancer syndrome we addressed in our recent publications. Specifically, we focused on predicting the likelihood of mutations in *BRCA1* and *BRCA2* genes using DST based on factors such as patient age, personal medical history, and familial cancer history [1]. Our model accounts for epistemic uncertainty by using intervals when the ages of individuals in the family history are not precisely known, and it applies interval arithmetic with result verification [2] for all operations related to DST.

In medical contexts, a further important aspect is algorithmic explainability, that is, the ability to make the model's decisions and the underlying data transparent and interpretable to end users. For example, physicians must understand how and why a particular risk prediction was generated in order to provide accurate, informed guidance on potentially life-altering decisions. Likewise, patients facing difficult treatments need to understand the rationale behind the risk score provided. Explainability thus transforms an algorithm from a black box into a trustworthy, human-centered precision tool. For this case as well, DST-based approaches may yield better results than traditional closed-source systems [4].

Accuracy and reliability in assigning patients to risk classes are, of course, also critically important. However, there are situations where accuracy may need to be balanced in favor of fairness. The concept of meta-fairness provides a framework for navigating such trade-offs, enabling the selection of appropriate quality criteria based on the specific context. This includes ethical considerations and the diverse utilities of the stakeholders involved, ultimately tending towards outcomes that are not only effective but also just and context-sensitive.

Beyond introducing the meta-fairness metric, this talk aims to explore the broader role of (meta-)fairness in healthcare and risk prevention. We revisit our earlier DST-based risk prediction models from this new perspective: Can these methods ensure appropriate classification of patient groups and their individual members or families into risk categories, as defined by our meta-fairness criterion? Are DST approaches genuinely superior to alternatives like logistic regression, or do they require generalization—such as incorporating interval-based probability bounds or alternative evidence combination rules—to fully align with the demands of clinical decision-making?

References

[1] L. Gillner and E. Auer. *Towards a Traceable Data Model Accommodating Bounded Uncertainty for DST Based Computation of BRCA1/2 Mutation Probability With Age*, Journal of Universal Computer Science, 29(11), pp. 1361-1384, 2023.

[2] R.E. Moore, R.B. Kearfott, and M.J. Cloud. *Introduction to Interval Analysis*. Society for Industrial and Applied Mathematics, 2009.

[3] J. Paulus and D. Kent. *Predictably unequal: understanding and addressing concerns that algorithmic clinical prediction may increase health disparities*, npj Digital Medicine, 3, 99, 2020.

[4] S. Penafiel, N. Baloian, H. Sanson, and J. Pino. *Predicting Stroke Risk With an Interpretable Classifier*, IEEE Access 9, pp. 1154-1166, 2021.

[5] G. Shafer. *A Mathematical Theory of Evidence*, Princeton University Press, 1976.

Thursday, September 25, 2025

Library Auditorium

9:00–10:30	**Plenary Lecture** Tino Teige: *Bringing Formal Methods from Academia to Real-World Applications in Industry: My Personal Two-Decades-Journey*
10:30–11:00	Coffee Break
11:00–12:30	**Regular Session A: Estimation**
11:00–11:30	Quentin Brateau, Fabrice Le Bars and Luc Jaulin: *Separator for the remoteness constraint*
11:30–12:00	Damien Esnault, Simon Rohou, Fabrice Le Bars and Luc Jaulin: *Computing Interval Detection-Probability Grids via Monte-Carlo method for Underwater Robotics*
12:00–12:30	Marit Lahme and Andreas Rauh: *Set-Based Identification of Characteristic Curves and Its Challenges for Real-Life Applications*
12:30–14:00	Lunch Break – Food truck
14:30–16:00	**Regular Session A: Linear Systems and Linear Algebra**
14:30–15:00	Haruto Kijima and Takeshi Ogita: *Fast Implementation of Interval Matrix Multiplication Using Infimum-Supremum Representation With SIMD Operations*
15:00–15:30	Takeshi Terao, Yoshitaka Watanabe and Katsuhisa Ozaki: *Verification of Singular Values under Oblique Inner Product Space for Matrices*
15:30–16:00	Katsuhisa Ozaki and Toru Koizumi: *Tight Enclosure of Matrix Multiplication using Fused Multiply-Add*
16:00–16:30	Coffee Break
16:30–17:30	**Regular Session A: Neural Networks**
16:30–17:00	Attila Szász and Balázs Bánhelyi: *Parameter Robustness of Neural Networks*
17:00–17:30	Tibor Csendes: *Interval Based Verification of Adversarial Example Free Zones for Neural Networks*
18:00–19:00	Meeting of the program committee including new member

Bringing Formal Methods from Academia to Real-World Applications in Industry – *My Personal Two-Decades-Journey* –

Tino Teige

BTC Embedded Systems AG
Department of Innovation & Technology
D-26135 Oldenburg, Germany
tino.teige@btc-embedded.com

Keywords: Formal Methods, Model Checking, Constraint Solving

Abstract

In this invited talk I will give insights into my personal experience in *bringing formal methods from academia to real-world applications in industry*. I will first elaborate on the development of the constraint solver iSAT during my academic years at the University of Oldenburg from 2005 to 2012. After that I will address the challenges and use cases from real-world applications I was faced with when I moved to the industrial test tool provider BTC Embedded Systems in 2012. One particular focus of this talk will be on how powerful methods and tools from academia like iSAT have been successfully transferred from their academic environment to industrial software development projects.

Separator for the remoteness constraint

Quentin Brateau[1], Fabrice Le Bars[1] and Luc Jaulin[1]

[1] Lab-STICC - ENSTA
2 rue François Verny, 29200 Brest, France
quentin.brateau@ensta.fr, fabrice.le_bars@ensta.fr, lucjaulin@gmail.com

Keywords: Interval methods, State Estimation, Remoteness

Introduction

Interval analysis is well suited for solving state estimation problems, which can be useful to deal with uncertainty in dynamical systems [4, 5].

The remoteness constraint [6] constitutes a fundamental geometric relationship in robotics, defining the distance measure between sensors with measurement directivity and obstacles in the environment. This constraint is particularly critical for acoustic sensors, where the directivity pattern can exhibit substantial angular coverage [1], making precise characterization of sensor-obstacle spatial relationships essential for reliable navigation and mapping applications.

We present an implementation of the separator [2] for the remoteness constraint. The proposed separator enables the complete characterization of the set of compatible sensor positions relative to obstacles, given distance measurements and sensor directivity constraints. Unlike previous approaches that were limited to inclusion testing [6], our implementation provides an efficient and modern way to characterize the feasible sensor positions.

Main results

Figure 1 shows a paving of separators [3] on the remoteness constraint relative to an obstacle segment shown in red, and the remoteness cone defined by vectors $u_1 = \begin{bmatrix}-0.5 & -1\end{bmatrix}$ and $u_2 = \begin{bmatrix}0.5 & -1\end{bmatrix}$. The pink area represent the set of positions for the sensor compatible with the measured distance d, the blue areas represent the set of positions not compatible with the measurement, and the yellow area is the unknown area. Figure 1a shows the separator for the case $d = [4, 5]$, and Figure 1b shows the separator for the case $d = [5, +\infty]$.

This separator can be used to localize the set of possible positions for an underwater robot in a known environment such as a pool or a harbor. Figure 1c shows the state estimation of a robot in a pool performing cycles and taking two measurements in the pool. The set of starting positions for the cycle is well enclosed in the pink area.

Acknowledgement

This work has been supported by the French Government Defense procurement and technology agency (AID-2022850).

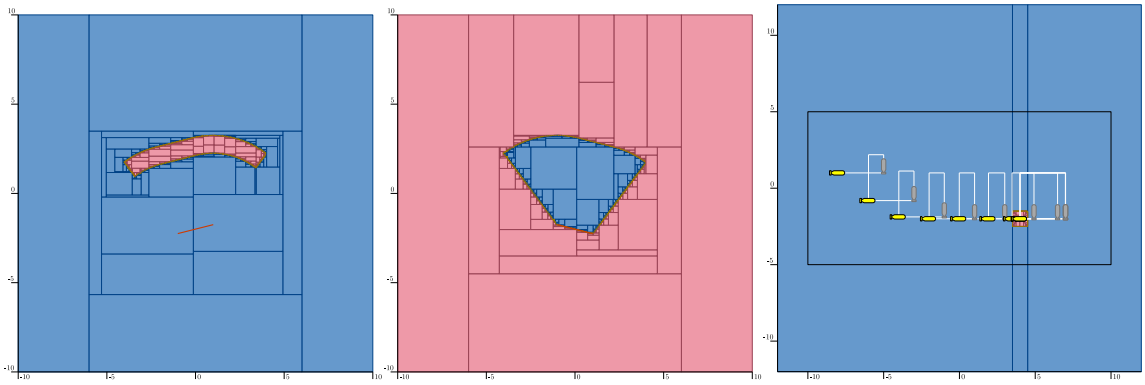

(a) $d = [4, 5]$ (b) $d = [5, +\infty]$ (c) Set of possible position of a robot performing cycles in a pool.

Figure 1: Paving of separators on the remoteness constraint

References

[1] Yang Cong, Changjun Gu, Tao Zhang, and Yajun Gao. Underwater robot sensing technology: A survey. *Fundamental Research*, 1(3):337–345, 2021.

[2] Luc Jaulin and Benoît Desrochers. Introduction to the Algebra of Separators with Application to Path Planning. *Engineering Applications of Artificial Intelligence*, 33:141–147, August 2014.

[3] Luc Jaulin, Michel Kieffer, Olivier Didrit, Eric Walter, Luc Jaulin, Michel Kieffer, Olivier Didrit, and Éric Walter. *Interval analysis*. Springer, 2001.

[4] Marit Lahme and Andreas Rauh. Set-valued approach for the online identification of the open-circuit voltage of lithium-ion batteries. *Acta Cybernetica*, 26:855–869, 11 2024.

[5] Ghalia Nassreddine, Fahed Abdallah, and Thierry Denoeux. State estimation using interval analysis and belief function theory: Application to dynamic vehicle localization. *IEEE Transactions on Systems, Man, and Cybernetics, Part B: Cybernetics*, 40(5):1205–1218, 2010.

[6] E. Seignez, M. Kieffer, A. Lambert, E. Walter, and T. Maurin. Experimental vehicle localization by bounded-error state estimation using interval analysis. In *2005 IEEE/RSJ International Conference on Intelligent Robots and Systems*, pages 1084–1089, 2005.

Separator for the remoteness constraint

Quentin Brateau, Fabrice Le Bars, Luc Jaulin
{quentin.brateau, fabrice.le_bars, luc.jaulin} @ ensta.fr
ENSTA, 2 rue François Verny, 29200 Brest, CNRS, UMR 6285, Lab-STICC, Pôle IA & Océans, ROBEX

Introduction

The remoteness constraint is fundamental in mobile robotics. It represents the constraint between the distance measured by a sensor within a measurement cone and an obstacle segment.

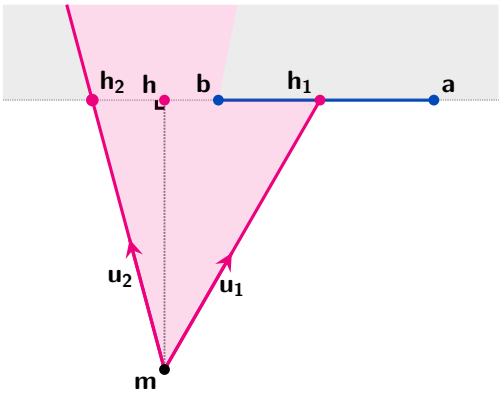

Figure 1 – Remoteness of a segment $[\mathbf{a}, \mathbf{b}]$ relative to a point $\mathbf{m}$ and two unit vectors $\mathbf{u_1}$ and $\mathbf{u_2}$

Measured distance

The remoteness constraint ensures that the measured distance d is on of $\{||\mathbf{ma}||, ||\mathbf{mb}||, ||\mathbf{mh}||, ||\mathbf{mh_1}||, ||\mathbf{mh_2}||, +\infty\}$, with

$$||\mathbf{mh}|| = \frac{det(\mathbf{ab}, \mathbf{am})}{||\mathbf{ab}||}$$
$$\forall \mathbf{p} \in \{\mathbf{a}, \mathbf{b}\}, ||\mathbf{mp}|| = \sqrt{(m_x - p_x)^2 + (m_y - p_y)^2}$$
$$\forall i \in \{1, 2\}, ||\mathbf{mh}_i|| = \frac{det(\mathbf{ab}, \mathbf{am})}{det(\mathbf{u}_i, \mathbf{ab})}$$

Case $\langle \mathbf{u}_1, \mathbf{ab} \rangle \geq 0 \wedge \langle \mathbf{u}_2, \mathbf{ab} \rangle \geq 0$

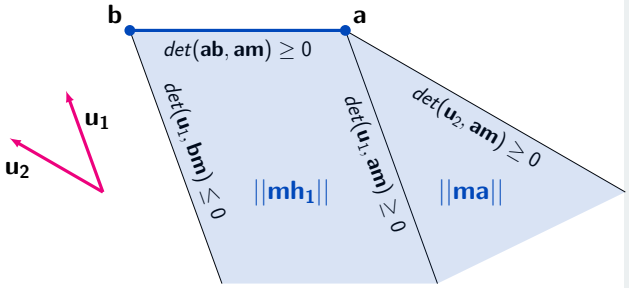

Figure 2 – Remoteness when $\langle \mathbf{u}_1, \mathbf{ab} \rangle \geq 0 \wedge \langle \mathbf{u}_2, \mathbf{ab} \rangle \geq 0$

Case $\langle \mathbf{u}_1, \mathbf{ab} \rangle < 0 \wedge \langle \mathbf{u}_2, \mathbf{ab} \rangle \geq 0$

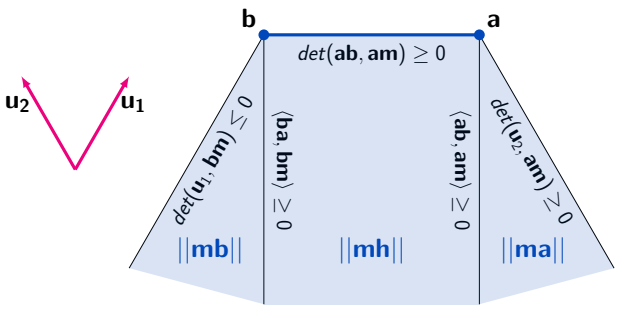

Figure 3 – Remoteness when $\langle \mathbf{u}_1, \mathbf{ab} \rangle < 0 \wedge \langle \mathbf{u}_2, \mathbf{ab} \rangle \geq 0$

Case $\langle \mathbf{u}_1, \mathbf{ab} \rangle < 0 \wedge \langle \mathbf{u}_2, \mathbf{ab} \rangle < 0$

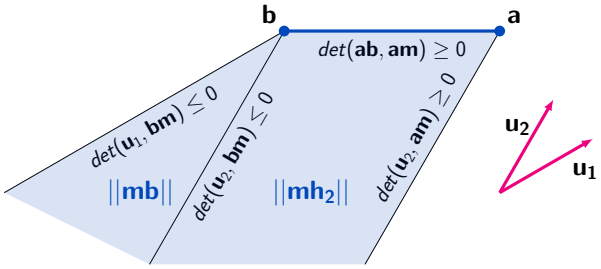

Figure 4 – Remoteness when $\langle \mathbf{u}_1, \mathbf{ab} \rangle < 0 \wedge \langle \mathbf{u}_2, \mathbf{ab} \rangle < 0$

Results

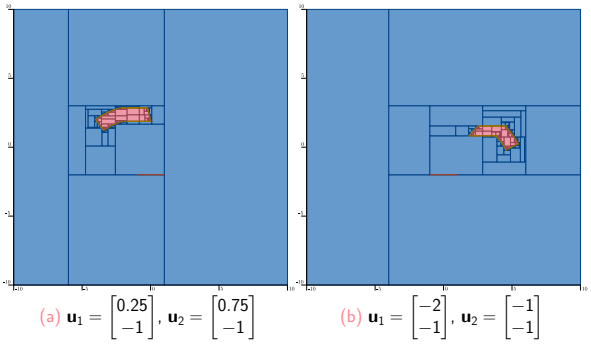

(a) $\mathbf{u}_1 = \begin{bmatrix} 0.25 \\ -1 \end{bmatrix}$, $\mathbf{u}_2 = \begin{bmatrix} 0.75 \\ -1 \end{bmatrix}$ (b) $\mathbf{u}_1 = \begin{bmatrix} -2 \\ -1 \end{bmatrix}$, $\mathbf{u}_2 = \begin{bmatrix} -1 \\ -1 \end{bmatrix}$

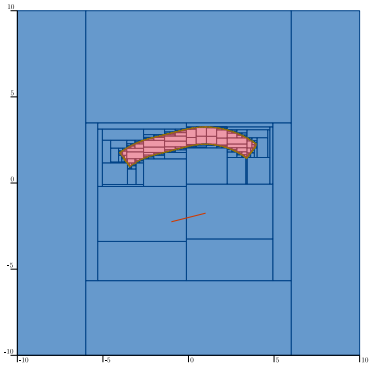

(c) $\mathbf{u}_1 = \begin{bmatrix} 0.75 \\ -1 \end{bmatrix}$, $\mathbf{u}_2 = \begin{bmatrix} 0.75 \\ -1 \end{bmatrix}$

Figure 5 – Paving of the separator for $d = [4, 5]$

Application

The remoteness constraint can be applied to the localization of an underwater robot in a known pool, using an echosounder to measure the distance to the pool walls, and by performing only two measurements.

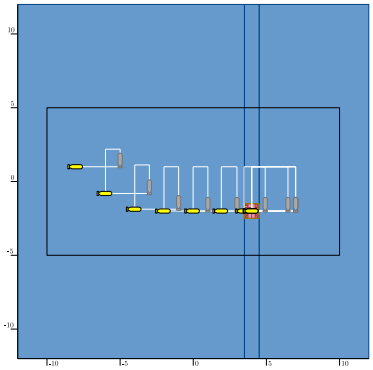

Figure 6 – Localization of an underwater robot in a known environment using remoteness constraint

Computing Interval Detection-Probability Grids via Monte-Carlo method for Underwater Robotics

D. Esnault[1,2], S. Rohou[2], F. Le Bars[2] and L. Jaulin[2]

[1] DGA Naval Systems (French Defense Ministry)
Naval mine warfare department
29200 Brest, France
damien.esnault@ensta.fr

[2] Lab-STICC, ENSTA
ROBEX team
29200 Brest, France
{simon.rohou,fabrice.le_bars,luc.jaulin}@ensta.fr

Keywords: Detection-Probability Grid, Monte-Carlo Method, Probabilities, Interval Methods and Underwater Robotics.

Introduction

Autonomous Underwater Vehicles (AUVs) are emerging as valuable assets in various domains due to their ability to operate autonomously in complex and hazardous environments [1]. To address the numerous sources of uncertainty—ranging from environmental disturbances (e.g., ocean currents, obstacles) to internal system limitations (e.g., sensor noise, state estimation errors)—AUVs are typically modeled and controlled using probabilistic approaches [2].

During mine-clearance missions, AUVs use onboard sensors to detect threats located on the seafloor. The area covered by these sensors during a mission can be represented as a set. Whether a target is detected then depends on whether its position falls within this set. However, due to the stochastic nature of the AUV's motion, the coverage area itself is random. As a result, detection becomes a probabilistic event: each point on the seafloor has an associated detection probability that depends on the mission plan and the AUV's behavior. To ensure mission effectiveness—especially when a list of potential mine positions is known—it is crucial to design the mission such that the detection probability for each target is close to 1.

Detection probability grid

A practical way to visualize the likelihood of detecting points on the seafloor is through a detection probability grid. This grid is a 2D matrix, where each cell corresponds to a specific point on the seafloor, and the associated value represents the probability of detection at that point [3].

We propose to compute an empirical estimation of this grid using a Monte-Carlo based method [3]. A large number of AUV simulations (trajectories) are generated based on a stochastic model. For each simulated trajectory, the area covered by the AUV's

sensor is computed [4]. A 2D grid is then overlaid on the seafloor, where each point represents a potential location for detection. For each point and each simulation, a binary realization value is assigned: 1 if the point lies within the covered area, and 0 otherwise. By averaging these values across all simulations, we obtain an empirical estimate of the detection probability for each grid point. By applying this procedure across all points in the grid, we obtain a full detection probability map.

Contribution

In practice, it is often infeasible to perfectly compute the covered area for each AUV trajectory due to the high computational cost. Instead, we typically compute an approximation of the covered area with a guaranteed precision. This approximation introduces ambiguity: rather than dividing the space into only two categories (covered and not covered), the seafloor is partitioned into three complementary regions: definitely covered, definitely not covered, and ambiguous, where it is uncertain whether a point has been covered or not. Instead of a binary outcome, we must now work within a three-valued logic [5].

To handle this new framework, the Monte-Carlo method must be adapted accordingly. Recent work has proposed the use of interval-valued realizations to model such uncertainty [6]. In this approach, each realization is no longer a number but an interval: [1] when the point is definitely covered, [0] when it is definitely not, and [0,1] when the status is uncertain.

By applying this interval-based Monte-Carlo method to each point in the 2D grid, the result is an interval detection probability grid, where each grid cell is associated with an interval of probability reflecting the uncertainty introduced by both uncertain factors and numerical approximations.

References

[1] R.B. Wynn, T. Le Bas, and al. *Autonomous Underwater Vehicles (AUVs): Their past, present and future contributions to the advancement of marine geoscience.* Marine Geology, vol. 352, no. 1, pp. 451–468, 2014.

[2] P. Corke. *Robotics, Vision and Control.* Springer Nature, 2023.

[3] S. Thrun, W. Burgard, and D. Fox. *Probabilistic robotics.* MIT Press, 2010.

[4] B. Desrochers, and L. Jaulin. *Computing a Guaranteed Approximation of the Zone Explored by a Robot.* IEEE Transactions on Automatic Control, vol. 62, no. 1, pp. 425–430, 2016.

[5] S.C. Kleene. *Introduction to Metamathematics.* Literary Licensing, LLC, 2012.

[6] D. Esnault, S. Rohou, F. Le Bars, and L. Jaulin. *Bounding the success probability of naval mine-clearance missions conducted by AUVs.* to appear in the Proceedings of "OCEANS 2025 - Brest", Brest, France.

Set-Based Identification of Characteristic Curves and Its Challenges for Real-Life Applications

Marit Lahme and Andreas Rauh

Carl von Ossietzky Universität Oldenburg
Distributed Control in Interconnected Systems
D-26111 Oldenburg, Germany
{marit.lahme,andreas.rauh}@uni-oldenburg.de

Keywords: Identification, Interval Observer, Contractor, Battery System

Introduction

The knowledge of the relationship between different physical quantities of a system is essential for various applications, such as monitoring its current state, predicting its future behavior, and designing appropriate controllers. These relationships can, for instance, be graphically represented by characteristic curves. For example, the characteristic curve of an ideal Ohmic resistor, showing the current-voltage relationship, is a linear function in $\mathbb{R}^2$. In certain applications, it is not feasible to directly obtain the characteristic curves of interest by measuring the corresponding physical quantities. One example is the open-circuit voltage (OCV) characteristic of a lithium-ion battery, which represents the dependence of the OCV on the state of charge (SOC), a quantity that cannot be measured directly. This characteristic is particularly valuable for modeling the dynamic behavior of the battery and for detecting aging or degradation effects [1]. Typically, obtaining the OCV characteristic involves measuring the OCV during a controlled charging or discharging cycle over several hours, while simultaneously estimating the SOC. Our goal is to identify this characteristic during system operation; in earlier work, we therefore proposed an online set-based identification scheme for this purpose [1, 4]. In this presentation, we outline the identification scheme with a primary focus on the challenges encountered when applying it to real-life systems with the identification of the OCV characteristic of a lithium-ion battery as an example. This work does not present a novel contribution, but rather provides a comprehensive overview of the identification scheme in a real-life context, highlighting the associated challenges and selected solution approaches.

Main results

The proposed identification scheme is a two-stage procedure. Since the SOC cannot be measured directly, it has to be estimated. For this purpose, an interval observer is employed, which provides estimated lower and upper bounds for the SOC that are guaranteed to enclose the true value. Based on this estimate together with structural information resulting from the application of Kirchhoff's voltage law to an equivalent circuit model the OCV can be computed, resulting in an interval enclosure for the true value of the OCV. The estimates for the OCV and SOC can be represented by interval boxes, which are the Cartesian products of their interval elements. During

battery charging/discharching, different interval boxes are obtained spanning different sections of the OCV-SOC characteristic. Intersecting overlapping interval boxes reduces the estimation uncertainty and enables the reconstruction of the characteristic curve [1].
Applying this identification scheme to real-life systems presents certain challenges, particularly in the state estimation part [2, 3, 5]. These challenges arise mainly from the structure of the system. The dynamic behavior of a lithium-ion battery can be captured by a quasi-linear state-space representation where the dynamics matrices depend on the SOC as one of the state variables. Furthermore, the state variables are scaled differently, and the output equation is nonlinear.
A classical Luenberger observer approach (a variant of a linear model-based state reconstruction scheme) does not yield sufficiently accurate or feasible estimation results in this case and is therefore unsuitable [3]. Instead, an interval observer which provides more design degrees of freedom is used. However, determining suitable observer gains that lead to feasible and accurate estimation results is challenging for the case of the lithium-ion batteries. We present several techniques for systematically parameterizing the observer gains to obtain estimated lower and upper bounds with a small interval width [5]. Additionally, uncertainties have to be taken into account during the observer design, which include measurement noise, process noise and parametric uncertainty. We present different techniques to address this during the observer parameterization [3].

References

[1] M. Lahme and A. Rauh. Set-Valued Approach for the Online Identification of the Open-Circuit Voltage of Lithium-Ion Batteries. *Acta Cybernetica (Special Issue of SWIM 2022)*, 26(4):855–869, 2024. DOI: 10.14232/actacyb.301185.

[2] M. Lahme and A. Rauh. Online Identification of the Open-Circuit Voltage Characteristic of Lithium-Ion Batteries with a Contractor-Based Procedure. *Proc. of the 27th International Conference on Methods and Models in Automation and Robotics (MMAR)*, IEEE 39–44, 2023. DOI: 10.1109/MMAR58394.2023.10242524.

[3] M. Lahme, A. Rauh, and G. Defresne. Interval Observer Design for an Uncertain Time-Varying Quasi-Linear System Model of Lithium-Ion Batteries. *Proc. of the 2024 European Control Conference (ECC)*, IEEE 3696-3702, 2024. DOI: 10.23919/ECC64448.2024.10591102.

[4] M. Lahme and A. Rauh. Combination of Stochastic State Estimation with Online Identification of the Open-Circuit Voltage of Lithium-Ion Batteries. *Proc. of the 1st IFAC Workshop on Control of Complex Systems (COSY)*, IFAC-PapersOnLine 55(40):97–102, 2022. DOI: 10.1016/j.ifacol.2023.01.055.

[5] M. Lahme and A. Rauh. Systematic Approach for Parameterizing TNL Interval Observers. *15th Summer Workshop on Interval Methods (SWIM 2024)*, Presentation, 2024. DOI: 10.13140/RG.2.2.33444.28800.

Fast Implementation of Interval Matrix Multiplication Using Infimum-Supremum Representation With SIMD Operations

Haruto Kijima[1], Takeshi Ogita[1]

[1] Waseda University
Graduate of Fundamental Science and Engineering
3-4-1 Okubo, Shinjuku-ku, Tokyo, Japan
khart@fuji.waseda.jp

Keywords: Interval Arithmetic, Matrix Multiplication, SIMD Operations

Introduction

Let $\mathbb{F}$ be a set of floating-point numbers. Let $\mathbb{IF}$ be a set of intervals whose endpoints are floating numbers. We propose a method of interval matrix multiplication using infimum-supremum representation. It is difficult to achieve high performance for interval matrix multiplication using the infimum-supremum representation. This is because in modern CPUs, comparing signs and switching rounding mode operations prevent efficient execution of floating-point operations. Therefore, Knüppel [1] proposed a method of calculating a product of a point matrix and an interval matrix, taking advantage of the fact that a product of a floating-point scalar a and an interval vector $[\boldsymbol{v}] = [\underline{\boldsymbol{v}}, \overline{\boldsymbol{v}}]$ ($\underline{\boldsymbol{v}}, \overline{\boldsymbol{v}} \in \mathbb{F}^n$) can be calculated as

$$\begin{array}{ll} \textbf{if } a > 0 \textbf{ then} & \underline{\boldsymbol{w}} = \mathtt{fl}_{\triangledown}(a \cdot \underline{\boldsymbol{v}});\ \overline{\boldsymbol{w}} = \mathtt{fl}_{\triangle}(a \cdot \overline{\boldsymbol{v}}); \\ \textbf{else} & \underline{\boldsymbol{w}} = \mathtt{fl}_{\triangledown}(a \cdot \overline{\boldsymbol{v}});\ \overline{\boldsymbol{w}} = \mathtt{fl}_{\triangle}(a \cdot \underline{\boldsymbol{v}}); \end{array}$$

However, since this is a level-1 BLAS operation, the execution performance is bounded by memory bandwidth. To overcome this, a fast algorithm of interval matrix multiplication was proposed using the midpoint-radius representation exploiting level-3 BLAS operations [2]. In the algorithm, the number of floating-point operations in the product of two interval matrices is $8n^3$. However, in the worst case, the resultant interval width is overestimated by 1.5 times. In response to this, Nguyen and Revol [3] proposed an algorithm that reduces the overestimation to 1.18, where the number of floating-point operations is $14n^3$. In addition, Rump [4] improved the algorithm, reducing the number of floating-point operations to $10n^3$.

Proposed Method

When implementing floating-point matrix multiplication, blocking technique is used for efficient computations. Here we focus on $m_b \times n_b$ register blocking for interval cases. Let $[\underline{A}, \overline{A}] \in \mathbb{IF}^{m_b \times l}$, $[\underline{B}, \overline{B}] \in \mathbb{IF}^{l \times n_b}$, $[\underline{C}, \overline{C}] \in \mathbb{IF}^{m_b \times n_b}$ be given. Consider computation of $[\underline{C}, \overline{C}] \leftarrow [\underline{A}, \overline{A}] \cdot [\underline{B}, \overline{B}] + [\underline{C}, \overline{C}]$. If the matrix multiplication is performed using rank-1 updates [5], the operation becomes

$$[\underline{C}, \overline{C}] \leftarrow [\underline{A}_{*1}, \overline{A}_{*1}] \cdot [\underline{B}_{1*}, \overline{B}_{1*}] + \cdots [\underline{A}_{*l}, \overline{A}_{*l}] \cdot [\underline{B}_{l*}, \overline{B}_{l*}] + [\underline{C}, \overline{C}]$$

where $\underline{A}_{*k}, \overline{A}_{*k}$ are the k-th column vectors of $\underline{A}$ and $\overline{A}$ and $\underline{B}_{k*}, \overline{B}_{k*}$ are the k-th row vectors of $\underline{B}$ and $\overline{B}$. Then, the calculation of each $[\underline{A}_{*k}, \overline{A}_{*k}] \cdot [\underline{B}_{k*}, \overline{B}_{k*}]$ is given by

$$\textbf{for } j = 1, \cdots, n_b \textbf{ do } [\underline{C}_{*j}, \overline{C}_{*j}] \leftarrow [\underline{A}_{*k}, \overline{A}_{*k}] \cdot [\underline{B}_{kj}, \overline{B}_{kj}] + [\underline{C}_{*j}, \overline{C}_{*j}].$$

We calculate the product of an interval vector $[\underline{A}_{*k}, \overline{A}_{*k}]$ and an interval scalar $[\underline{B}_{kj}, \overline{B}_{kj}]$ using the proposed multiplication algorithm as follows:

$$\begin{aligned}
&\textbf{if } \overline{B}_{kj} < 0 \textbf{ then}\\
&\quad \underline{C}_{*j} = \min(\mathtt{fl}_{\triangledown}(\underline{C}_{*j} + \overline{A}_{*k} \cdot \underline{B}_{kj}), \mathtt{fl}_{\triangledown}(\underline{C}_{*j} + \overline{A}_{*k} \cdot \overline{B}_{kj}))\\
&\quad \overline{C}_{*j} = \max(\mathtt{fl}_{\triangle}(\overline{C}_{*j} + \underline{A}_{*k} \cdot \underline{B}_{kj}), \mathtt{fl}_{\triangle}(\overline{C}_{*j} + \underline{A}_{*k} \cdot \overline{B}_{kj}))\\
&\textbf{elseif } \underline{B}_{kj} > 0 \textbf{ then}\\
&\quad \underline{C}_{*j} = \min(\mathtt{fl}_{\triangledown}(\underline{C}_{*j} + \underline{A}_{*k} \cdot \underline{B}_{kj}), \mathtt{fl}_{\triangledown}(\underline{C}_{*j} + \underline{A}_{*k} \cdot \overline{B}_{kj}))\\
&\quad \overline{C}_{*j} = \max(\mathtt{fl}_{\triangle}(\overline{C}_{*j} + \overline{A}_{*k} \cdot \underline{B}_{kj}), \mathtt{fl}_{\triangle}(\overline{C}_{*j} + \overline{A}_{*k} \cdot \overline{B}_{kj}))\\
&\textbf{else}\\
&\quad \underline{C}_{*j} = \min(\mathtt{fl}_{\triangledown}(\underline{C}_{*j} + \underline{A}_{*k} \cdot \overline{B}_{kj}), \mathtt{fl}_{\triangledown}(\underline{C}_{*j} + \overline{A}_{*k} \cdot \underline{B}_{kj}))\\
&\quad \overline{C}_{*j} = \max(\mathtt{fl}_{\triangle}(\overline{C}_{*j} + \underline{A}_{*k} \cdot \underline{B}_{kj}), \mathtt{fl}_{\triangle}(\overline{C}_{*j} + \overline{A}_{*k} \cdot \overline{B}_{kj}))
\end{aligned}$$

This is an improved version of Knüppel's algorithm. Based on this, we implement the proposed multiplication algorithm. The number of floating-point operations in the proposed algorithm is $8n^3$. The proposed algorithm is suitable for SIMD operations and has a high reusability of data. When using Intel AVX-512 instructions, it is possible to calculate $\overline{C}$ and $\underline{C}$ simultaneously without changing the rounding mode, since there are arithmetic operations with directed rounding for addition and multiplication. In this case, the number of comparing signs operations is $\frac{n^3}{m_b}$. In addition, since there is no data dependency between the calculations of $\overline{C}$ and $\underline{C}$, they can be calculated separately. If doing so, the number of rounding mode changes in the proposed algorithm becomes two and the number of comparing signs operations is $\frac{2n^3}{m_b}$. We will show numerical results in our talk.

References

[1] O. Knüppel. PROFIL/BIAS—A fast interval library, *Computing*, 53 (1994), pp. 277–287

[2] S. M. Rump. Fast and parallel interval arithmetic. *BIT Numerical Mathematics*, 39 (1999), pp. 534–554

[3] H. D. Nguyen. Efficient algorithms for verified scientific computing : Numerical linear algebra using interval arithmetic. Ph.D. thesis, Ecole normale supérieure de lyon - ENS LYON, 2011

[4] S. M. Rump. Fast interval matrix multiplication. *Numerical Algorithms*, 61 (2012), pp. 1–34

[5] S. M. Rump. INTLAB—Interval laboratory, in Developments in Reliable Computing, T. Csendes, ed., Kluwer Academic Publishers, Dordrecht, 1999, pp. 77-104

Verification of Singular Values under Oblique Inner Product Space for Matrices

Takeshi Terao[1], Yoshitaka Watanabe[1] and Katsuhisa Ozaki[2]

terao.takeshi.412@m.kyushu-u.ac.jp watanabe.yoshitaka.003@m.kyushu-u.ac.jp
[1] Research Institute for Information Technology, Kyushu University
744 Motooka, Nishi-ku, Fukuoka 819-0395, Japan
{terao.takeshi.412, watanabe.yoshitaka.003}@m.kyushu-u.ac.jp
[2] Department of Mathematical Science, Shibaura Institute of Technology
307 Fukasaku, Minuma-ku, Saitama, 337-8570, Saitama, Japan
ozaki@shibaura-it.ac.jp

Keywords: Verified numerical computation, Singular values, Interval arithmetic

Introduction

Let matrices $A \in \mathbb{R}^{n\times n}$ and $B \in \mathbb{R}^{n\times n}$ be given, where A is nonsingular and B is symmetric and positive definite. Let R denote the upper triangular Cholesky factor of B. This talk considers computing an enclosure of the spectral norm of $RA^{-1}R^T$, i.e.,

$$\underline{\rho} \leq \|RA^{-1}R^T\|_2 \leq \overline{\rho}. \tag{1}$$

To compute $\overline{\rho}$ and $\underline{\rho}$, the previous work employs the interval Cholesky decomposition [3] and spectral norm verification [2], which have been used in computer-assisted proofs for differential equations [1]. However, it is known that the interval Cholesky decomposition suffers from issues in terms of computational cost and numerical stability. Therefore, we propose a method to verify $\rho := \|RA^{-1}R^T\|_2$ without using interval Cholesky decomposition.

Proposed Method

The proposed method considers the smallest singular value $\sigma_{\min}$ of the matrix $R^{-T}AR^{-1}$, because $\sigma_{\min} = \rho^{-1}$. To develop the verification method, we define a singular value decomposition with respect to an oblique inner product [5] as follows:

$$A = U\Sigma V^T, \quad U^TBU = V^TBV = I, \quad U, \Sigma, V \in \mathbb{R}^{n\times n}, \tag{2}$$

where I is the identity matrix and Σ is a diagonal matrix with positive entries.

Let $\widehat{U}, \widehat{\Sigma}, \widehat{V}$ be approximations of U, Σ, V, respectively. Suppose

$$\alpha := \|\widehat{U}^TB\widehat{U}\|_2 < 1, \quad \beta := \|\widehat{V}^TB\widehat{V}\|_2 < 1. \tag{3}$$

Then for $S := \widehat{U}^TA\widehat{V}$, we have

$$\frac{\sigma_{\min}(S)}{\sqrt{(1-\alpha)(1-\beta)}} \leq \rho^{-1} \leq \frac{\sigma_{\min}(S)}{\sqrt{(1+\alpha)(1+\beta)}}, \tag{4}$$

where $\sigma_{\min}(S)$ denotes the smallest singular value of S.

Define

$$\bar{A} = \begin{pmatrix} O & A^T \\ A & O \end{pmatrix}, \quad \bar{B} = \begin{pmatrix} B & O \\ O & B \end{pmatrix}, \tag{5}$$

where O is the zero matrix. Then, $\bar{A}$ and $\bar{B}$ are symmetric, and $\bar{B}$ is positive definite. It follows that

$$\|\bar{R}\bar{A}^{-1}\bar{R}^T\|_2 = \rho, \tag{6}$$

where $\bar{R}$ is the upper triangular Cholesky factor of $\bar{B}$.

The matrix $\bar{R}\bar{A}^{-1}\bar{R}^T$ has eigenvalues $\pm\rho$. Therefore, if $\bar{A} - \theta\bar{B}$ with $\theta > 0$ has n positive and n negative eigenvalues, then it follows that $\rho < \theta^{-1}$. To count the number of positive and negative eigenvalues, one can use the method based on LDL^T decomposition [4]. A key advantage of this method is its applicability to sparse matrices A and B.

The proposed methods eliminate the need for interval Cholesky decomposition in enclosing ρ. We demonstrate through numerical experiments that the proposed method is superior in terms of computation time, accuracy, and numerical stability.

References

[1] M.T. Nakao, M. Plum, and Y. Watanabe. Numerical verification methods and computer-assisted proofs for partial differential equations. *Springer*, 2019.

[2] S.M. Rump. Verified bounds for singular values, in particular for the spectral norm of a matrix and its inverse. *BIT Numerical Mathematics*, 51:367–384, 2011.

[3] G. Alefeld and G. Mayer. The Cholesky method for interval data. *Linear Algebra and its applications*, 194:161–182, 1993.

[4] N. Yamamoto. A simple method for error bounds of eigenvalues of symmetric matrices. *Linear Algebra and its Applications*, 324:227–234, 2001.

[5] T. Terao, Y. Watanabe, and K. Ozaki. Verified error bounds for the singular values of structured matrices with applications to computer-assisted proofs for differential equations. *arXiv preprint arXiv:2502.09984*, 2025.

Tight Enclosure of Matrix Multiplication using Fused Multiply-Add

Katsuhisa Ozaki[1] and Toru Koizumi[2]

[1] Shibaura Institute of Technology
Department of Mathematical Sciences
307 Fukasaku, Saitama-shi, Saitma 337-8570, Japan
ozaki@shibaura-it.ac.jp
[2] Nagoya Institute of Technology
Department of Computer Science
Gokiso-cho, Showa-ku, Nagoya, Aichi 466-8555, Japan
koizumi@nitech.ac.jp

Keywords: Matrix Multiplication, Interval Methods, Verified Numerical Computations

Introduction

A verified enclosure of matrix multiplication results plays a fundamental role in reliable numerical computations arising in numerical linear algebra. Given an m-by-n floating-point matrix A and an n-by-p floating-point matrix B, the goal is to compute matrices (C_d, C_u) or (M, R) such that

$$C_d \leq AB \leq C_u, \tag{1}$$
$$M - R \leq AB \leq M + R, \tag{2}$$

where all entries of R are non-negative. The expressions (1) and (2) are referred to as the infimum-supremum form and the midpoint-radius form, respectively. Several enclosure methods have been proposed with a trade-off between computational cost, memory consumption, and the tightness of the resulting enclosures.

A typical method for obtaining C_d and C_u in (1) employs directed roundings as defined in the IEEE 754 standard. Let $\mathrm{fl}_{\bigtriangledown}(\cdot)$, $\mathrm{fl}(\cdot)$, and $\mathrm{fl}_{\bigtriangleup}(\cdot)$ denote floating-point evaluations of the expressions in parentheses, where the rounding modes are specified by IEEE 754 as follows: downward rounding for $\mathrm{fl}_{\bigtriangledown}(\cdot)$, rounding to nearest for $\mathrm{fl}(\cdot)$, and upward rounding for $\mathrm{fl}_{\bigtriangleup}(\cdot)$. Due to space limitations, we assume throughout this abstract that neither overflow nor underflow occurs.

The matrices C_d and C_u in (1) can be computed as

$$C_d := \mathtt{fl}_{\bigtriangledown}(AB), \quad C_u := \mathtt{fl}_{\bigtriangleup}(AB). \tag{3}$$

If a tighter enclosure than (3) is required, two methods are proposed in [1]. For the form (2), the matrices M and R can be computed as

$$M := \mathtt{fl}(AB), \quad R := nu\,|A||B|, \tag{4}$$

based on the method in [3], where u is the unit roundoff, and the absolute value symbol for a matrix denotes the matrix obtained by taking the absolute value of each entry. Approaches such as (3) and (4) make use of high-performance BLAS matrix multiplication routines.

The proposed method

We propose a fast and tight enclosure method that is not based on a BLAS function and that produces a tighter interval than (3). In addition, the proposed method exhibits lower memory consumption compared to the methods presented in [1]. For floating-point numbers a, b, and c, we obtain x and y such that $x + y \approx ab + c$. The following algorithm was introduced in [4]. If $2|ab| \leq |c|$, $|x + y - (ab + c)| \leq u^2|ab + c|$ holds [2].

---

function $[x, y] = \mathbf{FastTwoFMA}(a, b, c)$
$x = \texttt{fma}(a, b, c);$
$y = \texttt{fma}(a, b, c - x);$

We extend the above algorithm to $d_h + d_\ell \approx ab + c_h + c_\ell$ where $a, b, c_h, c_\ell, d_h, d_\ell \in \mathbb{F}$ and $\texttt{fl}(c_h + c_\ell) = c_h$.

---

function $[d_h, d_\ell] = \mathbf{FastTwoFMA\_s}(a, b, c_h, c_\ell)$
$[d_h,\ d_\ell] = \mathbf{FastTwoFMA}(a, b, c_h);$
$d_\ell = d_\ell + c_\ell;$

We introduce a floating-point matrix W and compute the matrix product AB as $(AB + W) - W$ using **FastTwoFMA_s**. We set W to satisfy $W \geq 3(1 + nu)|A||B|$. In this case, the condition $|c_h| \geq 2|ab|$ is always satisfied within **FastTwoFMA_s**. Let the computed result be $T_1 + T_2$; then we have $|T_1 + T_2 - AB| \leq n^2u^2(1 + u)^{n-2}W$. This result can be interpreted as a midpoint-radius form. In the presentation, we will provide a detailed comparison of the computational efficiency and the tightness of the resulting enclosures with those achieved by BLAS-based approaches. Although **FastTwoFMA_s** involves four arithmetic operations, recent CPUs support simultaneously executing both fused multiply-add (FMA) and addition, and thus it is faster than four FMA operations.

References

[1] K. Ozaki, T. Ogita, and S. Oishi. Tight and efficient enclosure of matrix multiplication by using optimized BLAS. *Numerical Linear Algebra With Applications*, 18:237–248, 2011.

[2] K. Ozaki and T. Koizumi. Fast and accurate algorithm for matrix multiplication using fused multiply-add. *JSIAM Letters*, 17:13–16, 2025.

[3] C.-P. Jeannerod and S.M. Rump. Improved error bounds for inner products in floating-point arithmetic. *SIAM. J. Matrix Anal. & Appl. (SIMAX)*, 34:338–344, 2013.

[4] T. Koizumi, T. Tsumura, H. Irie, and S. Sakai. A fast implementation of perfect-accuracy double-precision exponential function. *IPSJ SIG Technical Report*, 2023-HPC-192(21): 1–12, 2023.

Parameter Robustness of Neural Networks

Attila Szász[1], Balázs Bánhelyi[1]

[1] University of Szeged
Institute of Informatics
Hungary
{szasz, banhelyi}@inf.u-szeged.hu

Keywords: Neural Networks, Robust Optimization, Interval Methods

Introduction

In recent years neural networks have received considerable attention both from researchers and end-users. They are applied in numerous domains, such as computer vision and speech recognition. Most research efforts have been directed toward developing increasingly accurate and reliable networks. To train reliable, or so-called robust networks, various training techniques have been proposed. The vast majority of these methods fall into two categories. Adversarial training-based algorithms [1] optimize the network parameters on adversarial examples. Certified training [2] methods, on the other hand, compute bounds on the network outputs and minimize the worst-case scenario inferred from these bounds. While most existing research has concentrated on input-space attacks, parameter-space attacks on networks have also come into focus, which manipulate the network's parameters to induce adversarial behavior. In response, training methods have been developed to incorporate parameter stability into the training process. Among these, the most widely used in the literature is the Adversarial Weight Perturbation [3] (AWP) method. However, its main drawback is that it significantly underestimates the worst-case scenario, resulting in insufficient protection against parameter-space attacks.

In this work, we identify the primary weakness of the AWP algorithm by introducing a certified training framework that, in many cases, increased the networks' resistance to parameter-space attacks.

Training algorithms

The goal of input-robust training is to minimize the expected loss within a p-norm bounded ball around the input point x: $B_p(x, \epsilon) = \{\check{x} \mid ||\check{x} - x||_p \leq \epsilon\}$.

$$\theta = \arg\min_{\theta} \mathbb{E}_{x,y}[\max_{\check{x} \in B_p(x,\epsilon)} L_\theta(\check{x}, y)] \tag{1}$$

Here, θ denotes the parameters of the neural network, L is the loss function, and ϵ is the radius around x within which robustness is desired. During training, the inner maximization problem is typically approximated using either gradient-based optimization (adversarial training) or interval-based methods (certified training). While certified training is generally more unstable, it offers higher provable robustness by eliminating the unreliability inherent in gradient-based approaches.

When parameter perturbations are also taken into account, the robust training objective in Equation 1 is extended as shown in Equation 2, where λ defines the radius of allowable parameter perturbations:

$$\theta = \arg\min_{\theta} \mathbb{E}_{x,y}[\max_{\check{\theta}\in B_{p_1}(\theta,\lambda),\ \check{x}\in B_{p_2}(x,\epsilon)} L_{\check{\theta}}(\check{x}, y)] \tag{2}$$

The Adversarial Weight Perturbation (AWP) algorithm approximates the nested maximization problem using an iterative, gradient-based optimization procedure, which leaves the model vulnerable to both input- and parameter-based attacks.

In this work, the Adversarial Parameter Propagation (APP) algorithm was proposed to mitigate the shortcomings of AWP. Our method combines gradient-based search with interval arithmetic to compute a more accurate approximation of the inner maximization problem, thereby improving robustness against input and parameter perturbations.

Results

Several neural networks were trained based on the CNN7 architecture for the CIFAR-10 image classification task, employing different values of the regularization parameter λ. As presented in Table 1, the proposed models show better performance on both clean and adversarial inputs compared to the AWP algorithm. The parameter robustness of our models was evaluated using the Adversarial Parameter Attack [4]. For smaller attack radii, our models demonstrated approximately 15% greater resistance, while for larger radii, we observed up to a 30% improvement in robustness.

ϵ	λ	Algorithm	Accuracy	Robust Accuracy
$\frac{2}{255}$	0.01	APP	63.8%	49.63%
		AWP	60.68%	44.16%
	0.02	APP	60.77%	48.18%
		AWP	58.1%	43.70%

Table 1: Clean and robust accuracy on the CIFAR-10 test set

References

[1] Madry, A., Makelov, A., Schmidt, L., Tsipras, D. & Vladu, A. Towards Deep Learning Models Resistant to Adversarial Attacks. (2019)

[2] Gowal, S., Dvijotham, K., Stanforth, R., Bunel, R., Qin, C., Uesato, J., Arandjelovic, R., Mann, T. & Kohli, P. On the Effectiveness of Interval Bound Propagation for Training Verifiably Robust Models. (2019)

[3] Wu, D., Shu-Xia & Wang, Y. Adversarial Weight Perturbation Helps Robust Generalization. (2020)

[4] Yu, L., Wang, Y. & Gao, X. Adversarial Parameter Attack on Deep Neural Networks. (2022)

Interval Based Verification of Adversarial Example Free Zones for Neural Networks

Tibor Csendes[1]

[1] University of Szeged and
University of Pannonia
H-6720 Szeged, Hungary
csendes@inf.u-szeged.hu

Keywords: Adversarial Example, Artificial Intelligence, Interval Arithmetic, Verification

Introduction

Recent machine learning models are sensitive to adversarial input perturbation. That is, an attacker may easily mislead an otherwise well-performing image classification system by altering some pixels. It is quite challenging to prove that a network will have correct output when changing slightly some regions of the images. This is why only a few works targeted this problem. Although there are an increasing number of studies in this field, really reliable robustness evaluation is still an open issue. We will present some theoretical results on the dependency problem of interval arithmetic critical in interval based verification.

Main results

We investigate the overestimation amounts we can face while evaluating trained, fully connected feed forward networks with the ReLU activation function. We study the situation when the weights of such a network are given as real numbers, we fix an input (e.g. a picture), and we test how large intervals around the input values can be verified to result in the same classification we obtained for the real case. In the next theoretical investigations we assume that interval arithmetic is calculated in the precise way, i.e. we exclude the effect of outwards rounding.

Proposition 1. *For a fully connected feed forward standard artificial neural network the overestimation size $w(F(X))-w(f(X))$ of the inclusion function can be zero only if at least one of the following conditions are fulfilled:*

- *all input intervals are of zero width: $w(x_i) = b - a = 0$,*
- *For each output, the weights associated with all input variables x_i have the same sign, either all nonnegative or all nonpositive, and*
- *all the final evaluation functions calculating the outputs of the network have negative arguments.*

These conditions are sufficient one by one, and a proper combination of them is also necessary.

Consider now the question which are the major factors for the overestimation sizes in the same setting.

Proposition 2. *For a fully connected feed forward standard artificial neural network of k input intervals, m neurons in each of the even number of n hidden layers, and all weights w_i bounded by $|w_i| \leq W$, the amount of overestimation $w(F(X)) - w(f(X))$ of the inclusion function of an output is not more than $2^{n/2} m^{n/2} W^n \sum_{i=1}^{k} w(X_i)$.*

Corollary 1. *A direct consequence of Proposition 2 is that we can have the same amount of overestimation due to the dependency problem with decreasing the number of hidden layers while increasing the number of neurons in a layer and vice versa.*

The main consequence of our theoretical study is that we can control the amount of overestimation caused by the dependency effect of interval arithmetic by forcing advantageous parameters such as low absolute bound of weights, or minimizing the number of hidden layers – while keeping the expected level of precision and recall.

Acknowledgement

This research was supported by the project Extending the activities of the HU-MATHS-IN Hungarian Industrial and Innovation Mathematical Service Network EFOP3.6.2-16-2017-00015, 2018-1.3.1-VKE-2018-00033, and by the Subprogramme for Linguistic Identification of Fake News and Pseudo-scientific Views, part of the Science for the Hungarian Language National Programme of the Hungarian Academy of Sciences (MTA).

References

[1] T. Csendes. An interval method for bounding level sets of parameter estimation problems. *Computing*, 41:75–86, 1989.

[2] T. Csendes. Interval Based Verification of Adversarial Example Free Zones for Neural Networks – Dependency Problem. *Annales Mathematicae et Informaticae*, 60:19–26, 2024.

[3] T. Csendes, N. Balogh, B. Bánhelyi, D. Zombori, R. Tóth, and I. Megyeri. Adversarial Example Free Zones for Specific Inputs and Neural Networks, Proc. of the 2020 ICAI, Eger, Hungary, https://ceur-ws.org/Vol-2650/paper9.pdf

[4] C. Szegedy, W. Zaremba, I. Sutskever, J. Bruna, D. Erhan, I.J. Goodfellow, and R. Fergus. Intriguing properties of neural networks. Proc. of the 2014 Int. Conf. on Learning Representations, doi: 10.48550/arXiv.1312.6199

[5] V. Tjeng, K. Xiao, and R. Tedrake. Evaluating Robustness of Neural Networks with Mixed Integer Programming. Proc. of the 2019 International Conference on Learning Representations, doi: 10.48550/arXiv.1711.07356

[6] D. Zombori, B. Bánhelyi, T. Csendes, I. Megyeri, and M. Jelasity. Fooling a complete neural network verifier. Proc. of the 2021 Int. Conf. on Learning Representations, https://openreview.net/forum?id=4IwieFS44l

Thursday, September 25, 2025

A01-0-006

11:00–12:30	**Regular Session B: Uncertainty Quantification**
11:00–11:30	Olga Kosheleva and Vladik Kreinovich: *Inconsistencies in Fuzzy Estimations: Kaucher Arithmetic Naturally Appears*
11:30–12:00	Miroslav Svitek, Olga Kosheleva and Vladik Kreinovich: *Shapley Value Under Interval Uncertainty Revisited: Why Seemingly Natural Axiomatic Approach Is Not Fully Adequate*
12:00–12:30	Luc Jaulin: *A new wrapper for a reliable resolution of underdetermined nonlinear equations*
14:30–16:00	**Regular Session B: Optimization**
14:30–15:00	Milan Hladík: *Linear Programming Problems with Absolute Values and Interval Uncertainty*
15:00–15:30	Cyril Kotecký and Milan Hladík: *Basis stability in interval quadratic programming*
15:30–16:00	Christophe Jermann, Nathalie Revol and Christine Solnon: *B&P algorithms for continuous constraint problems: a survey of branching strategies*
16:30–17:30	**Regular Session B: Dynamic Systems**
16:30–17:00	Ramiz Dilji, Bernd Tibken, Robert Dehnert, Youping Fan, Regina Deisling and Laura Ackerschott: *Estimation of the Domain of Attraction for Nonlinear Systems using the Bihari Inequality*
17:00–17:30	Andreas Rauh and Marit Lahme: *Observer-Based Approaches for a Verified Simulation and Pseudo State Estimation of Fractional Dynamic Systems*

Inconsistencies in Fuzzy Estimations: Kaucher Arithmetic Naturally Appears

Olga Kosheleva[1] and Vladik Kreinovich[2]

[1] Department of Teacher Education, University of Texas at El Paso
El Paso, TX 79968, USA, olgak@utep.edu
[2] Department of Computer Science, University of Texas at El Paso
El Paso, TX 79968, USA, vladik@utep.edu

Keywords: Fuzzy logic, Interval-values fuzzy logic, Intuitionistic Fuzzy Logic, Interval Uncertainty, Kaucher Arithmetic

Interval-values and Intuitionistic fuzzy logics: a brief reminder

When experts describes how they solve tasks – e.g., how expert drivers control their cars – they usually use imprecise ("fuzzy") words from natural language such as *small*. To describe this knowledge in precise computer-understandable terms, Lotfi Zadeh proposed to ask the expert to assign, to each possible value x of the corresponding property, a degree $m \in [0,1]$ to which x satisfies the property – e.g., to which x is small. He called this technique *fuzzy*.

Experts often use logical connectives $*$ – e.g., "and" and "or" – in describing their decisions. For example, a condition for a certain action may be that a car in front is close *and* that it brakes a little bit. To estimate the degree c of a statement $A * B$ based on degrees a and b of its component statements A and B, Zadeh proposed to take $c = f(a,b)$, where $f : [0,1] \times [0,1] \to [0,1]$ is a (non-strictly) increasing continuous function for which for $a, b \in \{0,1\}$, the value $f(a,b)$ is the usual truth value of the corresponding logical operation.

This approach led to many successes, but its representation of expert knowledge was not always perfectly adequate. Two ideas were proposed to make it more adequate. The first idea was to take into account that, just like an expert cannot describe the exact value of control – e.g., he/she only says "a little bit" – this same expert cannot meaningfully describe his/her degree of belief by a single number. The expert's opinion would be described more adequately if we allow the expert to use the interval $[\underline{m}, \overline{m}]$ of possible values. This is known as *interval-valued* fuzzy logic. In line with general interval techniques, once we know the degrees $[a] = [\underline{a}, \overline{a}]$ and $[b] = [\underline{b}, \overline{b}]$ of statements A and B, it is reasonable to estimate the degree of $A * B$ as $f([a],[b]) \stackrel{\text{def}}{=} \{a * b : a \in [a], b \in [b]\}$. Since $f(a,b)$ is increasing, this leads to $f([a],[b]) = [f(\underline{a},\underline{b}), f(\overline{a},\overline{b})]$.

The second idea was to take into account that when the expert is not 100% sure that x is small, this means that he/she also has arguments that x is not small. So, in addition to the degree m to which the property is true, it makes sense to also ask for the degree m_- to which this property is false. This is known as *intuitionistic* fuzzy logic. We assume that there is no inconsistency, so $m + m_- \le 1$. Then, when we have pairs (a, a_-) and (b, b_-) corresponding to A and B, it is reasonable to apply f

to a and b, and to apply a de Morgan-dual operation $g(a,b) \stackrel{\text{def}}{=} 1 - f(1-a, 1-b)$ to the values a_- and b_-.

These two ideas have a different meaning, but from the purely mathematical viewpoint, they are equivalent: we can map an interval $[\underline{x}, \overline{x}]$ to a pair $(\underline{x}, 1-\overline{x})$ and, vice versa, a pair (a, a_-) to an interval $[a, 1-a_-]$; then, all operations remain the same.

Accounting for possible inconsistencies naturally leads to Kaucher arithmetic

In some cases, there is an inconsistency between arguments for and against the same statement. In such cases, it makes sense to consider pairs (a, a_-) for which $a + a_- > 1$; see, e.g., [1]. If we apply the above-mentioned transformation $(a, a_-) \mapsto [a, 1-a_-]$ to such pairs, we get an "interval" $[\underline{a}, \overline{a}]$ for which $\underline{a} > \overline{a}$. In interval computations community, such intervals are known as *improper*, with special arithmetic – first proposed by Kaucher – extending interval arithmetic to such intervals.

As shown in [2], Kaucher arithmetic operations can be interpreted as follows: while the usual interval operations describe the set of all possible values $f(a,b)$ when $a \in [a]$ and $b \in [b]$, Kaucher operations describe the intersection of all possible ranges of $f(S)$ over all connected sets $S \subseteq [a] \times [b]$ whose projections to a- and b-axis are exactly $[a]$ and $[b]$.

Our main result is that for every non-strictly increasing function $f(a,b)$, the results of applying f to thus extended intuitionistic pairs correspond exactly to Kaucher arithmetic.

Other relations between fuzzy and Kaucher arithmetic

If we know the sets $[a]$ and $[b]$ of all possible values of a and b, then the set of all *potentially possible* values of $a + b$ is the interval sum $[a] + [b]$, while the Kaucher sum $[a] +_K [b]$ is the set of all *definitely possible* values. These two intervals are the simplest case of a family of embedded intervals – which is exactly what a fuzzy number is.

References

[1] L. V. Arshinsky, On te third forms of conjunction and disjunction in logic with vector semantics, *Ontology of Designing*, 2025, Vol. 15, No. 2, pp. 262–269 (in Russian).

[2] V. Kreinovich, V. M. Nesterov, and N. A. Zheludeva, Interval methods that are guaranteed to underestimate (and the resulting new justification of Kaucher arithmetic), *Reliable Computing*, 1996, Vol. 2, No. 2, pp. 119–124.

Shapley Value Under Interval Uncertainty Revisited: Why Seemingly Natural Axiomatic Approach Is Not Fully Adequate

Miroslav Svitek[1], Olga Kosheleva[2], and Vladik Kreinovich[3]

[1] Faculty of Transportation Sciences, Czech Technical University in Prague
110 00 Prague 1, Czech Republic, miroslav.svitek@cvut.cz
[2] Department of Teacher Education, University of Texas at El Paso
El Paso, TX 79968, USA, olgak@utep.edu
[3] Department of Computer Science, University of Texas at El Paso
El Paso, TX 79968, USA, vladik@utep.edu

Keywords: Shapley value, Machine Learning, Interval Uncertainty

Shapley value: a brief reminder

Many successes are due to collaboration, be it in manufacturing or in research. How to fairly divide the dividends between all n participants? For example, when we evaluate individual researchers, how to fairly distribute the overall points-for-paper between paper co-authors? In this division, it is reasonable to take into account what would be the productivity $v(S)$ if only participants from the set $S \subseteq N \stackrel{\text{def}}{=} \{1, \ldots, n\}$ worked together.

The answer to this question was produced by the future Nobelist Lloyd Shapley. He formulated natural conditions: additivity; symmetry; and that a person who does not contribute anything, i.e., for whom $v(S \cup \{i\}) = v(S)$ for all S, should not get anything. He proved that there is only one distribution scheme that satisfies these conditions, in which Person i gets the amount $x_i(v) = \sum a(|S|) \cdot (v(S \cup \{i\}) - v(S))$, where the sum is taken overall all sets S for which $i \notin S$, $|S|$ denoted the number of elements in a set S, and

$$a(m) \stackrel{\text{def}}{=} \frac{m! \cdot (n-m)!}{n!}.$$

This expression for $x_i(v)$ is known as the *Shapley value*.

Lately, Shapley value has also been actively used in machine learning, to decide which of n features used to make a decision are most important. In this case, $v(S)$ is the effectiveness that we get when we only use features from the set S.

Need for interval uncertainty

In practice, we rarely know the exact values $v(S)$. Often, we only know an interval $[v](S) = [\underline{v}(S), \overline{v}(S)]$ that contains $v(S)$. The agreement about division is usually decided before the project starts, in which case even the future value $v(N)$ is not known exactly.

In this case, a reasonable idea is to come up with intervals $[x]_i([v]) = [\underline{x}_i([v]), \overline{x}_i([v])]$. Then we can use Hurwicz approach and make a distribution

$$x_i(v) = \alpha \cdot \overline{x}_i(v) + (1-\alpha) \cdot \underline{x}_i(v),$$

where α is determined from the condition that the sum of these values should be equal to the overall amount $v(N)$ – the overall monetary amount or the overall number of points for this particular paper.

Current interval method and its limitation

The paper [1] considers similar conditions to Shapley's and shows that under these conditions, we should take, as bounds on $x_i([v])$, the Shapley values corresponding to the functions $\underline{v}(S)$ and $\overline{v}(S)$. In many cases, this approach leads to reasonable results, but in other cases, it does not.

For example, for $n = 2$, if $\underline{v}(S) = 0$ for all S, $\overline{v}(\emptyset) = \overline{v}(\emptyset) = \overline{v}(\{x_2\}) = 0$, and $\overline{v}(\{x_1\}) = \overline{v}(\{1, 2\}) = 1$, then Person 2 gets nothing, although it is possible, e.g., that the actual values are $v(\{1, 2\}) = 1$ and $v(\{1\}) = v(\{2\}) = 0$, in which case, due to symmetry, Person 2 should get exactly the same amount as Person 1.

Analysis of the problem and resulting solution

The reason for the above problem is that while the condition that $v(S \cup \{i\}) = v(S)$ for all S indeed means that i did not contribute anything, but, as the above example shows, a similar interval equality $[v](S \cup \{i\}) = [v](S)$ for all S does not necessarily imply that Person i was not contributing.

So, a natural idea is to take, as $[x]_i([v])$, the set of all possible values $x_i(v)$ for all functions v for which $v(S) \in [v](S)$ for all S. To find these intervals, let us take into account that the Shapley value formula can be reformulated as

$$x_i(v) = \sum_{S: i \in S} a(|S| + 1) \cdot v(S) - \sum_{S: i \notin S} a(|S|) \cdot v(S).$$

Thus, by using usual interval computations, we get:

$$\underline{x}_i([v]) = \sum_{S: i \in S} a(|S| + 1) \cdot \underline{v}(S) - \sum_{S: i \notin S} a(|S|) \cdot \overline{v}(S);$$

$$\overline{x}_i([v]) = \sum_{S: i \in S} a(|S| + 1) \cdot \overline{v}(S) - \sum_{S: i \notin S} a(|S|) \cdot \underline{v}(S).$$

References

[1] K. Autchariyapanikul, O. Kosheleva, and V. Kreinovich, "Shapley value under interval uncertainty and partial information", In: V. Kreinovich, W. Yamaka, and S. Leurcharusmee (eds.), *Data Science for Econometrics and Related Topics*, Springer, Cham, Switzerland, to appear.

A new wrapper for a reliable resolution of underdetermined nonlinear equations

Luc Jaulin

ENSTA, Lab-STICC, France
lucjaulin@ensta.fr

Keywords: Nonlinear equations, Underdetermined system, Interval Methods

Introduction

This paper introduces a new wrapper called a *buche*, the French name for *log* (think of logs made from a straight trunk obliquely and bluntly cut with an axe). Buches are used to enclose a part of the solution set defined by nonlinear equations. We show that buches, combined with interval methods [2], may allow us to obtain a better accuracy for the approximation with less computations.

Notion of buche

The *buche* associated with a box $[\mathbf{x}] \subset \mathbb{R}^n$, a matrix $\mathbf{A}$, a vector $\mathbf{b}$ and the inflation rate ρ is the set $\langle \mathbf{x} \rangle$ defined by

$$\begin{array}{rcl} \langle \mathbf{x} \rangle & = & \langle [\mathbf{x}], \mathbf{A}, \mathbf{b}, \rho \rangle \\ & = & \{ \mathbf{x} \in [\mathbf{x}], \exists \mathbf{p}, \mathbf{A}\mathbf{p} = \mathbf{b} \text{ and } \|\mathbf{x} - \mathbf{p}\| < \rho \} \, . \end{array} \tag{1}$$

An illustration is given by the figure below. The quantity $\rho = \text{rad}(\langle \mathbf{x} \rangle)$ is called the *radius* of the buche $\langle \mathbf{x} \rangle$. The affine space $\mathbf{A}\mathbf{p} = \mathbf{b}$ is called a *flat*.

Our motivation for using buches is to have the following properties

- The box $[\mathbf{x}]$ in the structure of the buche will allow us to build a nonoverlapping covering of $\mathbb{X}$. This is not the case for zonotopes [4], [1].
- A buche can easily be bisected, contrary to ellipsoids [3].
- The axis-aligned projection is easy with buches, contrary to polyhedrons.
- A first order approximation is possible, contrary to boxes.

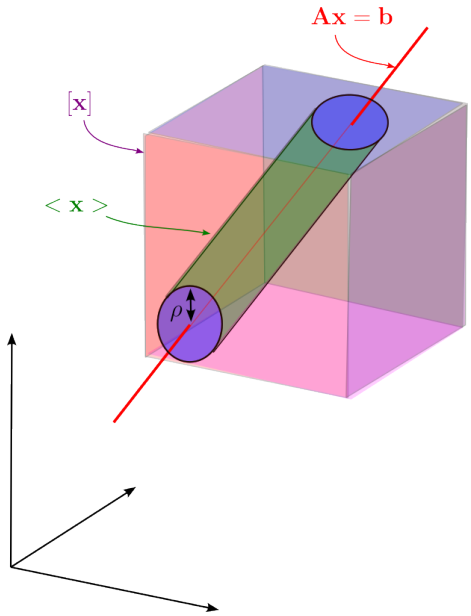

The buche (green) of the picture corresponds to the intersection between the box $[\mathbf{x}]$ and a cylinder

Contribution

Buches will be used to represent the solution set of an underdetermined set of non-linear equations. It will be shown that the use of buches makes it possible to increase the accuracy of the approximation of the solution set compared to classical interval techniques.

References

[1] C. Combastel. A state bounding observer for uncertain non-linear continuous-time systems based on zonotopes. In *44th IEEE Conference on Decision and Control*, 2005.

[2] R. Moore. *Methods and Applications of Interval Analysis*. Society for Industrial and Applied Mathematics, jan 1979.

[3] A. Rauh, J. Soueidan, S. Rohou, and L. Jaulin. Experimental validation of an ellipsoidal state estimation procedure for a magnetic levitation system. In *IFAC World Congress*, 2023, Yokohama, Japan. pp.8494-8499.

[4] J. Wan. *Computationally reliable approaches of contractive model predictive control for discrete-time systems*. PhD dissertation, Universitat de Girona, Girona, Spain, 2007.

Linear Programming Problems with Absolute Values and Interval Uncertainty

Milan Hladík[1]

[1] Charles University, Faculty of Mathematics and Physics
Department of Applied Mathematics
Malostranské nám. 25, 11800, Prague, Czech Republic
hladik@kam.mff.cuni.cz

Keywords: Linear Programming, Nonlinear Programming, Interval Analysis

Introduction

Absolute value linear programming (AVLP) problems [2, 3] are mathematical programming problems involving linear functions and absolute values. They can be expressed in a canonical form as follows

$$f(A,b,c,D) = \max\ c^T x \ \text{ subject to } \ Ax - D|x| \le b,$$

where $c \in \mathbb{R}^n$, $b \in \mathbb{R}^m$ and $A, D \in \mathbb{R}^{m\times n}$. We assume that $D \ge 0$; otherwise the negative coefficients can be equivalently reformulated by linear constraints. Note that the absolute values make the problem NP-hard.

We study the variations of the optimal value $f(A,b,c,D)$ when the input coefficients vary in the interval domains. Concretely, let interval vectors $\mathbf{c}$, $\mathbf{b}$ and interval matrices $\mathbf{A}, \mathbf{D}$ be given. Then the corresponding interval AVLP problem is a family of AVLP problems with $A \in \mathbf{A}$, $b \in \mathbf{b}$, $c \in \mathbf{c}$ and $D \in \mathbf{D}$.

Notation. Intervals, interval vectors and matrices are defined by their lower and upper bounds, such as $\mathbf{A} = [\underline{A}, \overline{A}]$, or by its midpoint and radius matrices, such as $\mathbf{A} = [A_c - A_\Delta, A_c + A_\Delta]$. We also make use of the Rohn's shortcuts: for an interval matrix $\mathbf{A}$, $r \in [-1,1]^m$ and $s \in [-1,1]^n$, we define

$$A_{r,s} = A_c - \operatorname{diag}(r) A_\Delta \operatorname{diag}(s) \in \mathbf{A},$$

and for an interval vector $\mathbf{c}$ and $s \in [-1,1]^n$, we define

$$c_s = c_c + \operatorname{diag}(s) c_\Delta \in \mathbf{c}.$$

Range of optimal values. The goal is to compute the best and the worst case optimal values defined, respectively, as

$$\overline{f} = \max\ f(A,b,c,D) \ \text{ subject to } \ A \in \mathbf{A},\ b \in \mathbf{b},\ c \in \mathbf{c},\ D \in \mathbf{D},$$
$$\underline{f} = \min\ f(A,b,c,D) \ \text{ subject to } \ A \in \mathbf{A},\ b \in \mathbf{b},\ c \in \mathbf{c},\ D \in \mathbf{D}.$$

This problem was thoroughly discussed for interval-valued linear programming problems [1] and certain types of interval nonlinear programming problems. However, for the AVLP problems, it seems that the optimal value range has not been investigated so far.

We assume that $\underline{D} \ge 0$. Basically, this assumption is without loss of generality, but simplifies the overall analysis.

Main results

Best case optimal value. The best case optimal value $\overline{f}$ can be completely characterized by means of a reduction to one real AVLP problem.

Proposition 1. *We have*

$$\overline{f} = \max\ c_c^T x + c_\Delta^T x \quad \textit{subject to} \quad A_c x - (A_\Delta + \overline{D})|x| \leq \overline{b}.$$

Worst case optimal value. A closed-form characterization of $\underline{f}$ is unknown so far. We can fix $b = \underline{b}$ and $D = \underline{D}$, since the worst case optimal value is attained in this setting. The other interval coefficients are much more difficult to handle. Nevertheless, we propose a convenient lower bound formula.

Proposition 2. *We have*

$$\underline{f} \geq \underline{f}^L,$$

where

$$\underline{f}^L = \max\ c_c^T x - c_\Delta^T |x| \quad \textit{subject to} \quad A_c x + (A_\Delta - \underline{D})|x| \leq \underline{b}.$$

The lower bound $\underline{f}^L$ may or may not be tight. However, under certain assumptions we can prove $\underline{f} = \underline{f}^L$.

Proposition 3. *Let s^* be the sign of the optimal solution for $\underline{f}^L$. If the optimal solution to*

$$f(A_{e,-s^*}, c_{-s^*}) = \max\ c_{-s^*}^T x \quad \textit{subject to} \quad A_{e,-s^*} x - \underline{D}|x| \leq \underline{b}$$

has the same sign s^*, then $\underline{f} = \underline{f}^L$.

Acknowledgement

The author was supported by the Czech Science Foundation Grant 25-15714S.

References

[1] M. Hladík. Interval linear programming: A survey. In Z. A. Mann, editor, *Linear Programming – New Frontiers in Theory and Applications*, chapter 2, pages 85–120. Nova Science Publishers, New York, 2012.

[2] M. Hladík and D. Hartman. Absolute value linear programming. preprint arXiv: 2307.03510, 2023.

[3] O. L. Mangasarian. Absolute value programming. *Comput. Optim. Appl.*, 36(1):43–53, 2007.

Basis stability in interval quadratic programs

Cyril Kotecký, Milan Hladík

Charles University
Faculty of Mathematics and Physics
Department of Applied Mathematics
Malostranské náměstí 25, Prague, Czech Republic
kotecky@kam.mff.cuni.cz, hladik@kam.mff.cuni.cz

Keywords: Quadratic programming, Basis stability, Interval Methods

Introduction

Basis stability is a topic that is well studied in the domain of interval linear programs [1], [2]. We define the stability of a given interval linear program with respect to a given basis as the condition that the basis is optimal for all realizations. There are some useful consequences of basis stability in some of the formulations, including the convexity of the set of optimal solutions.

The idea of generalizing basis stability is nothing new, one example is [3], where the authors define the notion of basis stability for the class of non-linear non-negative convex problems and describe its consequences. But there is still a lot of insight to be gained by applying the array of results in the area of interval analysis, namely characterizations of strong solvability and study of linear systems with linear parametric dependencies.

Our results

We propose a generalized definition of basis stability for the case of interval convex quadratic programs of the following forms

$$\min \frac{1}{2}x^T Qx + q^T x : Ax \leq b, \tag{A}$$

$$\min \frac{1}{2}x^T Qx + q^T x : Ax = b, x \geq 0, \tag{B}$$

$$\min \frac{1}{2}x^T Qx + q^T x : Ax \leq b, x \geq 0. \tag{C}$$

where Q is positive definite. We also examine the general form combining both equations and inequalities with both non-negative and free variables and the case with convex quadratic inequality constraints.

Consulting the KKT optimality conditions, we can define a basis analogously to that in the case of linear programs. The KKT conditions then yield a linear or a quadratic system of equations and inequalities which characterizes the optimality of the given basis.

If we now let the coefficients of Q, q, A, b vary within some intervals, we can thus define an interval quadratic program as a set of real quadratic programs. The

notion of basis stability now means a given basis is optimal for each real quadratic program from the given set, and stability under a given basis can now be characterized by the strong solvability of the interval version of the KKT system with some linear parametric dependencies.

The situation is however much less favorable than in the case of interval linear programming. The interval version of the KKT system has linear parametric dependencies, which greatly increases the complexity of verifying basis stability. On the other hand, for quadratic interval linear programs, basis stability does not guarantee convexity of the set of optimal solutions for any of the forms.

Under basis stability, we are still however guaranteed compactness and connectedness of the set of optimal solutions and we examine various special cases, where we can avoid parametric dependencies in the characterizing system and check basis stability more efficiently.

Acknowledgement

The authors were supported by the Czech Science Foundation Grant 25-15714S.

References

[1] M. Hladík. How to determine basis stability in interval linear programming. *Optim. Lett.*, 8(1):375–389, 2014a. ISSN 1862-4472. doi: 10.1007/s11590-012-0589-y. URL `https://doi.org/10.1007/s11590-012-0589-y`.

[2] M. Hladík. Interval Linear Programming and Extensions. *Springer, Cham*, 2025. ISSN 1931-6828. doi: 10.1007/978-3-031-85096-7. URL `https://doi.org/10.1007/978-3-031-85096-7`.

[3] D. Oelschlägel and H. Süße Interval Analytic Treatment of Convex Programming Problems. *Comput.*, 24 (2):213–225, 1980.

B&P algorithms for continuous constraint problems: a survey of branching strategies

Christophe Jermann[1], Nathalie Revol[2] and Christine Solnon[3]

[1] Nantes Université, École Centrale Nantes, CNRS
LS2N, UMR 6004, F-44000 Nantes, France
christophe.jermann@ls2n.fr
[2] INRIA, Pascaline team - LIP, UMR 5668 - ENS de Lyon, France
Nathalie.Revol@ens-lyon.fr
[3] INSA, Émeraude team - CITI
Villeurbanne, France
Christine.Solnon@insa-lyon.fr

Keywords: Discrete CSP, Continuous CSP, Branch-and-Propagate, Branch-and-Prune, Branching, Heuristics, Interval Methods

Introduction

We focus on Constraint Satisfaction Problems (CSPs) defined by a triple (X, D, C) such that $X = \{x_1, \ldots, x_n\}$ is a set of n variables, $D(x_i)$ is the domain of each variable $x_i \in X$, and $C = \{C_1, \ldots, C_m\}$ is a set of constraints such that each constraint is a relation defined over a subset of X. When variable domains are finite sets, the problem is called a *discrete CSP*; when they are intervals in $\mathbb{R}$, it is called a *continuous CSP*. A solution is a set of values $\{v_1, \ldots, v_n\}$ such that $v_i \in D(x_i)$ for each variable $x_i \in X$ and each constraint in C is satisfied, *i.e.*, the relation is verified for these values. The principle of algorithms solving a CSP, be it discrete or continuous, is *Branch-and-Propagate* or *Branch-and-Prune*: Branch involves selecting a variable and partitioning its domain to create subproblems that are recursively solved; Propagate/Prune involves exploiting constraints to reduce domains by removing inconsistent values.

In this work we survey the *Branch* procedure: our goal is to identify the heuristics that are successfully used to solve discrete CSPs, in order to determine if they could be useful for continuous CSPs. The *Propagate/Prune* procedure is already well studied for continuous CSPs and will not be addressed here.

Classical strategies

For continuous CSPs, *branching* usually means splitting a box into two subboxes and exploring each of them in turn. The algorithm maintains a list of boxes waiting to be explored. To ensure convergence of the algorithm, Neumaier in [8] suggests to choose either the oldest box and to bisect its oldest side, or to choose the largest box and to bisect its longest side. When the constraints appear in a global optimization problem, a classical choice [5] is to evaluate the cost function f on each box X in the waiting list: $f(\mathrm{X}) = [\underline{f}(\mathrm{X}), \bar{f}(\mathrm{X})]$, and to choose the one with the least $\underline{f}(\mathrm{X})$ (resp. $\bar{f}(\mathrm{X})$) in case of minimization (resp. maximization) problem.

Heuristics inspired from discrete CSP solving

A principle widely adopted for discrete CSPs is the fail-first principle. It has been adapted for continuous CSPs, e.g. in [1] as the "relative smear-based" strategy: the chosen variable is the one leading to the largest variation of some constraint.

Another principle widely adopted to solve discrete CSPs is the random restart, so that the search is not stuck in a long and inefficient branch. We are not aware of many similar approaches for continuous CSPs; however, partly random diversification search strategies for continuous CSPs were proposed in [3].

Along with random restarts goes the storage of a summary of the non-conclusive branches explored so far, known as "nogood recording" [6], with no direct equivalent for continuous CSPs.

Adaptive strategies

For discrete CSPs, adaptive strategies have been adopted. They consist in attaching a weight to each constraint and in increasing this weight when the corresponding constraint leads to a wipe-out of some domain [2]. Weights can also decrease with time, as some constraints are more useful to prune the domain when the search begins and some are more useful later: this is called *a decaying strategy*, see [7] which also gives a survey of classical strategies for discrete CSPs.

For continuous CSPs, reinforcement learning is introduced in [4].

References

[1] I. Araya, V. Reyes. C. Oreallana. More smear-based variable selection heuristics for NCSPs. In *ICTAI 2013*, 1004-1011, 2013.

[2] F. Boussemart, F. Hemery, C. Lecoutre, L. Sais. Boosting systematic search by weighting constraints. In *ECAI 2004*, 16(146):91-96, 2004.

[3] R. Chenouard and A. Goldsztejn and C. Jermann. Search strategies for an anytime usage of the branch and prune algorithm. In *International joint conference in artificial intelligence (IJCAI)*, 468-473, 2009.

[4] F. Goualard, C. Jermann. A reinforcement learning approach to interval constraint propagation. *Constraints* 13(1): 206-226, 2008.

[5] E. Hansen. *Global optimization using interval analysis*. Marcel Dekker, 1992.

[6] J. H. M. Lee, C. Schulte, Z. Zhu. Increasing nogoods in restart-based search. In *AAAI 2016*, 30(1), 2016.

[7] H. Li, M. Yin, Z. Li. Failure Based Variable Ordering Heuristics for Solving CSPs. In *Constraint Programming (CP 2021)*, p. 9-1, 2021.

[8] A. Neumaier. Complete search in continuous global optimization and constraint satisfaction. *Acta numerica*, 13:271-369, 2004.

Estimation of the Domain of Attraction for Nonlinear Systems using the Bihari Inequality

Ramiz Dilji, Bernd Tibken, Robert Dehnert, Youping Fan, Regina Deisling and Laura Ackerschott

University of Wuppertal
Institute of Automatic Control
D-42119 Wuppertal, Germany
{dilji,tibken,dehnert,yofan,deisling,laura.ackerschott}@uni-wuppertal.de

Keywords: stability analysis, nonlinear systems, integral inequalities

Introduction

In this contribution, we apply a long and well known integral inequality to the stability analysis of nonlinear systems. The main focus is on nonlinear systems with the state space representation

$$\dot{\boldsymbol{x}} = \boldsymbol{A}\boldsymbol{x} + \boldsymbol{g}\left(\boldsymbol{x}\right), \quad \boldsymbol{x}\left(0\right) = \boldsymbol{x}^0, \tag{1}$$

where $\boldsymbol{x} \in \mathbb{R}^n$ represents the state vector, $\boldsymbol{A} \in \mathbb{R}^{n\times n}$ is assumed to be Hurwitz, $\boldsymbol{g}$ represents the nonlinear part of the system starting with quadratic terms, and $\boldsymbol{x}^0$ is the initial condition, respectively. Note that in this work, matrices appear as bold italic uppercase letters, column vectors as bold italic lowercase letters, and scalars as italic lowercase letters.

We assume that the solutions of system (1) exist for all $t \geq 0$. Due to the eigenvalue condition of $\boldsymbol{A}$, the origin is asympotically stable, and the problem of estimating the domain of attraction arises. Using the well known method of Lyapunov is the main approach to tackle this problem. In this abstract, we will use a different approach based on the following theorem of Bihari [1].

Theorem 1. *Let u be a non-negative, continuous function satisfying*

$$u\left(t\right) \leq \alpha + \int_0^t f\left(s\right)\, w\left(u\left(s\right)\right)\, ds, \qquad t \in \left[0, \infty\right), \tag{2}$$

where $\alpha \geq 0$ is a constant, f is a non-negative continuous function and w is a continuous non-decreasing function with $w(u) > 0$ for all $u > 0$. Then it holds that

$$u\left(t\right) \leq G^{-1}\left(G\left(\alpha\right) + \int_0^t f\left(s\right)\, ds\right), \qquad t \in \left[0, T\right], \tag{3}$$

where G^{-1} is the inverse function of

$$G\left(x\right) = \int_{x_0}^{x} \frac{dy}{w\left(y\right)}, \qquad x \geq 0,\, x_0 > 0,$$

and T is determined such that the expression inside G^{-1} in inequality (3) remains within the domain of G^{-1} for all $t \in [0, T]$.

Application to the Nonlinear State Space Representation

The nonlinear system (1) is equivalent to the following integral equation

$$\boldsymbol{x}(t) = e^{\boldsymbol{A}t}\,\boldsymbol{x}^0 + \int_0^t e^{\boldsymbol{A}(t-\tau)}\,\boldsymbol{g}(\boldsymbol{x}(\tau))\,d\tau.$$

Taking the norm on both sides, we obtain

$$\|\boldsymbol{x}(t)\| \leq M\,\|\boldsymbol{x}(0)\|\,e^{-\beta t} + MC\,e^{-\beta t}\int_0^t e^{-\beta\tau}\,u(\tau)^2\,d\tau, \tag{4}$$

where $M > 0$, $\beta > 0$ and $C > 0$ are constants. Here, M and β arise from the bound

$$\|e^{\boldsymbol{A}t}\| \leq M\,e^{-\beta t},$$

and C provides an upper bound for the nonlinear term according to

$$\|\boldsymbol{g}(\boldsymbol{x}(\tau))\| \leq C\,\|\boldsymbol{x}(\tau)\|^2.$$

The constant β corresponds to the absolute value of the real part of the rightmost eigenvalue of the matrix $\boldsymbol{A}$. This choice of β ensures exponential decay of the linear part. Ideally, β should be as large as possible, while M and C should be as small as possible to ensure tight estimates. Introducing the substitutions

$$u(t) = e^{\beta t}\,\|\boldsymbol{x}(t)\|, \quad \alpha = M\,\|\boldsymbol{x}(0)\|, \quad f(\tau) = MC\,e^{-\beta\tau}, \quad \text{and} \quad w(y) = y^2,$$

we can now rewrite system (1) into inequality (2). This allows the use of inequality (3), which provides

$$u(t) \leq \frac{1}{\frac{1}{M\,\|\boldsymbol{x}(0)\|} - \frac{MC}{\beta}\left(1 - e^{-\beta t}\right)}.$$

For this inequality to be valid, the denominator on the right-hand side must remain positive. Taking the limit as $t \to \infty$, we obtain the condition

$$\|\boldsymbol{x}(0)\| \leq \frac{\beta}{M^2 C},$$

which provides an estimation of the domain of attraction for system (1). This estimate can, under certain circumstances, be larger than the one obtained using Lyapunov's method, which corresponds to a more precise estimate of the domain of attraction. This is caused by the fact that any matrix norm can be used to build the inequality (4). By contrast, Lyapunov's method usually requires a symmetric, positive-definite matrix to define the norm. This can result in conservative estimates of the domain of attraction, whereas the novel approach can provide a less conservative estimate.

References

[1] I. Bihari. A generalization of a lemma of Bellman and its application to uniqueness problems of differential equations. *Acta Mathematica Academiae Scientiarum Hungaricae* 7, 81–94 (1956). https://doi.org/10.1007/BF02022967

Estimation of the Domain of Attraction for Nonlinear Systems using the Bihari Inequality

Ramiz Dilji, Bernd Tibken, Robert Dehnert, Youping Fan, Regina Deisling, Laura Ackerschott

1 Problem Statement

- Stability analysis of nonlinear systems with state-space representation

$$\dot{\boldsymbol{x}} = \boldsymbol{A}\,\boldsymbol{x} + \boldsymbol{g}(\boldsymbol{x}), \quad \boldsymbol{x}(0) = \boldsymbol{x}_0 \tag{1}$$

$\boldsymbol{x} \in \mathbb{R}^n$: state vector
$\boldsymbol{A} \in \mathbb{R}^{n\times n}$: system matrix, assumed to be Hurwitz
$\boldsymbol{g}$: nonlinear part, starting with quadratic terms
$\boldsymbol{x}_0$: initial condition

- Due to eigenvalue condition of $\boldsymbol{A}$, the origin is asymptotically stable
- Goal: Estimation of the domain of attraction for the origin
- Classical approach: Lyapunov's method
  → requires a symmetric, positive-definite matrix to define the norm
  → can lead to conservative estimates of the domain of attraction for nonlinear systems

2 Theorem of Bihari

Let u be a non-negative, continuous function satisfying

$$u(t) \le \alpha + \int_0^t f(s)\, w(u(s))\, ds, \qquad t \in [0,\infty), \tag{2}$$

where $\alpha \ge 0$ is a constant, f is a non-negative continuous function and w is a continuous non-decreasing function with $w(u) > 0$ for all $u > 0$. Then it holds

$$u(t) \le G^{-1}\left(G(\alpha) + \int_0^t f(s)\, ds\right), \qquad t \in [0,T], \tag{3}$$

where G^{-1} is the inverse function of

$$G(x) = \int_{x_0}^{x} \frac{dy}{w(y)}, \qquad x \ge 0,\ x_0 > 0,$$

and T is determined such that the expression inside G^{-1} in inequality (3) remains within the domain of G^{-1} for all $t \in [0,T]$.

3 Application

- Equivalent integral equation of nonlinear system (1):

$$\boldsymbol{x}(t) = e^{\boldsymbol{A}t}\,\boldsymbol{x}_0 + \int_0^t e^{\boldsymbol{A}(t-\tau)}\,\boldsymbol{g}(\boldsymbol{x}(\tau))\,d\tau$$

- Estimation of the norm:

$$\|e^{\boldsymbol{A}t}\| \le M\, e^{-\beta t}$$

$$\|\boldsymbol{g}(\boldsymbol{x}(\tau))\| \le C\,\|\boldsymbol{x}(\tau)\|^2$$

$M > 0,\ \beta > 0,\ C > 0$: constants

- Taking the norm:

$$\|\boldsymbol{x}(t)\| \le M\,\|\boldsymbol{x}(0)\|\, e^{-\beta t} + MC\, e^{-\beta t} \int_0^t e^{-\beta\tau}\, u(\tau)^2\, d\tau$$

- Rewrite System (1) into inequality (2) by introducing the following substitutions

$$u(t) = e^{\beta t}\,\|\boldsymbol{x}(t)\|, \quad \alpha = M\,\|\boldsymbol{x}(0)\|,$$

$$f(\tau) = MC\, e^{-\beta\tau}, \quad w(y) = y^2$$

- The use of inequality (3) results in

$$u(t) \le \frac{1}{\frac{1}{M\,\|\boldsymbol{x}(0)\|} - \frac{MC}{\beta}\left(1 - e^{-\beta t}\right)}$$

- For this inequality to be valid, the denominator must remain positive. Taking the limit as $t \to \infty$ leads to the condition

$$\|\boldsymbol{x}(0)\| \le \frac{\beta}{M^2 C}$$

- Enables estimation of the domain of attraction for system (1)

4 Example

System: $\dot{\boldsymbol{x}} = \begin{pmatrix} 0 & 1 \\ -2 & -3 \end{pmatrix}\boldsymbol{x} + \begin{pmatrix} -2x_1^2 - 3x_1x_2 \\ -2x_1x_2 - 3x_2^2 \end{pmatrix}$

$M = 3.162277$	$\beta = 1.000000$	$C = 3.605551$	$\|\boldsymbol{x}(0)\| = 0.027735$

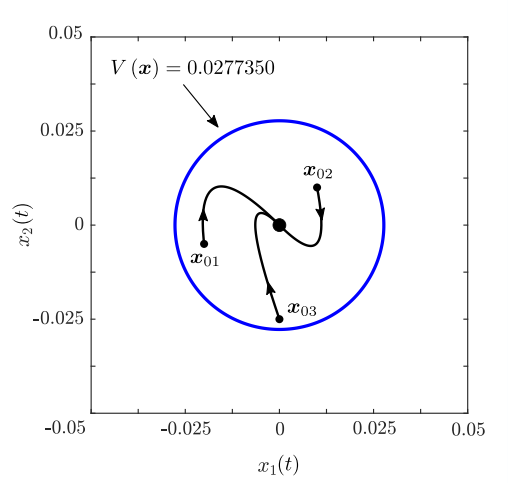

5 Conclusion / Outlook

- Novel approach
- Application of Bihari's Theorem for estimation of the domain of attraction
- Reformulates the problem into an integral inequality
- Provides an explicit bound on system trajectories $\boldsymbol{x}_0$
- Any matrix norm that satisfies the triangle inequality is acceptable
  → a positive-definite matrix is not required
  → here, for example, the Euclidean matrix norm was used for the presented example
- Can provide a less conservative estimate than Lyapunov's method
- Easier to compute, no hard optimization problem needs to be solved

6 References

[1] I. Bihari. A generalization of a lemma of Bellman and its application to uniqueness problems of differential equations. *Acta Mathematica Academiae Scientiarum Hungaricae* 7, 81-94 (1956). https://doi.org/10.1007/BF02022967

University of Wuppertal
Chair of Automatic Control
Prof. Dr.-Ing. Bernd Tibken

Rainer-Gruenter-Str. 21
42119 Wuppertal, Germany

School of Electrical, Information and Media Engineering

BERGISCHE UNIVERSITÄT WUPPERTAL

Observer-Based Approaches for a Verified Simulation and Pseudo State Estimation of Fractional Dynamic Systems

Andreas Rauh and Marit Lahme

Carl von Ossietzky Universität Oldenburg
Distributed Control in Interconnected Systems
D-26111 Oldenburg, Germany
{andreas.rauh,marit.lahme}@uni-oldenburg.de

Keywords: Fractional dynamic systems, Finite memory approximation, Verified state estimation

Introduction

Fractional system models [1, 3] have gained in importance during recent years. They account for non-standard dynamics with long-term memory effects. Such kind of dynamics can be found, for example, in electrochemical energy converters such as batteries and fuel cells. Despite capturing infinite horizon memory properties, the numerical evaluation may be complicated by a continuous increase in memory and computing time if no appropriate countermeasures are taken. This is especially critical in the frame of (pseudo) state estimation, where a periodic integrator reset takes place to limit both memory demand and computing times in real-time applications. Additionally, such resets occur when predictor–corrector state estimators are employed for systems with bounded uncertainty.

Solution Approach

This contribution provides an extension of recent work [4], in which the authors have proposed a novel method that allows for estimating errors in a set-based form that result from truncating the memory of fractional system simulators to a finite length. The general idea is based on error bounds published in [3] for Riemann-Liouville fractional differential equations. It is then extended by an interval observer similar to the one in [1] after including the approximation errors by means of integrator disturbance models. A verified enclosure of the solution sets becomes possible after converting the point-valued observer of Theorem 1 into a set-based formulation, cf. [4].

Theorem 1 ([4] Point-Valued Observer for Truncation Errors)**.** *The fractional differential equation model (derivative order $0 < \nu \leq 1$, initialized at $t_0 + T$)*

$$\begin{bmatrix} {}_{t_0+T}\mathcal{D}_t^{(\nu)}\hat{\mathbf{z}}(t) \\ {}_{t_0+T}\mathcal{D}_t^{(\nu)}\hat{\boldsymbol{\mu}}(t) \end{bmatrix} = \begin{bmatrix} \mathbf{f}\left(\hat{\mathbf{z}}(t)\right) + \hat{\boldsymbol{\mu}}(t) \\ \mathbf{0} \end{bmatrix} + \mathbf{H} \cdot \left(\mathbf{y}_{\mathrm{m}}(t) - \hat{\mathbf{y}}(t)\right) \tag{1}$$

with $\hat{\mathbf{z}}(t) = \mathbf{0}$ for $t \leq t_0 + T$ is an observer for state ($\hat{\mathbf{z}}$) and additive truncation error reconstruction ($\hat{\boldsymbol{\mu}}$) after an integrator reset at the point $t_0 + T$ with the sensor data $\mathbf{y}_{\mathrm{m}}(t)$ and the associated measurement model $\hat{\mathbf{y}}(t) = \mathbf{h}\left(\hat{\mathbf{z}}(t)\right)$. For stability, the gain $\mathbf{H}$ needs to be chosen so that the error dynamics are asymptotically stable.

Fig. 1 gives an example for the observer-based state reconstruction and truncation error estimation for the system model $x^{(0.5)}(t) = -x(t) + u(t)$, $z(t) = x(t) - x(t_0 + T)$, $u(t) = 1$ with the fractional differentiation order 0.5. It further contains a comparison between the integrator resetting with and without the proposed observer approach (obs.) and the true pseudo state evolution.

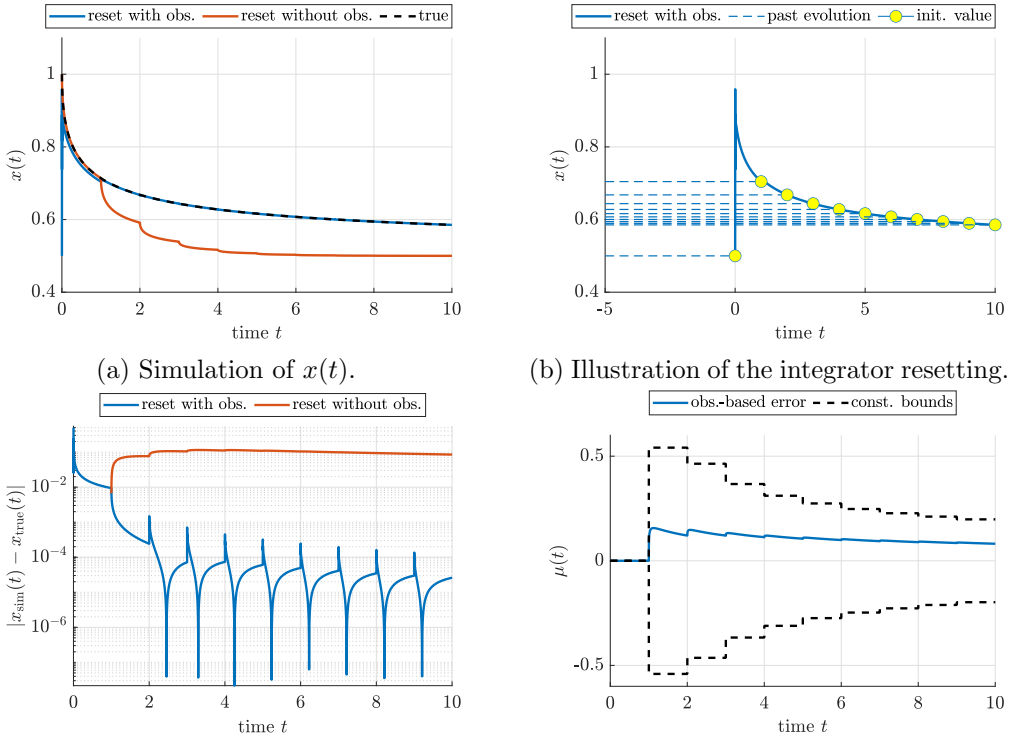

(a) Simulation of $x(t)$.

(b) Illustration of the integrator resetting.

(c) Approximation error of $x(t)$.

(d) Truncation error $\mu(t)$.

Figure 1: Illustration of the observer-based state and truncation error estimation.

References

[1] E. Hildebrandt, J. Kersten, A. Rauh, and H. Aschemann. Robust Interval Observer Design for Fractional-Order Models with Applications to State Estimation of Batteries, Proc. of the 21st IFAC World Congress, Berlin, Germany, 2020.

[2] G. Bel Haj Frej, R. Malti, M. Aoun, and T. Raïssi. *Fractional Interval Observers and Initialization of Fractional Systems.* Communications in Nonlinear Science and Numerical Simulation, 82:105030, 2020.

[3] I. Podlubny. *Fractional Differential Equations: An Introduction to Fractional Derivatives, Fractional Differential Equations, to Methods of Their Solution and Some of Their Applications.* Mathematics in Science and Engineering, Academic Press, London, 1999.

[4] A. Rauh and M. Lahme. A Finite Memory Approach Applied to Verified Pseudo State Estimation of Fractional Models of Lithium-Ion Batteries. *IFAC-PapersOnLine*, 12th IFAC Conference on Fractional Differentiation and its Applications, 58:185–190, Bordeaux, France, 2024.

Friday, September 26, 2025

Library Auditorium

9:00–10:30	**Plenary Lecture** Christoph Matheja: *Automated Verification of Discrete Probabilistic Programs*
10:30–11:00	Coffee Break
11:00–12:30	**Regular Session A: Dynamic Systems**
11:00–11:30	Robert Szczelina, Anna Gierzkiewicz and Jakub Kural: *Investigating chaos in Delay Differential Equations with rigorous numerical methods*
11:30–12:00	Jakub Kural, Anna Gierzkiewicz and Robert Szczelina: *Computer assisted proof of existence of periodic solutions to ENSO delay differential equation model*
12:00–12:30	Théo Le Terrier, Marie Babel and Vincent Drevelle: *Ultra-wideband Based Smart Wheelchair Pose Estimation using Interval Analysis*
12:30–14:00	Lunch Break – Food truck
14:00–15:30	**Regular Session A: Dynamic Systems**
14:00–14:30	Andreas Rauh and Friederike Bruns: *Set-Based Contracts for Systematic Controller Tuning in Interconnected Dynamic Systems*
14:30–15:00	Anna Gierzkiewicz, Maciej Capinski and Pau Martin: *Oscillating orbits in the Sitnikov model: equal masses case*
15:00–15:30	Mohamed Fnadi and Régis Lherbier: *Interval Particle Filter for LiDAR-Based Object Tracking*
16:00–. . .	**Closing of SCAN 2025**

Automated Verification of Discrete Probabilistic Programs

Christoph Matheja

Carl von Ossietzky Universität Oldenburg
Theory of Correct Systems
D-26129 Oldenburg, Germany
christoph.matheja@uni-oldenburg.de

Keywords: probabilistic programs, deductive verification, formal methods

Introduction

Probabilistic programs are ordinary computer programs with the ability to base decisions on samples drawn from probability distributions. They appear as implementations of randomized algorithms and communication protocols, as well as descriptions of physical and statistical models (cf. [1] for an overview). Common questions in the analysis of probabilistic programs concern quantifying their expected behavior, e.g. how large is the expected runtime of an algorithm, the expected number of retransmissions of a network protocol, or the probability that a particle reaches its destination? Writing correct probabilistic programs is notoriously hard, arguably even harder than ordinary software development [3].

Over the last 15+ years, verification techniques for probabilistic programs have thus received much attention. By now, there exists a plethora of proof techniques for quantifying, amongst others, the termination probability or expected runtimes of such programs. To enable reasoning about the correctness of feature-rich probabilistic programs, those techniques must be adapted and combined. However, many of the existing verification techniques are inspired by different fields in computer science, mathematics, and engineering, such as control theory, program logics, probabilistic model checking, probability theory, and domain theory. Comparing—let alone combining—those techniques can thus be non-trivial (cf. [8]).

Modern program verifiers often have a front-end that translates a program and its specification into an intermediate language, such as Boogie [6]. Such intermediate languages enable the encoding of complex verification techniques, while allowing for the separate development of efficient back-ends, e.g. verification condition generators or symbolic execution engines. In the same spirit, HeyVL [7] is a recently developed *quantitative* intermediate verification language, which aims to enable researchers to (i) prototype and automate new verification techniques for probabilistic programs, (ii) combine those techniques, and (iii) benefit from improvements to common back-ends. It is part of the caesar automated verification infrastructure[2], which has been applied successfully to analyze probabilistic programs with different techniques. Figures 1 and 2 depict examples of probabilistic programs together with a description of the verified property and the technique encoded in HeyVL.

[2] https://www.caesarverifier.org

```
while (1 < i) {
  n := i;
  while (0 < n) {
    d := flip(0.5);
    i := i − d; n := n − 1
  } }
```

Figure 1: Model of Rabin's Mutal Exclusion Protocol [4]. Property: the probability to select exactly one process (i.e. $i = 1$) plus the probability of nontermination is at least $\frac{2}{3}$ if $n \geq 2$ holds initially. Verified by encoding weakest liberal preexpectations [5].

```
while (0 < x) {
  i := N + 1;
  while (0 < x < i) {
    i := unif(1, N)
  }; x := x − 1
}
```

Figure 2: Model of the Coupon Collector's Problem. Property: the expected number of loop iterations is bounded from above by $N \cdot H_N$, where H_N is the N-th harmonic number. Verified by encoding the expected runtime calculus [2].

Outline

This lecture will provide an overview of verification techniques for discrete probabilistic programs. Along the way, we will demonstrate how those techniques can be automated using the HeyVL intermediate language and caesar.

References

[1] G. Barthe, J.-P. Katoen, and A. Silva. Foundations of Probabilistic Programming. *Cambridge University Press*, 2020.

[2] B. L. Kaminski, J.-P. Katoen, C. Matheja, and F. Olmedo. Weakest precondition reasoning for expected runtimes of randomized algorithms. *Journal of the ACM*, 65(5), 1-68. 2018.

[3] B. L. Kaminski, J.-P. Katoen, and C. Matheja On the Hardness of Analyzing Probabilistic Programs. *Acta Informatica* 56(3), 255–285, 2019.

[4] E. Kushilevitz and M. O. Rabin. Randomized Mutual Exclusion Algorithms Revisited. *PODC.* 1992.

[5] A. McIver and C. Morgan. Abstraction, Refinement and Proof for Probabilistic Systems. *Monographs in Computer Science.*, Springer, 2005.

[6] K. R. M. Leino. This is Boogie 2. 2008.

[7] P. Schröer, K. Batz, B. L. Kaminski, J.-P. Katoen, and C. Matheja. A Deductive Verification Infrastructure for Probabilistic Programs. *Proc. ACM Program. Lang.* 7(OOPSLA2): 2052–2082, 2023.

[8] T. Takisaka, Y. Oyabu, and N. Urabe, and I. Hasuo. Ranking and Repulsing Supermartingales for Reachability in Randomized Programs. *ACM Trans. Program. Lang. Syst.* 43(2), 5:1–5:46 2021.

Investigating chaos in Delay Differential Equations with rigorous numerical methods

Anna Gierzkiewicz[1], Jakub Kural[1], Robert Szczelina[1,2]

[1] Jagiellonian University
Institute of Computer Science and Computational Mathematics
Gołębia 24 street, 31-007 Kraków, Poland
[2] {robert.szczelina}@uj.edu.pl

Keywords: Delay Differential Equations, Pseudospectral method, Interval Newton Operator, Infinite-dimensional Dynamical Systems

Abstract

We are studying the Cauchy problem for Delay Differential Equations with constant delays of the following form:

$$\begin{aligned} x'(t) &= f(x(t), x(t-\tau)) && t \geq 0 \\ x(t) &= \psi(t) && t \in [-\tau, 0], \end{aligned}$$

with $\tau > 0$ fixed, $x \in \mathbb{R}^d$, $\psi \in \mathcal{C}^0([-\tau, 0], \mathbb{R}^d) =: \mathcal{C}$.

In recent years, a significant effort was made to study and prove various dynamical phenomena in such systems such as periodic motions, with a particular attention given to proving chaos in canonical examples such as the Mackey–Glass equation [9]. Several of the techniques require rigorous numerical computations of a considerable scale, for instance, see [1, 3, 4, 7, 8, 10, 11] and references therein. However, the infinite-dimensional nature of the DDEs presents some challenges, such as the complicated setup, finding good approximations, and carrying out the computer assisted proofs.

For several years we have been working on methods for proving complicated dynamics (for example, periodic orbits and symbolic dynamics in DDEs) using rigorous, forward in time integration of the DDE in the (subspace of) the phasespace $\mathcal{C}$ [5, 11]. However, our current method uses a very high dimensional projection of the solutions, and thus is unfeasible for numerical investigations, especially when preparing data for computer assisted proofs, for instance, when looking for initial sets in computer assisted proofs. To address this issue we propose another approach: by using a pseudospectral approximation [2] we reduce the DDE to a finite-dimensional system of Ordinary Differential Equations (ODEs) while preserving numerically observed dynamical features of the original system. Due to the low-dimensionality of the resulting approximation, the computations are less demanding and can be done using known tools, such as CAPD rigorous ODE solvers [1], to efficiently verify some dynamical phenomena that closely mirror those of the full system.

We present some rigorous results for both DDE and the approximating projection to ODE and we discuss some problems that arise in this approximation. Based on the experiments, we believe those complications are intrinsic to the nature of DDEs and solving them in the reduced system might guide the search for the computer assisted proof of chaotic (symbolic) dynamics in the full DDE system.

Acknowledgement

The author would like to acknowledge the support of Polish National Science Center (NCN) grant no. 2023/49/B/ST6/02801 and Polish NAWA Bekker project no. BPN/BEK/2023/1/00170.

References

[1] F.A. Bartha, T. Krisztin, and A. Vígh. Stable periodic orbits for the Mackey–Glass equation. *J Diff.l Eq.*, Vol. 296 pp. 15–49, 2021.

[2] D. Breda, O. Diekmann, M. Gyllenberg, F. Scarabel, and R. Vermiglio. Pseudospectral Discretization of Nonlinear Delay Equations: New Prospects for Numerical Bifurcation Analysis. *SIAM J. Appl. Dyn. Sys.*, Vol. 15(1), pp. 1–23, 2016.

[3] K.E.M. Church. Validated integration of differential equations with state-dependent delay. *Commun. Nonlinear Sci. Numer. Simul.*, 115:106762, 2022.

[4] J. Gimeno, J-P. Lessard, J.D. Mireles James and J. Yang, Persistence of Periodic Orbits under State-dependent Delayed Perturbations: Computer-assisted Proofs, *SIAM J. Appl. Dyn. Sys.*, Vol. 22(3), pp. 1743–1779, 2023

[5] A. Gierzkiewicz, R. Szczelina. Sharkovskii theorem for infinite dimensional dynamical systems. *Commun. Nonlinear Sci. Numer. Simul.*, Vol. 146, 108770, 2025.

[6] T. Kapela, M. Mrozek, D. Wilczak, and P. Zgliczyński. CAPD::DynSys: A flexible C++ toolbox for rigorous numerical analysis of dynamical systems. *Commun. Nonlinear Sci. Numer. Simul.*, 101:105578, 2021.

[7] G. Kiss and J.P. Lessard. Computational fixed-point theory for differential delay equations with multiple time lags. *J. Diff. Eq.*, Vol. 252(4), pp. 3093–3115, 2012.

[8] J-P. Lessard and J.D. Mireles James. A rigorous implicit C^1 Chebyshev integrator for delay equations. *J. Dyn. Diff. Eq.*, 33:1959–1988, 2021.

[9] M. C. Mackey and L. Glass. Oscillation and chaos in physiological control systems. *Science*, 197(4300), pp. 287–289, 1977.

[10] A. Rauh and E. Auer. Verified Integration of Differential Equations with Discrete Delay. *Acta Cybernetica*, 25(3), pp. 677–702, 2022.

[11] R. Szczelina and P. Zgliczyński. High-order Lohner-type algorithm for rigorous computation of Poincaré maps in systems of delay differential equations with several delays. *Found. Comput. Math.*, 24(4), pp. 1389–1454, 2024.

Computer assisted proof of existence of periodic solutions to ENSO delay differential equation model

Anna Gierzkiewicz, Jakub Kural, Robert Szczelina

Jagiellonian University, Faculty of Mathematics and Computer Science
ul. Prof. S. Łojasiewicza 6, 30-348 Kraków, Poland
{anna.gierzkiewicz,robert.szczelina}@uj.edu.pl
jakub.kural@student.uj.edu.pl

Keywords: Mathematics, Computer Science, Interval Methods, Delay Differential Equations

El Niño–Southern Oscillation (ENSO) is a recurring climate phenomenon where the temperatures of oceanic waters at the western coast of equatorial South America deviate from their mean annual values, coupled with changes in the surface air pressure [1]. We study a following delay differential equation model for ENSO [1]

$$h'(t) = -a\tanh(\kappa h(t-\tau)) + b\cos(2\pi t) \tag{1}$$

and a limiting case as $\kappa \to \infty$

$$h'(t) = -a\,\mathrm{sgn}(h(t-\tau)) + b\cos(2\pi t) \tag{2}$$

where h represents the thermocline depth deviation from its annual mean.

These equations exhibit interesting, but only numerically checked properties, such as bistability and existence of periodic and quasi-periodic solutions. Our goal is to study and prove the existence of periodic orbits for these equations through the use of interval arithmetic and rigorous numerical algorithms [2, 3]. Computations were conducted with the CAPD C++ Library [4].

Acknowledgement

The research was funded by the program Excellence Initiative – Research University at the Jagiellonian University in Kraków.

References

[1] A. Keane, B. Krauskopf and C. Postlethwaite. Delayed Feedback Versus Seasonal Forcing: Resonance Phenomena in an El Niño Southern Oscillation Model. *SIAM Journal of Applied Mathematics*, 14.3:1229–1257, 2015

[2] R. Szczelina and P. Zgliczyński. Algorithm for rigorous integration of delay differential equations and the computer-assisted proof of periodic orbits in the Mackey–Glass equation. *Foundations of Computational Mathematics*, 18:1299–1332, 2018

[3] R. Szczelina and P. Zgliczyński. High-order lohner-type algorithm for rigorous computation of Poincaré maps in systems of delay differential equations with several delays. *Foundations of Computational Mathematics*, 24.4:1389–1454, 2018

[4] T. Kapela, M. Mrozek, D. Wilczak and P. Zgliczyński. CAPD::DynSys: A flexible C++ toolbox for rigorous numerical analysis of dynamical systems. *Communications in Nonlinear Science and Numerical Simulation*, 101:105578, 2021

Ultra-wideband Based Smart Wheelchair Static Pose Estimation using Interval Analysis

Théo Le Terrier, Marie Babel and Vincent Drevelle

Univ Rennes, INSA Rennes, Inria, CNRS, IRISA - UMR 6074, F-35000 Rennes, France
{theo.le-terrier,marie.babel,vincent.drevelle}@irisa.fr

Keywords: Localization, Interval Analysis, Ultra-wideband, Smart Wheelchair

Introduction

Autonomous power wheelchairs (PW) indoor navigation requires reliable positioning. In a clinical environment, e.g., a rehabilitation center, a PW is often moved while it is switched off, preventing the positioning method to rely on any prior information. We propose an indoor positioning method that leverages ultra-wideband (UWB) beacons to provide a confidence domain for the pose of a PW, i.e., a subpaving in which the true position and orientation of the PW are guaranteed to belong [1].

A typical UWB-based positioning ([2]) setup consists of a set of fixed UWB nodes, or *anchors*, measuring their range from UWB nodes installed on the robot, or *tags*. UWB range measurements between tags and anchors are performed using two-way ranging by measuring the time of flight of the UWB signal. The actual range between the two UWB nodes can be determined, assuming line-of-sight (LOS) propagation. In practice, UWB signals are also reflected or blocked by the environment. This may result in non-line-of-sight (NLOS) distances exceeding the true value.

Interval-Based Reliable Pose Estimation

The PW configuration in the world frame $\mathcal{F}_w$ is denoted $\mathbf{q} = (x, y, \theta)^{\mathbf{T}}$. The local frame attached to the PW is denoted $\mathcal{F}_r$. Let n_T be the number of tags installed on the PW, and n_A the number of anchors. We denote $T_i,\ i \in \{1, \ldots, n_T\}$, the i^{th} tag, and $A_j,\ j \in \{1, \ldots, n_A\}$, the j^{th} anchor. The coordinates of T_i, expressed in $\mathcal{F}_r$, are denoted ${}^r\mathbf{x}_{T_i} = ({}^r x_{T_i}, {}^r y_{T_i}, {}^r z_{T_i})$. The coordinates of T_i in $\mathcal{F}_w$, denoted $\mathbf{x}_{T_i} = (x_{T_i}, y_{T_i}, z_{T_i})$, can be expressed as a function of the PW configuration as

$$\mathbf{x}_{T_i}(\mathbf{q}) = \begin{pmatrix} x + {}^r x_{T_i} \cos\theta - {}^r y_{T_i} \sin\theta \\ y + {}^r x_{T_i} \sin\theta + {}^r y_{T_i} \cos\theta \\ {}^r z_{T_i} \end{pmatrix}. \tag{1}$$

The fixed coordinates of A_j in $\mathcal{F}_w$, are denoted $\mathbf{x}_{A_j} = (x_{A_j}, y_{A_j}, z_{A_j})$. The measured range between T_i and A_j is denoted $r_{i,j}$ and is defined as

$$r_{i,j} = \|\mathbf{x}_{T_i}(\mathbf{q}) - \mathbf{x}_{A_j}\|_2 + \beta_{i,j}, \tag{2}$$

where the range measurement error $\beta_{i,j}$ is assumed to belong to an interval $[\beta] = [\underline{\beta}, \overline{\beta}]$.

The PW pose domain computation is defined as a constraint satisfaction problem (CSP). NLOS or multipath propagation leads to range measurements that are

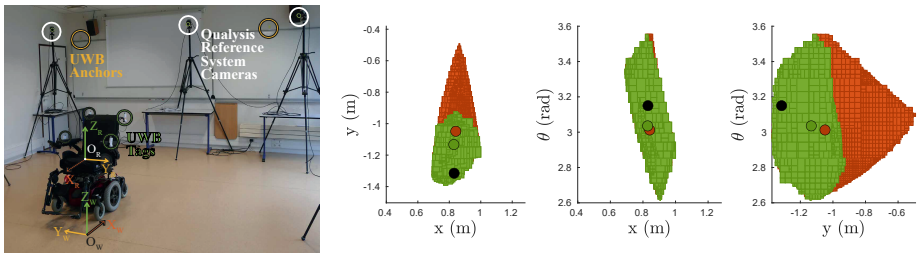

Figure 1: Left: Experimental setup. Right: Subpavings from $\mathcal{S}_{UB}$ (orange) and $\mathcal{S}$ (green). Black circles are ground truth; orange/green circles are the domain centroids.

greater than the actual ones. For a tag T_i measuring its range to an anchor A_j, a range upper-bound constraint (corresponding to disk membership) is defined by $\mathcal{L}^{\text{UB}}_{r_{i,j}} : \{\|\mathbf{x}_{T_i}(\mathbf{q}) - \mathbf{x}_{A_j}\|_2 \leq r_{i,j} - \underline{\beta}\}$. The set $\mathcal{L}_{\text{UB}}$ of range upper-bound constraints for all pairs of tags and anchors at a given epoch is then defined by $\mathcal{L}_{\text{UB}} = \bigcap_{i,j} \mathcal{L}^{\text{UB}}_{r_{i,j}}$.

As the PW approaches or exits the anchors' polygon boundaries, the volume of the solution set will increase, leading to higher uncertainties and less accurate pose estimations. To prevent such drawbacks in our positioning method, range lower-bound constraints can be added to our CSP: $\mathcal{L}^{\text{LB}}_{r_{i,j}} : \{\|\mathbf{x}_{T_i}(\mathbf{q}) - \mathbf{x}_{A_j}\|_2 \geq r_{i,j} - \overline{\beta}\}$. Since these constraints may be violated by NLOS outliers, the set $\mathcal{L}_{\text{LB}}$ of range lower-bound constraints is defined by the q-relaxed intersection of tag/anchor pair constraints at a given epoch: $\mathcal{L}_{\text{LB}} = \bigcap^{\{q\}}_{i,j} \mathcal{L}^{\text{LB}}_{r_{i,j}}$

A separator $\mathcal{S}_{UB}$ is created from the set of constraints $\mathcal{L}_{\text{UB}}$, using the *forward-backward* interval constraint propagation algorithm [3]. The SIVIA algorithm is applied with the defined separator to compute inner and outer subpavings of all feasible PW poses that are consistent with the range upper-bound constraints. Finally, the SIVIA algorithm is applied again with a separator $\mathcal{S} = \mathcal{S}_{UB} \cap \mathcal{S}_{LB}$. The obtained subpaving is taken as the confidence domain for the PW pose.

Results The proposed method has been tested on a real PW with 4 UWB tags (Fig. 1). It provided consistent confidence domains over 99.6% of the dataset, containing 4.800 epochs of data. It uses the centroid of all the subpaving boxes to estimate of the PW configuration. With a mean horizontal positioning error (HPE) of 8.0 cm, and a mean absolute heading error of 4.5°, the centroid is shown to be an accurate pose estimate. The computed domains of feasible PW poses can be used for safety assessment with respect to the worst-case required navigation performance criteria or, e.g., to focus the initialization step of a particle filter.

References

[1] B. Desrochers, S. Lacroix, and L. Jaulin. Set-membership approach to the kidnapped robot problem. *IEEE/RSJ IROS*, 2015, 3715-3720.

[2] H. Jiang, W. Wang, Y. Shen, X. Li, X. Ren, B. Mu, and J. Wu. Efficient planar pose estimation via UWB measurements. *IEEE ICRA*, 2023, 1954-1960.

[3] L. Jaulin, M. Kieffer, O. Didrit, and E. Walter. Interval Analysis *Springer*, 2001.

Ultra-wideband Based Smart Wheelchair Static Pose Estimation using Interval Analysis

Théo Le Terrier, Marie Babel and Vincent Drevelle
Univ Rennes, INSA Rennes, Inria, CNRS, IRISA - UMR 6074, F-35000 Rennes, France

SCAN 2025
20th International Symposium on Scientific Computing, Computer Arithmetic, and Verified Numerical Computations
Oldenburg, 22-26 September 2025

Background and Objective

- Fully autonomous navigation systems for smart wheelchairs (SW) can significantly enhance user independence by enabling tasks such as safe transfers or autonomous docking at charging stations.
- Designing such systems requires a reliable localization method that balance robustness, efficiency, cost, and acceptability [1].
- Low-cost ultra-wideband (UWB) sensors are used for indoor localization [2]. The precision of the pose (position/orientation) estimation suffers from non-line-of-sight (NLOS) signal propagation, uncorrected biases, or multipath [3]. Hence the aim to compute the uncertainty associated with the estimation, using interval analysis [4].

Objective: design a **set-membership UWB** based reliable **static positioning method** to provide **confidence domain** of the pose of a **smart wheelchair.**

UWB interval-based reliable pose estimation

- A typical UWB-based positioning setup consists of fixed anchors in the room and mobile tags on the SW to estimate its pose $\boldsymbol{q}$ through range measurements.

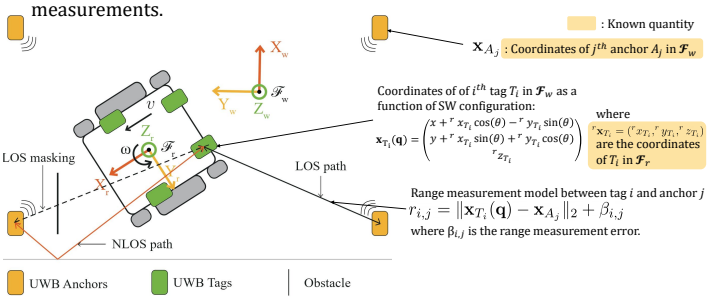

- UWB range measurements are mostly affected by **non-line-of-sight** conditions and **multipath** signal propagation, leading to **overestimated range measurements**.

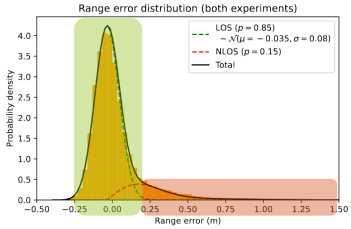

Histogram of the UWB range measurement error.

Line-of-sight conditions

Ranging error can be modeled by a centered interval, i.e., each $\beta_{i,j}$ should belong to an interval $[\beta] = [\underline{\beta},\ \overline{\beta}]$.

Non-line-of-sight conditions

Because the outliers are only positive, the lower bound $\underline{\beta}$ remains satisfied, while the upper bound $\overline{\beta}$ is violated.

Range upper-bound constraints
➢ Constraints always satisfied

$$\mathcal{L}^{\mathrm{UB}}_{i,j} : \{\|\mathbf{x}_{T_i}(\mathbf{q}) - \mathbf{x}_{A_j}\|_2 \leq r_{i,j} - \underline{\beta}\}$$

A separator $\mathcal{S}_{UB}$ is created from the set of constraints

$$\mathcal{L}^{\mathrm{UB}} = \bigcap_{i,j} \mathcal{L}^{\mathrm{UB}}_{i,j}$$

Range lower-bound constraints
➢ Constraints only satisfied in line-of-sight conditions

$$\mathcal{L}^{\mathrm{LB}}_{i,j} : \{\|\mathbf{x}_{T_i}(\mathbf{q}) - \mathbf{x}_{A_j}\|_2 \geq r_{i,j} - \overline{\beta}\}$$

A separator $\mathcal{S}_{LB}$ is created from **the q-relaxed intersection [5]** of tag/anchor pair constraints

$$\mathcal{L}^{\mathrm{LB}} = \bigcap_{i,j}^{\{q\}} \mathcal{L}^{\mathrm{LB}}_{i,j}$$

- Apply SIVIA algorithm with separator $\mathcal{S}_{UB}$ to compute inner and outer subpavings of the pose uncertainty domain with range upper-bound constraints only.
- Estimate minimal number of outliers q_{box} by counting, for each inner box, inconsistent theoretical ranges.
- Increment q_{box} by one to add robustness against undetected outliers in $\mathcal{S}_{LB}$.
- Compute the domains of $\mathcal{S} = \mathcal{S}_{UB} \cap \mathcal{S}_{LB}$ with SIVIA algorithm.
- The outer subpaving is taken as the confidence domain for the SW pose. The centroid of all the boxes is used as an estimate of the SW configuration.

Experiment

➢ 4 anchors in the room, 4 tags on a real SW, manually driven by a user with a joystick.
➢ 4800 epochs of data.
➢ Error bounds for the UWB range measurements are set to $\pm 3\sigma$, i.e., ± 24 cm.

Experimental setup

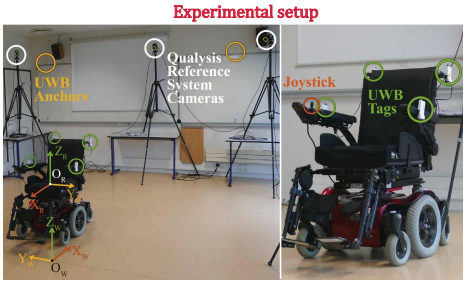

Results

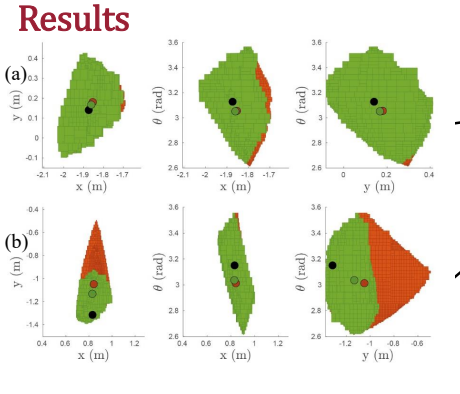

Domains computed with Sub (orange) and S (green), inside the anchors polygon (up) and close to the anchors polygon boundary (bottom). Black circle corresponds to the ground truth. Orange and green circles are the centroids of the corresponding domains.

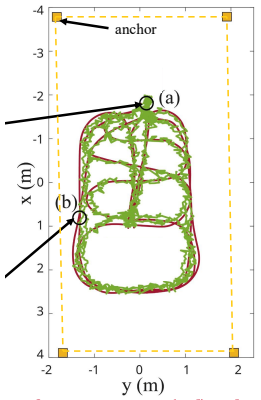

Reference trajectory (red) and estimated trajectory (green) with the S solution. The anchors polygon is represented by yellow dotted lines.

➢ $\mathcal{S}_{UB}$ and $\mathcal{S}$ provide almost identical domains in configuration (a), showing that the $\mathcal{S}_{UB}$-only solution can be used as a positioning method, as long as the wheelchair stays close to the center of the anchors' polygon.

➢ Configuration (b) highlights the contribution of $\mathcal{S}_{LB}$ in unfavorable geometrical configurations (i.e., close to, or outside the anchors' polygon boundary).

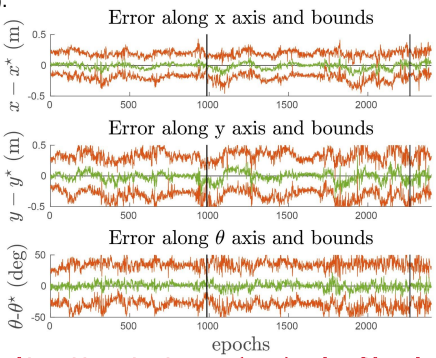

Set-membership position estimation error (green), and confidence lower and upper-bounds (orange). The reference is at zero (black).

Consistent confidence domains **over 99.6%** of the dataset epochs. Mean horizontal planimetric error of 9.8 cm for the $\mathcal{S}_{UB}$ solution, and 8.0 cm for the $\mathcal{S}$ solution.

Conclusion

➢ The proposed **set-membership UWB** based **reliable static positioning** method provides consistent pose uncertainty domains, and sufficient pose estimation accuracy.
➢ Within the anchors' polygon, a robust solution can be obtained without using q-relaxed intersections by leveraging the positive bias of outliers. To extend this approach to the entire geometric space, q-relaxed constraints can be incorporated, which are only satisfied under line-of-sight conditions.
➢ The positioning method is a step towards a smart wheelchair control law that explicitly accounts for pose estimation uncertainties.

References

[1] Simpson, Richard C. "Smart wheelchairs: A literature review." Journal of rehabilitation research & development 42.4 (2005).
[2] H. Jiang et al., "Efficient Planar Pose Estimation via UWB Measurements," 2023 IEEE International Conference on Robotics and Automation (ICRA), London, United Kingdom, 2023, pp. 1954-1960.
[3] D. Dardari et al., "Ranging With Ultrawide Bandwidth Signals in Multipath Environments," in Proceedings of the IEEE, vol. 97, no. 2, pp. 404-426, Feb. 2009.
[4] L. Jaulin et al. "Interval analysis." Applied Interval Analysis: With Examples in Parameter and State Estimation, Robust Control and Robotics. London: Springer London, 2001. 11-43.
[5] Drevelle, Vincent, and Philippe Bonnifait. "Robust positioning using relaxed constraint-propagation." 2010 IEEE/RSJ International Conference on Intelligent Robots and Systems. IEEE, 2010.

Set-Based Contracts for Systematic Controller Tuning in Interconnected Dynamic Systems

Andreas Rauh and Friederike Bruns

Carl von Ossietzky Universität Oldenburg
Distributed Control in Interconnected Systems
D-26111 Oldenburg, Germany
{andreas.rauh,friederike.bruns}@uni-oldenburg.de

Keywords: Set-based reachability analysis, Contract-based performance specification, Controller tuning, Cyber-physical systems

Introduction

In Cyber-Physical Systems (CPSs), numerous hardware and software components interact with each other to achieve a dynamic system behavior that cannot be obtained with the hardware components alone. The design of large-scale CPSs typically needs to be supported by systematized development, testing, and verification approaches. In this frame, the so-called Contract-Based Design (CBD) methodology provides benefits for reusability of system specifications, supports a correct-by-construction approach guaranteeing a desired system behavior, and prevents costly design-cycle reiterations [2, 4].

Following this design approach, the desired overall system behavior can be ensured by a suitable composition of the formalized specification of the dynamic behavior of the individual subsystem components. In recent work [5], we have shown how methods for a set-based reachability analysis can be used to systematically derive contracts for interconnected dynamic systems with bounded uncertainty. For that purpose, an iterative procedure was presented that allows for a decentralized determination of contracts. Its advantage is a reduced computational effort in comparison with the immediate consideration of the overall system structure. In general, this approach is applicable to a subset of system models that can be shown to be asymptotically stable on the basis of the system property of passivity or the small-gain theorem. In this work, we propose to use this approach for contract-based controller tuning.

Considered System Classes

The iterative derivation of set-based contracts for the specification of the admissible system behavior is applicable to a large variety of systems, such as the structures shown in Fig. 1, cf. [5]. These include bi- and uni-directional couplings of subsystems, parallel connections, as well as nested combinations of each of these structures. With these basic structures, also classical control loops such as the standardized output feedback loop, cascaded controllers, and internal model control structures can be taken into consideration. The iterative derivation of set-based contracts according to [5] is a generalization of the approach proposed in [3], where we have made use of a constraint satisfaction differential problem formulation as derived in [1].

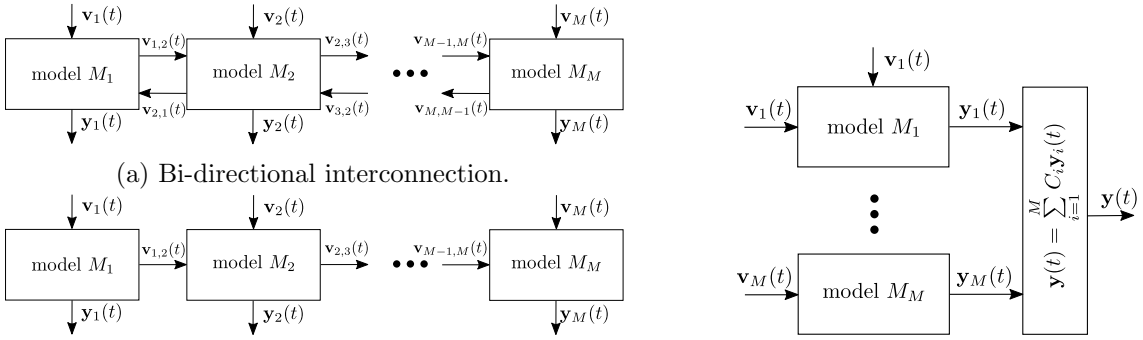

(a) Bi-directional interconnection.

(b) Uni-directional interconnection.

(c) Parallel connection.

Figure 1: Representation of the structure of interconnected subsystems in CPSs [5].

Contract-Based Controller Tuning

In this contribution, we extend the work sketched above by the following multi-stage approach. Firstly, base contracts are derived by means of the procedure published in [5] for an interconnected system with bounded parameter uncertainty and disturbances. Second, we establish an approach for a replacement of controller components in the sense of *contract refinement*. This approach leads to outcomes of the reachability analysis which are true subsets of the results of the first development stage. As such, the overall structure is still proven to be feasible for the refined system model, however, it also possesses a reduced sensitivity against the considered uncertainties in comparison with the baseline solution. It is further shown how this procedure can be used to validate the use of alternative hardware components (such as actuators or sensors) in a complex interconnected CPS.

References

[1] J. Alexandre dit Sandretto, A. Chapoutot, and O. Mullier. Formal Verification of Robotic Behaviors in Presence of Bounded Uncertainties. Proc. of 2017 First IEEE International Conference on Robotic Computing (IRC), pages 81–88, 2017.

[2] A. Benveniste, B. Caillaud, and R. Passerone. A Generic Model of Contracts for Embedded Systems. 2007.

[3] F. Bruns, A. Rauh, and M. Fnadi. Set-Based Assumption-Guarantee Reasoning for Handling Uncertainty in Functionality and Safety Verification of Dynamic Systems. In A. Rauh, B. Finkbeiner, and P. Kröger, editors, *Design and Verification of Cyber-Physical Systems: From Theory to Applications*, A Springer Nature Computer Science book series, 2025.

[4] B. Meyer. Applying 'Design by Contract'. Computer, 25(10):40–51, 1992.

[5] A. Rauh and F. Bruns. A Set-Based Approach to Derive Contracts for Dynamic Behavior in Interconnected Systems, Proc. of the 29th Intl. International Conference on Methods and Models in Automation and Robotics (MMAR), Międzyzdroje, Poland, 2025. Accepted.

Oscillating orbits in the Sitnikov model: equal masses case

M. J. Capiński[1], A. Gierzkiewicz[2], and P. Martín[3,4]

[1] AGH University of Science and Technology, al. Mickiewicza 30, 30-059 Kraków, Poland
mcapinsk@agh.edu.pl
[2] Jagiellonian University, ul. Łojasiewicza 6, 30-348 Kraków, Poland
anna.gierzkiewicz@uj.edu.pl
[3] Universitat Politècnica de Catalunya, Departament de Matemàtiques & IMTECH, Pau Gargallo 14, Barcelona, Spain
[4] Centre de Recerca Matemàtica, Campus de Bellaterra, Edifici C, Barcelona, Spain
p.martin@upc.edu

Keywords: Sitnikov problem, oscillatory motion, computer-assisted proof.

Abstract

The Sitnikov three body problem (S3BP) is an example of a spatial elliptic 3BP with oscillatory motion. The configuration has a planar binary consisting of two symmetric bodies of mass m running around the common center of mass, and the other body of mass m_1, allowed to move along their perpendicular axis of symmetry. Originally [3] $m_1 = 0$, which made the system a 1.5 degrees of freedom Hamiltonian problem. Sitnikov showed the existence of oscillatory motion for this case. By 'oscillatory motion' we mean an orbit with the mass m_1 going closer and closer to infinity but always returning to a fixed bounded region.

In our case of $0 \neq m_1 = m$, after rescaling, the system can be seen as a 2 d.o.f. Hamiltonian system with the energy function

$$H(r, \rho, R, y) = \frac{1}{2}R^2 + \frac{1}{2}\left(y^2 + \frac{1}{\rho^2}\right) - \frac{1}{\sqrt{r^2+\rho^2}} - \frac{1}{4\rho}, \tag{1}$$

where r is the position of the third body on the perpendicular axis, ρ roughly describes the size of the binary, and R, y are the conjugate momenta.

In a joint work with M. Capiński and P. Martín, we prove the existence of oscillatory orbits for the Sitnikov 3BP in the case of three equal masses ($m_1 = m$). The proof relies on analyzing the stable and unstable invariant manifolds of infinity and their intersections. We construct orbits shadowing these invariant manifolds by the method of correctly aligned windows, which is a modification of the method used in [2]. The proof is computer assisted with the use of `CAPD C++` library for rigorous integration of ODEs and computation of Poincaré maps derived from ODEs [1].

Acknowledgement

AG and MC were supported by Polish NCN grant 2021/41/B/ST1/00407.

References

[1] T. Kapela, M. Mrozek, D. Wilczak and P. Zgliczyński. `CAPD::DynSys`: a flexible `C++` toolbox for rigorous numerical analysis of dynamical systems. *Communications in Nonlinear Science and Numerical Simulation*, 101:105578, 2021.

[2] M. J. Capiński, M. Guardia, P. Martín, T. M. Seara, P. Zgliczyński *et al.* Oscillatory motions and parabolic manifolds at infinity in the planar circular restricted three body problem. *Journal of Differential Equations*, 320:316–370, 2022.

[3] K. Sitnikov. The existence of oscillatory motions in the three-body problem. *Soviet Physics Doklady*, 5:647, January 1961.

Interval Particle Filter for LiDAR-Based Object Tracking

Mohamed Fnadi and Régis Lherbier

LISIC – UR4491, Université du Littoral Côte d'Opale F-62228, France
{mohamed.fnadi,regis.lherbier}@univ-littoral.fr

Keywords: Interval Particle Filter, Target Tracking, LiDAR Sensor

Introduction

Accurate target tracking remains challenging for autonomous systems due to sensor noise and inherent uncertainties. Particle filters (PF) [1, 2] handle non-Gaussian noise effectively but require precise noise and accurate models, while set-membership methods [3, 4] guarantee bounded estimates yet often remain overly conservative. Building on [5], we propose an *Interval Particle Filter* (IPF) that integrates the probabilistic robustness of PF with the bounded-error guarantees of interval analysis for robust LiDAR-based tracking. The IPF represents the target state using weighted interval particles $\{[\mathbf{x}_k^{(i)}], \omega_k^{(i)}\}_{i=1}^{N_p}$, updated through prediction–correction cycles. As illustrated in Figure 1, the proposed IPF algorithm processes uncertain LiDAR measurements $[\mathbf{y}_k] = \{[\mathbf{r}_k], [\boldsymbol{\alpha}_k]\}$, where $[\mathbf{r}_k]$ denotes the bounded radial distance to the target's barycenter and $[\boldsymbol{\alpha}_k]$ the orientation deviation between LiDAR and target frames.

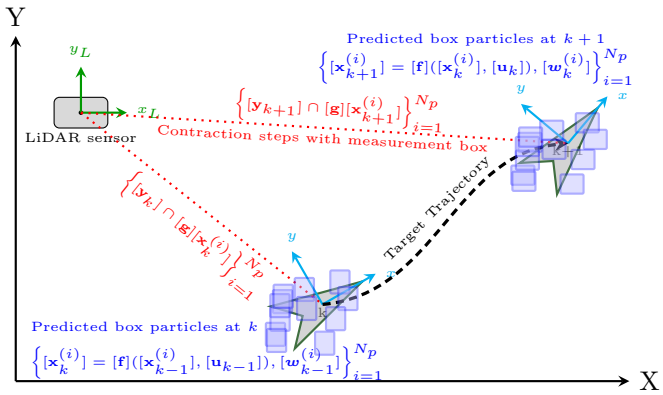

Figure 1: Principle of the IPF filter.

During prediction, each particle's state interval is propagated via the inclusion function $[\mathbf{f}]([\mathbf{x}_{k-1}^{(i)}], [\mathbf{u}_{k-1}], [\mathbf{w}_{k-1}^{(i)}])$, where $[\mathbf{u}_{k-1}]$ captures bounded control inputs and $[\mathbf{w}_{k-1}^{(i)}]$ represents process noise bounds. In correction, predicted measurements $[\mathbf{y}_k^{(i)}] = [\mathbf{g}]([\mathbf{x}_k^{(i)}])$ are compared with actual measurements, and the state intervals are contracted via set inversion as $[\tilde{\mathbf{x}}_k^{(i)}] = [\mathbf{x}_k^{(i)}] \cap [\mathbf{g}]^{-1}([\mathbf{y}_k] \ominus [\mathbf{v}_k^{(i)}])$, where $[\mathbf{v}_k^{(i)}]$ bounds measurement noise. Weights are updated based on the contraction ratio $\omega_k^{(i)} \propto \mu([\tilde{\mathbf{x}}_k^{(i)}])/\mu([\mathbf{x}_k^{(i)}])$, and the final state estimate $\hat{\mathbf{x}}_k$ is obtained from the weighted midpoints of contracted particles. Systematic resampling is performed when the effective sample size $N_{\text{eff}} = 1/\sum(\omega_k^{(i)})^2$ falls below $N_p/3$ to maintain particle diversity.

Main results

The IPF was implemented using `INTLAB` and evaluated against a conventional PF for Autonomous Surface Vehicle (ASV) tracking using LiDAR measurements. Both filters processed identical LiDAR datasets under bounded noise and initial uncertainty. As illustrated in Fig. 2, the IPF achieved superior accuracy (e.g., RMSE of 0.0246 m with 200 particles versus 0.0823 m for the PF with 1000 particles) while providing guaranteed state bounds. However, this came at the cost of higher computation time (e.g., 0.34 s), highlighting the need for further optimization.

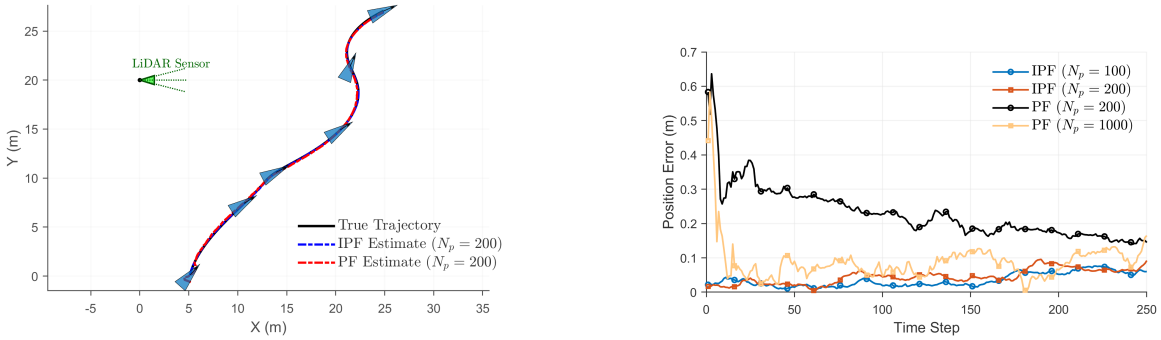

Figure 2: Comparison of tracking performance: (a) shows the computed trajectories of IPF and PF methods, (b) displays the corresponding lateral errors during ASV tracking.

References

[1] M. S. Arulampalam, S. Maskell, N. Gordon, and T. Clapp. *A tutorial on particle filters for online nonlinear non-Gaussian Bayesian tracking.* IEEE Transactions on signal processing, 50(2), pp. 174–188, 2002.

[2] B. Fortin, J. C. Noyer, and R. Lherbier. *A particle filtering approach for joint vehicular detection and tracking in lidar data.* 2012 IEEE Inter Instrumentation and Measurement Technology Conference Proceedings, pp. 391–396, 2012.

[3] A. Rauh, M. Lahme, S. Rohou, L. Jaulin, T. N. Dinh, T. Raissi, and M. Fnadi. *Offline and Online Use of Interval and Set-Based Approaches for Control and State Estimation: A Review of Methodological Approaches and Their Application.* Logical Methods in Computer Science, 2024.

[4] M. Fnadi, and A. Rauh. *Exponential State Enclosure Techniques for the Implementation of Validated Model Predictive Control.* Acta Cybernetica, 26(4), 839–854, 2024.

[5] F. Abdallah, A. Gning, and P. Bonnifait. *Box particle filtering for nonlinear state estimation using interval analysis.* Automatica, 44(3), pp. 807–815, 2008.

Friday, September 26, 2025

A01-0-006

11:00–12:30	**Regular Session B: Optimization**
11:00–11:30	Mihály Gencsi and Boglárka G.-Tóth: *Improvements of the Geometrical Test in Interval Branch and Bound methods*
11:30–12:00	Verlein Radwan, Simon Rohou and Gilles Trombettoni: *Exhaustive Interval-based 2-D Shape Registration Under Similarity Transformation*
12:00–12:30	Maël Godard, Luc Jaulin and Damien Massé: *Adaptative parallelepipedic approximation of the image of a set by a nonlinear function*
14:00–15:30	**Regular Session B: Optimization**
14:00–14:30	Yuki Uchino, Katsuhisa Ozaki and Toshiyuki Imamura: *High-Performance Emulation of Matrix Multiplication using INT8 Matrix Engines and its Error Analysis*
14:30–15:00	Lorenz Gillner and Ekaterina Auer: *Efficient Acceleration Strategies for Interval Branch-and-Bound Type Methods*
15:00–15:30	Diego Romano, Ekaterina Auer, Francesco Gregoretti and Lorenz Gillner: *GPU-Accelerated Algorithmic Differentiation For Reliable Computing: Comparing Different Architectures*

Improvements of the Geometrical Test in Interval Branch and Bound methods

Mihály Gencsi, Boglárka G.-Tóth

University of Szeged
Department of Computational Optimization
H-6720 Szeged, Hungary
{gencsi,boglarka}@inf.szte.hu

Keywords: Interval Methods, Branch and Bound method, Fritz-John optimality conditions, Geometrical Test

Introduction

In many real-world applications, finding a guaranteed solution is crucial. We focus on the following nonlinear inequality-constrained global optimization problem,

$$\begin{array}{ll} \underset{x \in \boldsymbol{y} \subseteq \mathbb{R}^n}{\text{minimize}} & f(x) \\ \text{subject to} & g_i(x) \leq 0, \quad i \in M_c, \end{array} \tag{1}$$

where $f, g_i : \mathbb{R}^n \to \mathbb{R}, i \in M_c$ are continuously differentiable nonlinear functions. The interval box $\boldsymbol{y} = [\underline{y}, \overline{y}]$ defines the general bound constraints. These constraints can be expressed as $p_{i_u}(x) = x_i - \overline{y_i}$ and $p_{i_l}(x) = \underline{y_i} - x_i$, which can be written compactly as $p_j(x) \leq 0, j \in M_b$, where $M_b = \{i_u, i_l \mid i = 1, \ldots, n\}$.

In this study, we improve the efficiency of the IBB method using optimality conditions. We improve the Advanced Geometrical Test to discard non-optimal boxes and avoid using optimality conditions when they are ineffective.

The Normalized Interval Fritz-John Condition System

The normalized interval Fritz-John condition system (NIFJ-CS), as used in [1], defines a system of interval linear equations for a given box $\boldsymbol{x}$:

$$\boldsymbol{\phi}(\boldsymbol{t}) = \begin{bmatrix} \boldsymbol{\mu}_0 + \sum_{i \in B \cup C} \boldsymbol{\mu}_i - 1 \\ \boldsymbol{\mu}_0 \cdot \boldsymbol{\nabla}\mathbf{f}(\boldsymbol{x}) + \sum_{i \in B} \boldsymbol{\mu}_i \cdot \boldsymbol{\nabla}\mathbf{p}_i(\boldsymbol{x}) + \sum_{j \in C} \boldsymbol{\mu}_j \cdot \boldsymbol{\nabla}\mathbf{g}_j(\boldsymbol{x}) \\ \boldsymbol{\mu}_i \cdot \mathbf{p}_i(\boldsymbol{x}) \qquad i \in B \\ \boldsymbol{\mu}_j \cdot \mathbf{g}_j(\boldsymbol{x}) \qquad j \in C \end{bmatrix} = 0, \tag{2}$$

where $\mathbf{f}(\boldsymbol{x})$, $\mathbf{p}_i(\boldsymbol{x})$, $\mathbf{g}_j(\boldsymbol{x})$ are the inclusion functions and $\boldsymbol{\nabla}\mathbf{f}(\boldsymbol{x})$, $\boldsymbol{\nabla}\mathbf{p}_i(\boldsymbol{x})$, $\boldsymbol{\nabla}\mathbf{g}_j(\boldsymbol{x})$ are the inclusions of the gradients. The system includes only active constraints ($B = \{i \in M_B \mid 0 \in \mathbf{p}_i(\boldsymbol{x})\}$, $C = \{i \in M_C \mid 0 \in \mathbf{g}_j(\boldsymbol{x})\}$). The variables are $\boldsymbol{t} = [\boldsymbol{x}, \boldsymbol{\mu}]^T$.

Several approaches to solving Fritz-John optimality conditions have been proposed in the literature. As discussed in [2, 3], two main methods are: computing only the bounds for the Lagrange multipliers (Lagrange estimator method) and enclosing both the multipliers and the optimal point location (Lagrange estimator+NIFJ-CS method). Both methods are computationally expensive and often ineffective. Therefore, an efficient modification is needed.

Advanced Geometrical Test

Instead of applying the Lagrange estimator or combining it with the NIFJ-CS method, we perform a preliminary test, the Advanced Geometrical Test. This test discards the nonoptimal boxes or avoids the unnecessary use of the optimality conditions.

The Advanced Geometrical Test is based on the geometrical interpretation of the optimality conditions [4]. Geometrically, in the interval settings, the optimality conditions require that there exists a direction in the negative cone of the objective's gradient, $\mathbf{CF} = \{d \in \mathbb{R}^n \mid d \in -\mu_0 \boldsymbol{\nabla} \mathbf{f}(\boldsymbol{x}), \mu_0 \geq 0\}$, which lies in the conic hull of the gradient enclosures, $\mathbf{CH} = \left\{ d \in \mathbb{R}^n \mid d \in \sum_{i \in B} \mu_i \boldsymbol{\nabla} \mathbf{p}_i(\boldsymbol{x}) + \sum_{i \in C} \mu_i \boldsymbol{\nabla} \mathbf{g}_i(\boldsymbol{x}), \mu \geq 0, \mu \neq 0 \right\}$. So, if $\mathbf{CF} \cap \mathbf{CH} \neq \emptyset$, then the interval box $\boldsymbol{x}$ can contain a local optimizer.

The test performs step-by-step checks on the conic hull **CH** and the cone **CF**, which allows for early termination and saves computation time. The procedure begins with a check to see if the gradient, denoted by $\boldsymbol{\nabla} \mathbf{f}(\mathbf{x})$, contains zero, or if any active constraint's gradient has zero in its interior. If either condition is satisfied, the box cannot be reduced. Next, we analyze the sign patterns of the gradient enclosures in each dimension and classify them as "+", "–", "0+", "0–", or "+–". If the signs of the conic hull and the cone differ in any dimension, the necessary optimality conditions cannot hold, and the box is discarded. Then, we check if the gradient enclosures of the active constraints cover all orthants. In this case, **CH** is full, so the box cannot be reduced. For an active constraint, we compute the inclusion of the Lagrange multipliers in each dimension. If the intersection of these inclusions is empty, the box is discarded. For multiple active constraints, we compute the same inclusions using the interval hull of the active gradients. Again, if the intersection is empty, the box is discarded. Lastly, we consider pairs of dimensions where at least one has sign-consistent gradient enclosure. For each pair, we compute the slope intervals $\mathbf{M}_f$ and $\mathbf{M}_g$. If $\mathbf{M}_f \cap \mathbf{M}_g = \emptyset$, the box is eliminated. Efficient pairing strategies reduce the running time of the pairing method.

We show that the above Advanced Geometrical Test is very efficient on a large benchmark. The best variant can save more than 40% of the computational time on average using the designed test.

References

[1] M. Gencsi and B. G.-Tóth. The Fritz-John condition system in interval branch and bound method. *Annales Mathematicae et Informaticae*, 58:56–68, 2023.

[2] E. Hansen and G.W. Walster. Global Optimization Using Interval Analysis: Revised And Expanded. CRC Press, 2003.

[3] E.R. Hansen and G.W. Walster. Bounds for Lagrange multipliers and optimal points. *Computers & Mathematics with Applications*, 25(10):59–69, 1993.

[4] M. Gencsi and B. G.-Tóth. Efficient use of optimality conditions in Interval Branch and Bound methods. *EURO Journal on Computational Optimization*, 13, 2025.

Exhaustive Interval-based 2-D Shape Registration Under Similarity Transformation

Verlein Radwan[1], Simon Rohou[2] and Gilles Trombettoni[1]

[1] LIRMM - Lab. d'Informatique, de Robotique et de Microélectronique de Montpellier
161 Rue Ada, 34095 Montpellier, France
{vradwan,gilles.trombettoni}@lirmm.fr
[2] ENSTA, Institut Polytechnique de Paris, Lab-STICC
2 Rue François Verny, 29200 Brest, France
simon.rohou@ensta.fr

Keywords: Procrustes Analysis, Registration, Separators, Interval Analysis

Motivation

The registration of two sets aims at getting all the transformation parameters that map them. This work covers the case of bounded subsets of $\mathbb{R}^2$ and similarity transforms, consisting of a composition of translation, rotation and uniform scaling. The classical Procrustes-like approach [1] to this problem is to switch from the original 4D transformation to a 1D orientation problem. Since rotational symmetries induce several solutions for the orientation problem, state-of-the-art methods based on local optimization are *de facto* unsuitable when they appear.

We propose a set-membership approach capable of approximating all solutions by reproducing the Procrustes-like approach and solving the orientation problem, thanks to set manipulation using descriptive operators called *separators* [2].

A Procrustes set-membership approach

The algorithmic sequence used to perform the registration of two sets $\mathbb{A}$ and $\mathbb{B}$ starts by centering and normalization steps, followed by rotational mapping. The usual centers and scaling factor come from the fact that $\mathbb{A}$ and $\mathbb{B}$ are represented as point clouds in state-of-the-art methods. In our set-membership approach, we have to find appropriate substitute for these (centers and scaling factors) parameters.

Proposition 1. *The minimum enclosing circle [3] provides different but suitable parameters for the centering and normalization.*

Thus, the whole algorithm consists of the following steps:

1. Find the minimum circles centers $\mathbf{c}^{\mathbb{A}}_{1,2}$, $\mathbf{c}^{\mathbb{B}}_{1,2}$ and radii $c^{\mathbb{A}}_3$, $c^{\mathbb{B}}_3$. (Fig. 1.A),
2. Describe the normalized sets $\mathbb{A}_N := \left(\mathbb{A} - \mathbf{c}^{\mathbb{A}}_{1,2}\right)/c^{\mathbb{A}}_3$, $\mathbb{B}_N := \left(\mathbb{B} - \mathbf{c}^{\mathbb{B}}_{1,2}\right)/c^{\mathbb{B}}_3$. (Fig. 1.B–C),
3. Describe the set of possible rotations $\Theta = \{\theta \mid \mathbb{B}_N = \mathrm{R}_\theta \cdot \mathbb{A}_N\}$, where R_θ is the rotation matrix of parameter θ. (Fig. 1.D).

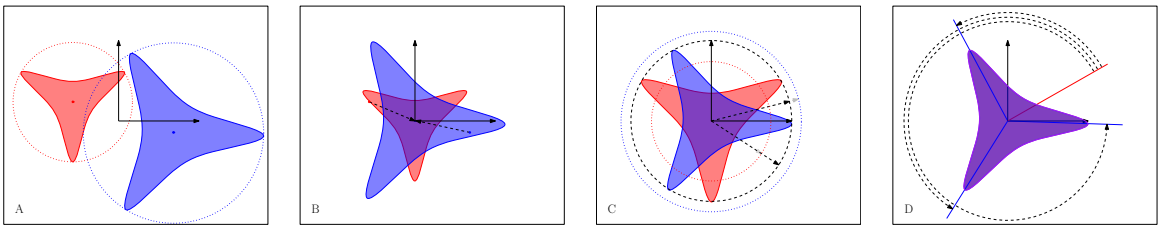

Figure 1: Algorithm in 4 steps: A: Identification of smallest circles (centers and sizes). B: Centering of sets. C: Normalization of sets. D: Identification of rotation parameters.

Approximation using separators

Usually involved in a branch and separate algorithm, a separator [2] is an algorithmic operator capable of representing a set: from an initial domain, it can remove non-solution parts (contraction) as well as parts containing only solutions.

Using the Codac library (`www.codac.io`, [4]) which offers a catalog of separators, it is possible to define a new separator as a sequence of separators handling constraints involving sets and set operations.

To implement the Procrustes approach, we first give the system of constraints that defines the problem, and for each variables we propose a separator consistent with it.

As a result, the algorithm returns separators describing respectively all possible sets Θ, $\mathbb{K}$, $\mathbb{T}$ of rotations θ, (unique) uniform scaling k and translations $\mathbf{t}$.

Finally, by slightly modifying the chain of separators, we will see that the same approach allows similarity transformations to be approximated completely, including reflection symmetries.

References

[1] P.H. Schönemann and R.M. Carroll. Fitting one matrix to another under choice of a central dilation and a rigid motion. *Psychometrika*, vol 35, 245–255, 1970.

[2] L. Jaulin and B. Desrochers. Introduction to the Algebra of Separators with Application to Path Planning. *Engineering Applications of Artificial Intelligence*, vol 33, 141–147, 2014.

[3] J.J. Sylvester. A question in the geometry of situation. *Quarterly Journal of Pure and Applied Mathematics*, vol 1, 79–80, 1857.

[4] S. Rohou and B. Desrochers and F. Le Bars. The Codac Library. *Acta Cybernetica, Special Issue of SWIM 2022*, vol 26, 871–887, 2024.

Adaptative parallelepipedic approximation of the image of a set by a nonlinear function

Maël Godard[1], Luc Jaulin[1] and Damien Massé[2]

[1] ENSTA
Lab-STICC, ROBEX Team
2 rue François Verny, Brest, 29200, France
{mael.godard,luc.jaulin}@ensta.fr
[2] Université de Bretagne Occidentale (UBO)
Lab-STICC, ROBEX Team
20 avenue Le Gorgeu, Brest, 29200, France
damien.masse@univ-brest.fr

Keywords: Parallelepipeds, Adaptative enclosure, Interval Methods

Introduction

We propose a method to compute an adaptative inner and outer approximation of the image of a set by a function. This approximation relies on a cover of the boundary with parallelepipeds [1]. As any set-based method, it gives a guaranteed yet pessimistic result when approximating the image set. If the system has to respect some constraints (e.g. obstacle avoidance), this pessimism can cause a false alarm. The method presented here relies on an adaptative slicing of the initial set to limit the false alarms while saving computation time around the safe states.

Adaptative parallelepipedic approximation

Let us denote by $\mathbb{Y}$ the image set and $\langle\mathbb{Y}\rangle$ its parallelpipedic outer-approximation. Figure 1 shows two possible outer-approximations of $\mathbb{Y}$. On Figure 1a the pessimism is too important and we can not conclude if the situation is safe. On the other hand on Figure 1b the situation is clearly safe, but this result was longer to get.

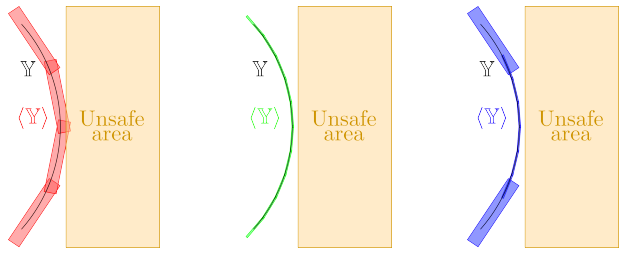

(a) False alarm (b) No false alarm (c) Adaptative approximation

Figure 1: Outer approximations of $\mathbb{Y}$ next to an unsafe area

The idea presented in this paper is then to use a low resolution everywhere, and to refine the approximation where needed. This is depicted on Figure 1c where two different resolutions are used to get an adaptative parallelepipedic enclosure of $\mathbb{Y}$.

Main results

We propose an algorithm to generate an adaptative outer approximation of the image of a set. This algorithm is n-dimensionnal, and allows to verify if the image set satisfies a given property (or set of properties). Applications in three dimensions will be displayed.

Figure 2a shows an application where we want to assert that a robotic arm will not collide in a cylinder [2] [3]. The arm is composed of three segments (red, green and blue) and we want to compute its workspace, i.e. the possible positions of the orange effector. The position of the effector can be computed directly from the three angles of the arm : one between the black base and the red segment, one between the red and green segments and one between the green and blue segments.

Figures 2b and 2c show the projected workspace of the robotic arm in green, with the cylinder in orange. We can see that thanks to our adaptative slicing we are able to assert that the arm will not collide with the cylinder.

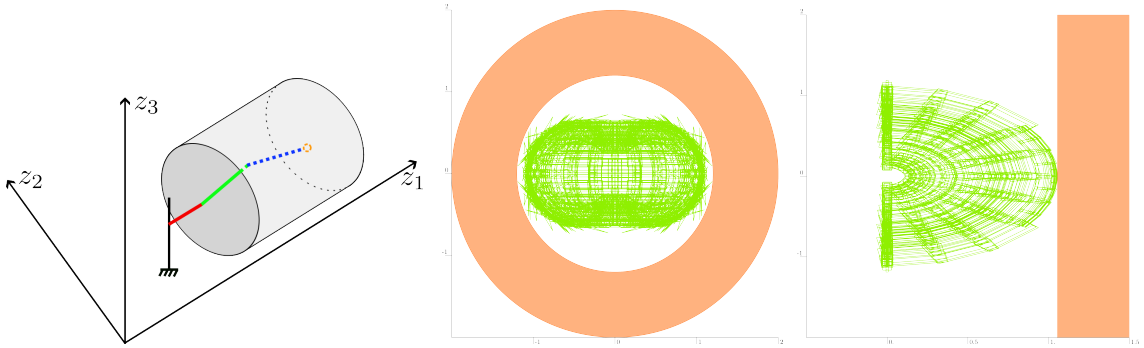

(a) Robotic arm in a cylinder (b) Workspace projected in the (z_2, z_3) plane (c) Workspace projected in the (z_1, z_2) plane

Figure 2: Constraints validated thanks to an adaptative slicing

Acknowledgement

This work was supported by the Defense Innovation Agency (AID) and the Brittany Region.

References

[1] L. Chisci, A. Garulli, and G. Zappa, "Recursive state bounding by parallelotopes," *Automatica*, vol. 32, no. 7, pp. 1049–1055, 1996.

[2] J.-P. Merlet, "Trajectory verification in the workspace for parallel manipulators," *International Journal of Robotics Research*, vol. 13, no. 4, pp. 326–333, 1994.

[3] O. Khatib, "Real-time obstacle avoidance for manipulators and mobile robots," *International Journal of Robotics Research*, vol. 5, no. 1, pp. 90–98, 1986.

Adaptative parallelepipedic approximation of the image of a set by a nonlinear function

Maël Godard – Luc Jaulin – Damien Massé

SCAN 2025, Oldenburg, Germany

Parallelepipedic Approximation

Let us consider a function $\mathbf{f}: \mathbb{R}^m \to \mathbb{R}^n$, $m \leq n$. A **parallelepiped inclusion function** of f is a function

$$\langle \mathbf{f} \rangle : \begin{array}{c} \mathbb{IR}^m \to \mathbb{PR}^n \\ [\mathbf{x}] \to \langle \mathbf{f} \rangle([\mathbf{x}]) \end{array}$$

For a given box $[\mathbf{x}]$, this function returns a parallelepiped enclosing $\mathbf{f}([\mathbf{x}])$.

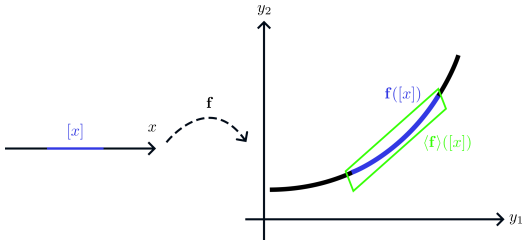

Parallelepipeds are efficient wrappers to enclose a set. They are a compromise between the **simplicity of boxes** and the **precision of zonotopes**.

Need for adaptivity

As any set based method, the use of parallelepipeds to enclose a set gives a **pessimistic** result. If the final objective is to assert that a constraint is satisfied, this pessimism can create an **ambiguity**.

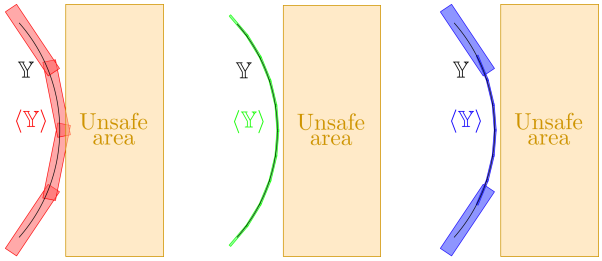

Ambiguity | No ambiguity | Adaptative

Using a high number of parallelepipeds everywhere is expensive time-wise and computational-wise. The idea presented here is then to use a low resolution everywhere, and to refine only the areas where it is needed. The result is an **adaptative parallelepipedic approximation**.

Use cases

Direct image computation

This method can be used to compute the **direct image of a set by a function**. For example, the computation of the workspace of a robotic arm.

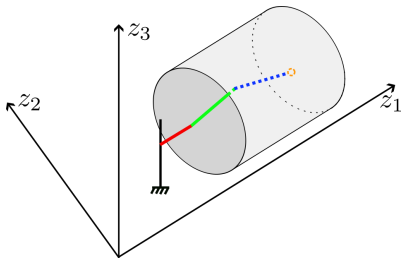

In this example we consider the set of the possible angles for each joint. The image set contains all the achievable positions for the effector. The constraint is that we want to **avoid collisions** between the effector and the grey cylinder (in red in both planes below).

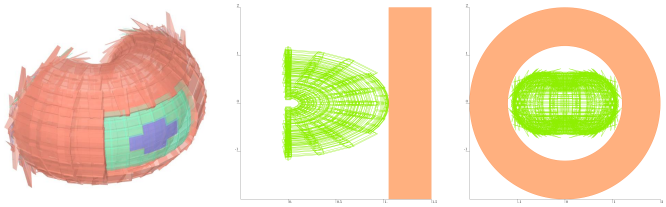

3D workspace | (z_1, z_2) plane | (z_2, z_3) plane

Reachable set computation

This method can be used to compute the **reachable set** of a dynamical system of the form $\dot{\mathbf{x}} = \mathbf{f}(\mathbf{x}, \mathbf{u})$.The state of the system is $\mathbf{x}$ and $\mathbf{u}$ is a **known input**.
As an example we will consider that the system is a robot defined by its position and its heading.

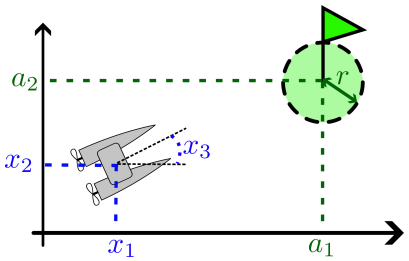

Here we consider the set of possible initial states for the robot. The image set contains all the possible states of the robot after a given time. We want to assert that the robot reaches the green area after a specific duration.

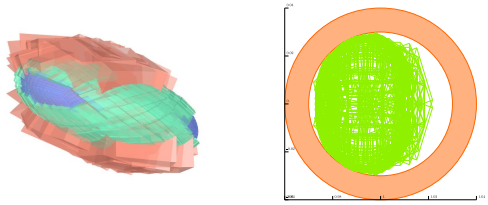

3D reachable set | (x_2, x_3) plane

High-Performance Emulation of Matrix Multiplication using INT8 Matrix Engines and its Error Analysis

Yuki Uchino[1], Katsuhisa Ozaki[2] and Toshiyuki Imamura[3]

[1] RIKEN Center for Computational Science
650-0047 Hyogo, Japan
yuki.uchino.fe@riken.jp
[2] Department of Mathematical Sciences
Shibaura Institute of Technology
337-8570 Saitama, Japan
ozaki@sic.shibaura-it.ac.jp
[3] RIKEN Center for Computational Science
650-0047 Hyogo, Japan
imamura.toshiyuki@riken.jp

Keywords: Matrix Multiplication, High-Performance Computing, Emulation, Error Analysis

Introduction

The field of AI is evolving daily, and handling data center-scale AI workflows with high throughput is essential. Modern architectures feature high-performance and power-efficient units (e.g., NVIDIA Tensor Cores, AMD Matrix Cores, and Google Cloud Tensor Processing Units) to process low-precision matrix multiplication in AI workflows rapidly. However, the performance of single- and double-precision computations required in scientific computing has stagnated. The key to reconcile contemporary hardware advancements with the requirements of scientific computing is utilizing low-precision units. We present methods for emulating single- and double-precision general matrix-matrix multiplication (SGEMM and DGEMM) using INT8 matrix engines.

Previous Study

The authors proposed Ozaki scheme II [1], emulation of high-precision matrix multiplication based on the Chinese Remainder Theorem. For $N \in \mathbb{N}$, we let $p_1, \ldots, p_N \in \mathbb{N}_{\geq 2}$ be pairwise coprime integers and $q_1, \ldots, q_N \in \mathbb{N}$ be modular multiplicative inverses of $\prod_{j \neq i} p_j$ (i.e., $\prod_{j \neq i} p_j \cdot q_i \equiv 1 \mod p_i$). For integer matrices $A' \in \mathbb{Z}^{m \times k}$ and $B' \in \mathbb{Z}^{k \times n}$, the approximation of a matrix product $C' \approx A'B'$ can be obtained as follows:

$$C' \leftarrow \mathrm{mod}\left(\sum_{i=1}^{N} \mathrm{mod}(A''B'', p_i) \cdot \prod_{j \neq i} p_j \cdot q_i, \prod_{j \neq i} p_j\right), \tag{1}$$

where $A'' := \mathrm{mod}(A', p_i)$, $B'' := \mathrm{mod}(B', p_i)$, and $\mathrm{mod}(x, y)$ is the remainder of x/y. Note that this accumulation must be computed with high precision. For floating-point matrices $A \in \mathbb{R}^{m \times k}$ and $B \in \mathbb{R}^{k \times n}$, we first apply scaling and chopping to obtain

A' and B'. We then compute $C' \approx A'B'$, and subsequently apply inverse scaling to obtain an approximation of AB.

Main results

We chose the moduli p_i such that the remainders fit within the INT8 range, enabling emulation of the matrix multiplications $A''B''$ in (1) using INT8 matrix engines. The performance of matrix multiplication using INT8 matrix engines is overwhelmingly faster than that of FP64, FP32, and others. Therefore, even if the computational cost of FP64, FP32, and similar operations is much lower than that of matrix multiplication, their execution time remains non-negligible. Consequently, if Ozaki scheme II implemented in a straightforward manner, it can become a performance bottleneck. Hence, in emulation using INT8 matrix engines, it is crucial to skillfully apply techniques such as table lookups and error-free computations to avoid division and high-precision computations.

Numerical experiments to evaluate the accuracy, throughput performance, and power efficiency were conducted on an NVIDIA GH200 Grace Hopper Superchip, an NVIDIA Ampere A100 SXM4 GPU, and an NVIDIA GeForce RTX 5080 Blackwell GPU. On GH200, the proposed DGEMM emulation achieved a 1.3x speedup and a 43% improvement in power efficiency compared to native DGEMM. The proposed SGEMM emulation achieved a 3.4x speedup and a 173% improvement in power efficiency compared to native SGEMM. Numerical results obtained on A100 and RTX 5080 also showed high performance and power efficiency.

A deterministic error analysis of the emulation was also conducted. In the presentation, we will discuss the validity of this error analysis by comparing it with numerical results. Error analysis of matrix multiplication has been widely used to verify the results of various problems in numerical linear algebra. Likewise, the proposed emulation and its error analysis can be applied to such verification methods.

Acknowledgement

This study was supported by Japan Society for the Promotion of Science Grant-in-Aid for Research Activity Start-up No. 24K23874, Grant-in-Aid for Scientific Research (A) No. 25H01109, and Grant-in-Aid for Scientific Research (B) (General) Numbers 23K28100 and 25K03126.

References

[1] K. Ozaki, Y. Uchino, and T. Imamura. Ozaki Scheme II: A GEMM-oriented emulation of floating-point matrix multiplication using an integer modular technique. preprint arXiv:2504.08009, 2025.

Efficient Acceleration Strategies for Interval Branch-and-Bound Type Methods

Lorenz Gillner and Ekaterina Auer

Department of Electrical Engineering
University of Applied Sciences Wismar
D-23966 Wismar, Germany
{lorenz.gillner,ekaterina.auer}@hs-wismar.de

Keywords: Interval Methods, Parallelization, Parameter Estimation, GPU

Interval analysis [9] is a valuable tool for addressing a wide range of applications that require reliable methods for such tasks as, for example, root-finding, global optimization, or parameter estimation. Despite its versatility in deterministic handling of bounded uncertainty, the adoption of interval analysis in computer-aided problem-solving has been constrained by computational overhead and the possibility of too conservative estimations of the result domains. A promising approach to alleviate this is the use of parallelization on specialized hardware, such as GPUs. Leveraging GPUs can potentially enable computations that were previously considered infeasible.

Interval branch-and-bound (IBB) methods, which systematically reduce an initial search domain, are particularly well-suited for estimation problems involving bounded uncertainty. IBB algorithms rely on iterative subdivision strategies to isolate regions of interest. Although this process can be implemented efficiently in a sequential manner, it has potential for parallelization on GPUs. Naive implementations often conflict with the GPU's massively parallel architecture in practice, leading to suboptimal performance and therefore undermining the advantages of hardware acceleration. While GPU-based IBB methods have been addressed in the literature, the employed parallelization strategies are not unified and vary widely from brute-force techniques to more structured, vectorized implementations [3, 4, 10].

Recently, we have tested our own versions of GPU interval optimization methods based on brute-force techniques in the context of communication and energy systems [1, 2]. We applied monotonicity, convexity and SIVIA-like [7, 8] tests in parallel on a multi-dimensional, uniform grid in order to eliminate boxes from the search that cannot contain a solution. For automatic differentiation, we ported the widely used FADBAD++ to the CUDA framework, with interval support provided by a modified version of the CUDA interval library [5]. This approach proved to be faster than comparable CPU-based ones. However, our brute-force method on the GPU does not scale well due to its memory-intensive processing of redundant boxes. Depending on the structure and size of a problem, different forms of parallelized space subdivision can accelerate the optimization process even further.

In this contribution, we investigate and compare several ways to parallelize subdivision methods on the example of the SIVIA algorithm. Our goal is to identify strategies that maximize utilization of GPUs' computational capabilities by benchmarking throughput performance in a series of standard examples. We also introduce a new GPU interface for the Boost interval library to enable a seamless integration

of GPUs into existing CPU-based code. Additionally, we assess our findings using a close-to-life application.

Finally, we consider the implications of GPU acceleration with respect to power consumption. Although GPUs offer substantial performance improvements with each new generation, they also require significant amounts of energy. To quantify our energy-related costs, we not only benchmark throughput performance but also perform detailed energy measurements for both CPU-only and GPU-accelerated interval implementations. Unlike our previous studies [1, 6], which relied on software-based estimates, this work presents our results using hardware-based measurements, offering a more accurate assessment of the trade-offs between performance and power consumption in parallelized IBB methods.

References

[1] E. Auer, A. Ahrens and L. Gillner. GPU-Based Interval Optimization in the Context of Optical MIMO Systems. In: R. Wyrzykowski, J. Dongarra, E. Deelman, and K. Karczewski (Eds.), *Parallel Processing and Applied Mathematics*, 360–374, 2025.

[2] E. Auer, A. Rauh and L. Gillner. Parameter Identification for Cooperative SOFC Models on the GPU. In: T. N. Dinh, A. Rauh, S. Z. Yong, Z. Wang (Eds.), *Set-Valued Approaches to Control and Estimation of Uncertain Systems – Theory and Applications*, to be published.

[3] Z. Bagóczki and B. Bánhelyi. A Parallel Interval Arithmetic-based Reliable Computing Method on a GPU. *Acta Cybernetica*, 23:491–501, 2017.

[4] P.-D. Beck and M. Nehmeier. Parallel Interval Newton Method on CUDA. *Applied Parallel and Scientific Computing*, 454–464, 2013.

[5] C. Collange, M. Daumas, D. Defour. Interval Arithmetic in CUDA. In: W. W. Hwu (Ed.): *GPU Computing Gems Jade Edition*, 99–107, 2012.

[6] L. Gillner and E. Auer. GPU-Accelerated, Interval-Based Parameter Identification Methods Illustrated Using the Two-Compartment Problem. *Acta Cybernetica*, 26:913–932, 2024.

[7] E. Hansen and G. W. Walster (Eds.). *Global Optimization Using Interval Analysis: Revised and Expanded*. CRC Press, 2004.

[8] L. Jaulin and E. Walter. Set Inversion via Interval Analysis for Nonlinear Bounded-error Estimation. *Automatica*, 29:1053–1064, 1993.

[9] R. E. Moore, R. B. Kearfott, and M. J. Cloud. *Introduction to Interval Analysis*. Society for Industrial and Applied Mathematics, 2009.

[10] D. P. Sanders and V. Churavy. Branch-and-bound interval methods and constraint propagation on the GPU using Julia. *SCAN*, 2020.

Efficient Acceleration Strategies for Interval Branch-and-Bound Type Methods

Lorenz Gillner and Ekaterina Auer

Wismar University of Applied Sciences
Department of Electrical Engineering and Computer Science

Motivation

Classical interval algorithms for problems such as root-finding, global optimization and parameter estimation iteratively apply branching and bounding/pruning on an initial search domain until a satisfactory result is reached. These types of algorithms are often **restricted** to problems of low dimensions due to their dependence on **space subdivision**. As a result of the **growing interest** in GPU applications for scientific computing in general, the topic of **GPU-accelerated interval methods** has also gained more attention in recent years. We explore ways to **enhance** the speed of **interval branch-and-bound type methods** using GPUs to scale them beyond their current limits. Given today's growing **demand for computing power**, we must evaluate accelerated algorithms based not only on their speed, but also on their **energy requirements**.

GPU Computing

Key considerations:

- Fit tasks to thread block model
- Reduce main memory accesses
- Maximize occupancy
  ➥ Avoid idle threads
- Kernels operate in *warps* (groups of 32 threads)

Thread Block Model

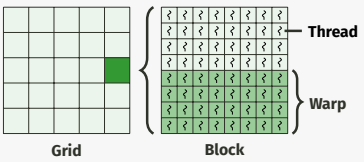

Parallelization of Branching Algorithms

Two main categories of parallelization for tree-like procedures:

Node Level
Work distribution across a *coarse* grid (subtasks)

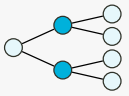

Leaf Level
Subdivision of a problem into *fine* grid (brute-force)

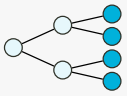

General search space reduction scheme used previously [1, 2, 3]:

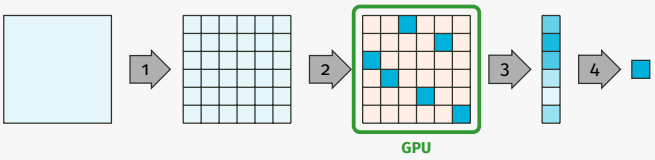

Drawbacks: High memory saturation; scalability limited by problem dimensions
Improvement: Unify steps 1 and 2 to maximize computational efficiency

if $f([x]) \subset [y]$: keep $[x]$
elif $f([x]) \cap [y] = \emptyset$: reject $[x]$
else: bisect $[x]$

SIVIA (Set Inversion Via Interval Analysis [5]): good example for branching-based interval algorithms suitable for parallelization

☞ We consider 3 basic parallelized versions, as well as combinations thereof:

NSIVIA Multiple (independent) instances of SIVIA in parallel over a coarse grid
PSIVIA Massively parallel, one-time evaluation of single boxes over a fine grid
VSIVIA Vectorized »bisect – evaluate – partition« cycle [4]

Boost.Interval: New GPU Mode

To streamline development, we added GPU support to the Boost.Interval library:

- ➤ Direct rounding mode for GPU arithmetic ➟ fast operations
- ➤ Extensive use of generic programming ➟ same source code for CPU and GPU
- ➤ First cross-platform, GPU-compatible interval library for CUDA C++

```
/* Classic interval type definition */
typedef interval<double, policies<save_state<rounded_transc_std<double> >,
        checking_base<double> > > host_interval;

/* Interval data type definition for the GPU */
typedef interval<double, policies<save_state_nothing<rounded_transc_gpu<double> >,
        checking_base_gpu<double> > > device_interval;

/* Cross-platform interval type (without bounds checking) */
typedef interval<double, policies<save_state_nothing<rounded_transc_exact<double> >,
        checking_base<double> > > cross_interval;
```

https://github.com/lorenzgillner/boost-interval

Performance Benchmarks

Benchmarks: SIVIA of the Griewank test function

$$g(\mathbf{x}) = \frac{1}{K}\sum_{i=1}^{n} x_i^2 - \prod_{i}^{n} \cos\left(\frac{x_i}{\sqrt{n}}\right) + 1, \; K = 4000$$

- Optimization of the method itself
  ➥ All results are qualitative the same
- 16 variations of SIVIA implementations
- Selection of parallelization frameworks
  ➥ OpenMP, OpenMPI, TBB and CUDA
- Tests on consumer grade hardware

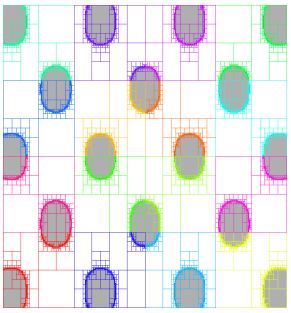

Power Profiling

➤ Per-component measurements of power consumption during benchmarks

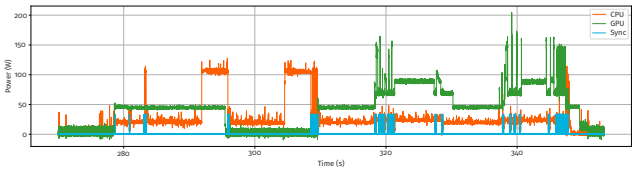

Results

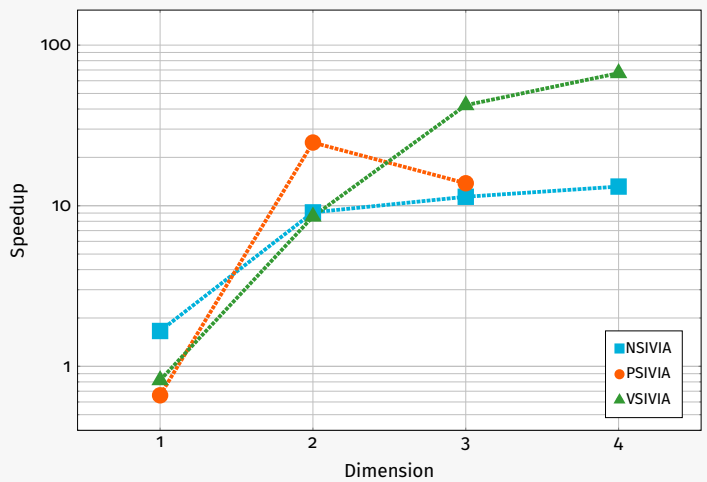

- ➤ Choice of parallelization method depends on the problem dimensions
- ➤ Brute-force methods are best suited for small problems
- ➤ A-priori subdivision combined with vectorization yields best time to solution
- ➤ 67× speedup on a four-dimensional problem compared to traditional version
  ➥ Reduction of energy requirements by 90%

References:
[1] L. Gillner and E. Auer. GPU-accelerated, interval-based parameter identification methods illustrated using the two-compartment problem. *Acta Cybernetica*, 2024.
[2] M. B. Eriksen and S. Rasmussen. GPU accelerated parameter estimation by global optimization using interval analysis, 2013.
[3] K. Nasiotis. Accelerating SIVIA (set inversion via interval analysis). an interval set membership technique to evaluate the generalization of neural classifiers, 2023.
[4] S. Tzeng and J. D. Owens. Finding convex hulls using quickhull on the GPU. 2012.
[5] L. Jaulin and E. Walter. Guaranteed nonlinear parameter estimation from bounded-error data via interval analysis. *Mathematics and computers in simulation*, 1993.
[6] E. Auer, A. Ahrens, and L. Gillner. GPU-based interval optimization in the context of optical MIMO systems. In *International Conference on Parallel Processing and Applied Mathematics*. Springer, 2024.

20th International Symposium on Scientific Computing, Computer Arithmetic, and Verified Numerical Computations, Sept. 22–26, 2025, Oldenburg, Germany

GPU-Accelerated Algorithmic Differentiation For Reliable Computing: Comparing Different Architectures

Diego Romano[1], Ekaterina Auer[2], Francesco Gregoretti[1] and Lorenz Gillner[2]

[1] Institute for High Performance Computing and Networking
National Research Council, Italy
{diego.romano, francesco.gregoretti}@cnr.it
[2] Department of Electrical Engineering
University of Applied Sciences Wismar,
D-23966 Wismar, Germany
{ekaterina.auer,lorenz.gillner}@hs-wismar.de

Keywords: Interval Methods, Algorithmic Differentiation, GPU

As the need for trustworthy simulations grows, reliable computations are becoming increasingly important in such varied areas as robotics, medical imagining, computational biology, and many others. In such applications, accurately propagating bounded epistemic uncertainty is crucial for achieving dependable results in both static and dynamic systems. Beyond simulation, parameter identification under uncertain conditions plays a vital role in solving real-world engineering and scientific problems. The demand for reliability is offset by an equally important requirement of efficiency, often resulting in a compromise that prioritizes one over the other.

Interval methods [3] have emerged as a valuable tool in the context of reliability, since they inherently propagate bounded uncertainty while fulfilling their primary purpose of result verification. This kind of verification involves providing a guaranteed enclosure of the exact result, despite potential rounding, discretization, or method errors that may affect computer-based calculations.

An important step in the verification of higher-level numerical methods, such as those used for solving differential equations or global optimization, is the computation of exact partial derivatives of the underlying functions. While users can provide the code for derivatives manually or with the aid of a computer algebra system, it is more desirable to compute derivatives automatically within the normal program code. Algorithmic differentiation [2] offers a well-established approach to achieve this goal. Over the past three decades, numerous tools have been developed to support its implementation, primarily targeting serial execution on the CPU. While algorithmic differentiation simplifies the process from the point of view of human effort, it must not necessarily result in improved overall runtime performance of a simulation.

Parallelization has been successfully employed within the high-performance computing framework to accelerate traditional result verification methods. The use of graphic processing units (GPUs) can be particularly beneficial, owing to their high computational throughput and relatively low cost. Nevertheless, the GPU architecture diverges significantly from its CPU counterpart, necessitating innovative approaches to porting CPU code to the GPU in order to fully exploit the GPUs' capabilities.

This poses a particular challenge for algorithmic differentiation, as only a few GPU implementations currently exist[1], and none are designed to support interval data types. To address this gap, we have recently ported the popular template-based CPU tool FADBAD++ to the GPU and implemented a differentiation-algebra-based approach for the first and second derivative[2]. Although FADBAD++ has the big advantage of enabling the computation of derivatives of any order on the CPU, a naive porting to the GPU proves to be inefficient [1].

In this contribution, we initiate a systematic approach to optimizing the implementation of algorithmic differentiation on the GPU. By analyzing the performance characteristics of various GPU architectures, we aim to pinpoint the primary bottlenecks and identify opportunities for improvement. To this end, we examine the computational efficiency of a classic global optimization problem using the Griewank function, alongside a real-world case from the field of multiple-input multiple-output (MIMO) systems, a key technology in broadband wireless communications.

References

[1] E. Auer, A. Ahrens, and L. Gillner. GPU-based interval optimization in the context of optical MIMO systems. In: R. Wyrzykowski, J. Dongarra, E. Deelman, and K. Karczewski (Eds.), *Proceedings of Parallel Processing and Applied Mathematics*, 2025.

[2] A. Griewank. Evaluating Derivatives: Principles and Techniques of Algorithmic Differentiation. Frontiers in Applied Mathematics Series, 2000.

[3] R.E. Moore, R.B. Kearfott, and M.J. Cloud. *Introduction to Interval Analysis*. Society for Industrial and Applied Mathematics, 2009.

[1] e.g., `https://github.com/vgvassilev/clad`

[2] `https://github.com/lorenzgillner/tada`